Transcriptional and signaling analysis as a means of investigating the complexity of aging processes in human and mouse

Dissertation zur Erlangung des akademischen Grades des Doktors der Naturwissenschaften (Dr. rer. nat.)

eingereicht im Fachbereich Biologie, Chemie, Pharmazie der Freien Universität Berlin

vorgelegt von

Thore C. Brink
aus Herdecke

August 2008

1. Gutachter: Prof. Dr. Hans Lehrach,
Max-Planck-Institut für Molekulare Genetik

2. Gutachter: Prof. Dr. Volker Erdmann
Freie Universität Berlin

Disputation am 27.03.2009

Acknowledgment

Ich danke Herrn Professor Lehrach für die Betreuung, das Interesse und die Unterstützung beim Durchführen dieser Arbeit sowie für die Überlassung des Themas und die Möglichkeit die Dissertation am Max-Planck-Institut für Molekulare Genetik anzufertigen.

Des Weiteren danke ich Herrn Professor Erdmann für das Interesse und die Unterstützung beim Durchführen dieser Arbeit.

Ein besonderer Dank gebührt Herrn Dr. James Adjaye für die Korrektur, Unterstützung und Anleitung bei der Anfertigung meiner Dissertation sowie für die angenehme Zusammenarbeit während der letzten Jahre.

Den Mitgliedern meiner Arbeitsgruppe sowie allen anderen Mitarbeitern und Doktoranden des Max-Planck-Instituts für Molekulare Genetik danke ich für die gute Zusammenarbeit und das gute Arbeitsklima.

Meiner Familie danke ich herzlich für vielerlei Unterstützung, Aufmunterung und Anerkennung während der zurückliegenden Zeit. Hervorzuheben sind meine Frau Nicole und meine Eltern Dr. Kurt und Carmen Brink.

Ich danke herzlich meinen Freunden für ihre Unterstützung und Aufmunterung während der zurückliegenden Zeit. Danke Andreas und Marc für die tatkräftige Unterstützung bei der Korrektur und viele anregende Gespräche.

Vielen Dank Metzler für das Erstellen der PDF Version dieser Arbeit.

Contents

Abbreviations

Abbreviations

AGEs	advanced glycation end products
aRNA	amplified ribonucleic acid
ATP	adenosine triphosphate
BP	biological process
BSA	bovine serum albumin
CC	cellular compartment
cDNA	complementary deoxyribonucleic acid
CLS	chronological life span
CR	caloric restriction
Ct	threshold cycle
DNA	deoxyribonucleic acid
dNTP	deoxyribonucleotide triphosphate
DR	dietary restriction
GO	gene ontology
LPO	lipid hydroperoxide
MHC	major histocompatibility complex
mRNA	messenger ribonucleic acid
PBS	phosphate buffered saline
PCR	polymerase chain reaction
PFA	paraformaldehyde
RLS	replicative life span
RNA	ribonucleic acid
ROS	radical oxygen species
RT	room temperature
SDS	sodium dodecyl sulfate
SSC	sodium chloride/sodium citrate

Semantics

°C	degrees Celsius
µg	micrograms
µl	microlitres
µM	micromol
g	grams / gravity
hr/hrs	hours
M	mol
mA	milliampere
mg	milligrams
min	minutes
ml	millilitres
mm	millimetres
mM	millimol
ng	nanograms
nm	nanometres
pg	picograms
pmol	picomol
s	seconds
U	units
V	volt

List of Figures

List of Tables

Abstract

There has been a dramatic increase in the life expectancy of men and women in the last century. Along with the increased life span the incidence of age-related diseases such as Alzheimer's disease has also increased. This increase has led to an elevated interest to understand and investigate the mechanisms that underlie age-related diseases. Consequently, there is an increased awareness of the necessity to understand the mechanisms of aging to better cope with age-related diseases. However, the process of aging is complex and many different mechanisms are involved, including transcriptional regulation occurring with advanced age. Studies investigating age-related transcriptional changes mainly revealed that the magnitude of these changes is small and that it is difficult to find conserved regulated age-related genes between diverse species and tissues using microarray analysis.

This study was aimed at elucidating mechanisms involved in human skin and general mouse aging as well as potentially conserved mechanisms involved in mammalian aging by conducting microarray analyses using RNA derived from male and female human skin biopsies and mouse brain, heart and kidney tissues and using the same array platform and standardized parameters. The data analysis was not solely based on highlighting age-related genes but also biological processes, cellular compartments and pathways. The influence of age-dependent hormonal decline on gene expression has also been tested on a different microarray platform using two different human skin cell types – sebocytes and fibroblasts.

These experiments revealed that human skin aging is accompanied by a reduction in skin collagen structure. Furthermore, the potential involvement of WNT signaling in human skin aging was observed for the first time. The analysis of hormone-treated skin cells revealed significant differences between cell types and underscores the potential that age-related transcriptional changes are cell-type specific. The studies on mouse aging identified a conserved increase of immune responses on the transcriptional level. In addition, elevated levels of radical oxygen species (ROS) suggest the oxidative stress-mediated activity of NF-kB signaling. Comparisons of the human and mouse results confirm the conserved involvement of immune responses and of metabolism-related processes including for instance glutathione metabolism a regulator of endogenous ROS levels in mammalian aging.

In summary, the results suggest that transcriptional changes are most probably the downstream effect of environmental and endogenous factors constantly affecting the organism during age. In addition, the finding that similar processes are age-regulated including different genes in varying tissues such as immune and metabolism-related genes, suggests that aging is not dependent on single genes but rather on a network of genes.

Abstract (german)

Die menschliche Lebenserwartung hat sich im letzten Jahrhundert dramatisch erhöht. Damit verbunden sind auch altersspezifische Krankheiten wie Alzheimer vermehrt aufgetreten, wodurch heutzutage großes Interesse daran besteht, die Mechanismen zu untersuchen und zu verstehen, welche altersspezifischen Krankheiten zugrunde liegen. Um diese Krankheiten besser behandeln zu können, ist es auch notwendig, die Mechanismen der Alterung besser zu verstehen. Das Altern ist jedoch sehr komplex, da viele verschiedene Mechanismen eine Rolle spielen, wie z.B. transkriptionelle Regulation. Transkriptionsstudien haben gezeigt, dass das Ausmaß der Regulation für einzelne Gene eher gering ist und dass es schwer ist, mittels Arrayanalysen konservierte Alterungsgene zu finden, welche unabhängig von Spezies oder Organ im Alter reguliert werden.

Das Ziel dieser Arbeit war es mit Hilfe von Arrayanalysen mit standardisierten Parametern, Mechanismen aufzudecken, welche in der menschlichen Hautalterung, in der Alterung von Mäusen sowie generell im Alterungsprozess von Säugetieren eine Rolle spielen. Benutzt wurde dafür die RNA von menschlichen Hautproben (Mann und Frau) sowie von Mausgeweben (Gehirn, Herz und Niere) weiblicher Mäuse. Die Datenanalyse wurde nicht auf die Entschlüsselung von Alterungsgenen beschränkt, sondern bezog die Analyse von z.B. Gengruppen bestimmter biologischer Prozesse mit ein. Der Einfluss verringerter Hormonlevel auf die Genexpression im Alter wurde zusätzlich in Zellkulturen zweier Hautzelltypen untersucht (Sebozyten und Fibroblasten).

Die Experimente zeigten, dass die menschliche Hautalterung mit einem Verlust der Kollagenstruktur verbunden ist und dass der WNT Signalweg eine potentielle Rolle spielt, was zum ersten Mal beobachtet wurde. Die Analyse der Hormon behandelten Zellkulturen wies signifikante Unterschiede der beiden Zelltypen auf und unterstreicht damit die Theorie, dass transkriptionelle Veränderungen im Alter Zelltyp spezifisch sind. Die Untersuchung der Mausalterung identifizierte eine über die drei untersuchten Gewebe konservierte Aktivierung der Immunantwort auf Transkriptionsebene. Zusätzlich weisen erhöhte Konzentrationen von ROS auf eine mögliche durch Stress vermittelte Aktivierung des NF-kB Signalweges hin. Vergleiche der Daten von Mensch

und Maus bestätigen die im Alter konservierte Beteiligung der Immunantwort sowie von Prozessen, die im Zusammenhang mit Metabolismus stehen.

Zusammengefasst zeigen die Daten, dass transkriptionelle Unterschiede im Alter wahrscheinlich die Antwort auf äußere oder innere Faktoren sind, welchen der Organismus ein Leben lang ausgesetzt ist. Die geringe Übereinstimmung an altersspezifischen Genen und die im Gegensatz dazu signifikante Konservierung bestimmter Prozesse suggerieren, dass die Alterung nicht von einzelnen Genen, sondern vielmehr von Gennetzwerken reguliert wird.

1. Introduction

1.1 Aging

1.1.1 Aging theories

Aging research is mainly focused on the goal of facilitating a healthy long life. To reach this optimistic and overwhelming aim we first need to understand the underlying processes, which are involved in the aging process and which further lead to age-related diseases and ultimately to death. Today, the most common believe in the aging research field is that aging is a very complex process (McClearn 1997), which is clearly demonstrated by the many different theories on aging being postulated over the last decades. In the following paragraphs the most accepted theories will be shortly explained.

The DNA and genetic theories

Many aging theories have been evolved, which are related to the DNA. Some scientists believe that there exists a 'planned obsolescence' in the genetic code of species and of each individual within the same species. Additionally, this genetic code can be easily manipulated by environmental factors such as radical oxygen species (ROS), which lead to either mutations within the code or to cross links with for instance sugars. Another fact concerning DNA and aging is a loss in telomere length with age. Telomeres are repetitive regions at the end of chromosomes, which mainly protect the chromosomes from destruction but also from fusing and rearranging with each other. The problem of linear DNA is a continuous loss of nucleotides in the telomere regions in each replication step, limiting most cells in the number of replications until they exhibit cellular senescence. Therefore, unlimited dividing cells like e.g. stem cells need ways to rebuild their telomeres after each replication, which can for instance be accomplished by hormones or by the enzyme telomerase reverse transcriptase (TERT). The activity of this enzyme in somatic cells can lead to cancers, which might explain why it is normally not expressed, thus protecting the organism from cancers.

In the following theories all of these above mentioned genetic-related mechanisms in aging appear again in another context, showing that most theories are also inter-related.

The free radical theory

The free radical theory of aging is maybe the most famous aging theory. Developed in 1956 by Denham Harman, the theory (Harman 1956) describes the fact that ROS are harmful to the organism and are the main cause of age-related morphologies. ROS are produced by many exogenous factors like UV light, inflammatory cytokines or environmental toxins and also endogenously in the mitochondria during cell respiration or in the peroxisomes. Accordingly, cells have some enzymatic (e.g. catalase (CAT)) and non-enzymatic (e.g. glutathione) systems to reduce the produced ROS. The main tenet of the theory is that life span is related to the rate of ROS production in the organism. The increased rate of ROS production with age could explain the accumulation of damaged nucleic acids (DNA, RNA), proteins and lipids with age, which would then lead to age-related loss of physiological function in all parts of the body.

The cross-linking theory

The basis of this theory (Sinex 1964) is a spontaneously occurring reaction of proteins and sugars in the presence of oxygen called glycation. In contrast to glycolysation, which is the enzyme-controlled functional addition of sugars, glycation leads in many cases to a loss of function or at least a decrease in efficiency of the protein. Additionally, some cross-linked proteins cannot be degraded and therefore accumulate in the cells causing other downstream problems. Cross-linked proteins are correlated to many age-related diseases and morphologies such as senile cataract (Dawczynski and Strobel 2006), leathery skin (Avery and Bailey 2006) and diabetes (Goh and Cooper 2008).

The Hayflick limit theory

This theory (Hayflick 1965) describes the limitation of cells in the number of possible divisions. From observations made in 1961, Hayflick postulated that human cells are limited to approximately 50 cycles of cell division followed by senescence. In addition, he could show that caloric restriction (CR) – the only approved method to slow down

aging in mammals, lead to a slower rate of divisions and therefore an increased 'life span' of the cultured cells. As described above in the DNA and genetic theories, the reason why limited number cells are able to divide could be an accumulation of mutations or a decrease in telomere length.

The mitochondrial decline theory

With age the number of mitochondria declines and the existing mitochondria are less efficient and larger. The mitochondria are the energy factories of each cell by producing huge amounts of adenosine triphosphate (ATP), which cannot be stored for a long time in the cells. The cells of an organ are therefore responsible for providing enough energy for the function of the corresponding organ. If this is not possible, ATP cannot be transferred from other parts of the body and the affected organ will literally die. The mitochondrial decline theory is closely linked to the free radical theory of aging, as the mitochondria are one of the main endogenous producers of ROS and therefore subject themselves continuously with oxidative stress. As described above, ROS damages DNA, RNA, proteins and lipids and because mitochondria are limited in defence mechanisms compared to other parts of the cell their number declines with age. (Harman 1972)

The membrane theory of aging

According to this theory (Zs-Nagy 1978) the cell's impairment with age is the reduced ability of the membranes to transfer chemicals, heat and electrical processes. The theory evolved from the observation that aged membranes become less lipidic and therefore exhibit a more solid structure, which leads to less efficiency in normal function and an accumulation of the cellular toxin lipofuscin. Lipofuscin deposits become more and more present with age in brain, heart, lung and skin. In the skin these deposits are visible as some of the so-called age-spots. Interestingly, patients suffering from Alzheimer's disease – a known age-related disease, show higher levels of lipofuscin than corresponding healthy patients of the same age. Although the theory is mainly based on lipofuscin accumulation, impaired heat and electrical transfer as well as impaired sodium and potassium transfer is expected to play a role, which would lead for instance to impaired cell communication.

The neuroendocrine theory

The neuroendocrine theory (Dilman et al. 1986) completely focuses on the endocrine system. This system is a complex biochemical network responsible for the release of hormones in the body. A small gland in the brain – the hypothalamus, regulates it. With age, this system is continuously losing its precision by decreased release of hormones by the responsible organs and by a loss of the hormones effectiveness due to down-graded hormone receptors. The main cause of these functional losses in this theory is also a hormone – cortisol. This hormone is one of the few hormones which exhibit an increased release with age, and it is considered to be responsible for stress. Cortisol could therefore directly damage the hypothalamus, which would then lead to further dysregulation leading ultimately to a vicious cycle.

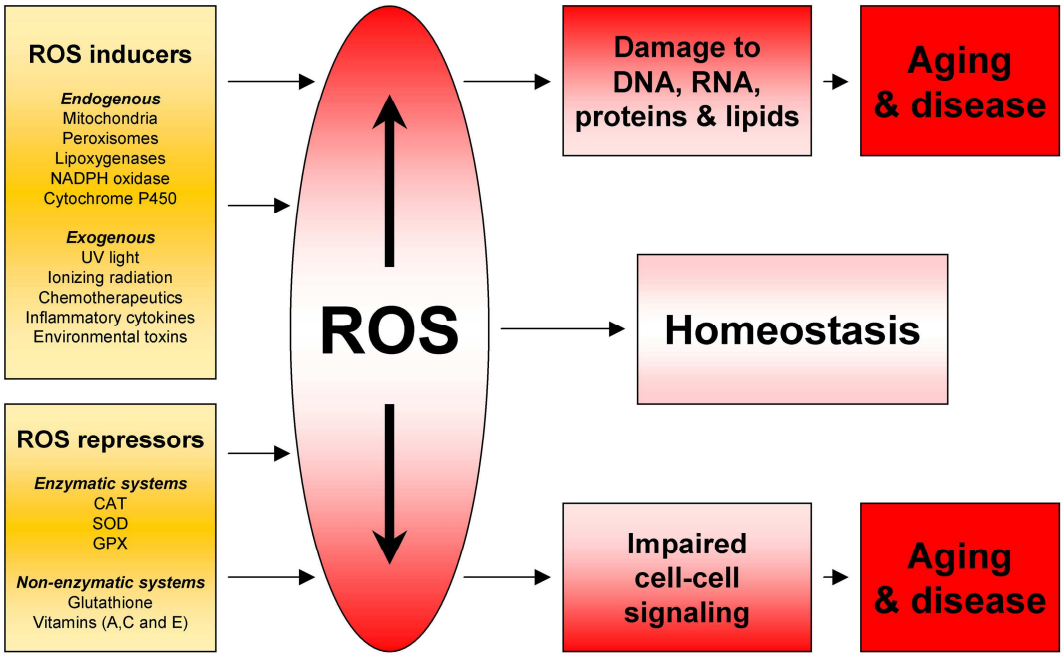

Figure 1.1 The dual role of ROS and its contribution to aging.

The figure shows that oxidants are generated as a result of normal intracellular metabolism in mitochondria and peroxisomes, as well as from a variety of cytosolic enzyme systems. In addition, a number of exogenous agents can trigger ROS production. Increased levels of ROS lead to aging, disease and cell death by damaging DNA, RNA, proteins and lipids whereas decreased levels lead to decreased proliferative response, impaired signaling and ultimately aging, disease and cell death. This dual role of ROS indicates the importance to keep homeostasis for normal cellular function, which will presumably lead to increased health and life span.

All the theories presented here describe mechanisms occurring during the process of aging. However, none of them is able to explain every aspect of aging.

Figure 1.1 – adapted from (Finkel and Holbrook 2000) – shows a simplified model of aging focussing on the role of ROS. The global message is that the ability of an organism, tissue or cell to keep a steady state could be the main aspect responsible for the rate of aging. The importance of homeostasis is of course not only valid for ROS but also other metabolites, temperature and electric potentials to ensure the effectiveness and function of the whole organism.

1.1.2 Model systems in aging research

In addition to the complex processes underlying aging and age-related diseases, large differences in aging processes exist between different species and even between different tissues within the same species. The most commonly used species in research are the yeast *Saccharomyces cerevisiae*, the nematode *Caenorhabditis elegans*, the fruit fly *Drosophila melanogaster*, and the mammalian species *Mus musculus* and *Homo sapiens*. Due to differences in number and size of samples, the genetic background and also ethic aspects, the strategy and experimental design to investigate the aging process in these five species differ from one another. In the following paragraphs, some strategies of aging research focussing mainly on whole genome gene expression studies in these species and, in addition, the potentially best-conserved age-related processes will be shortly discussed.

S. cerevisiae

The yeast *Saccharomyces cerevisiae* is a widely used model system in research. Aging research in yeast is divided in two major models that define aging in different ways – replicative life span (RLS), which is defined as the number of daughter cells produced by the mother cell, and chronological life span (CLS), which is defined as the mean life span of non-dividing cells (Kaeberlein et al. 2007). Therefore, the yeast model of aging provides the interesting possibility to compare proliferating and non-proliferating aspects of aging on the single cell level. Both RLS and CLS studies rely on the measurement of life span. Whether there is a direct relation of life span and aging is likely but still not fully proved. However, studies in yeast revealed some interesting results for eukaryotic aging. Caloric or dietary restriction for instance extends both RLS

and CLS (Jiang et al. 2000; Lin et al. 2000; Reverter-Branchat et al. 2004). In addition, genome wide screens (Kaeberlein et al. 2005; Powers et al. 2006) have identified nutrient-responsive TOR signaling pathway as an important mediator of both RLS and CLS. Decreases in TOR activity increase the life span of both dividing and non-dividing cells. The TOR signaling pathway, which acts downstream of the insulin signaling pathway mediates various downstream processes, which may influence the life span of yeast. These are for instance cell cycle progression, translational regulation, stress response, and autophagy.

C. elegans

In contrast to yeast, the nematode *C. elegans* provides a more complex but still well defined model system. While it is small-sized (~1mm) and has a relatively short life expectancy (~3days) it has a sophisticated neuroendocrine system that regulates development, metabolism and life span (Houthoofd and Vanfleteren 2007; Artal-Sanz and Tavernarakis 2008). For instance, this system performs the task to shift the worm from the metabolically active reproductive mode to the non-reproducing, non-feeding dauer larva upon e.g. perturbed food availability or temperature. For aging studies it is therefore of major importance to distinguish longer life span as a cause of prolonged adult stage or as a cause of entering the dauer diapause. Comparable to yeast, the aging of *C. elegans* is evaluated by the mean life span of the investigated cohort of animals. Due to this investigation method, the aging of different tissue types of the worm is not highlighted although it is in contrast to yeast a complex animal. However, these life span studies in *C. elegans* revealed some mechanisms involved in extended life span of the worm, which are for instance low temperature, the insulin signaling pathway, caloric or dietary restriction, mitochondrial dynamics, and protein synthesis (Curran and Ruvkun 2007; Houthoofd and Vanfleteren 2007; Artal-Sanz and Tavernarakis 2008). Additionally, chronological aging in C. elegans has been investigated by comparing gene expression in worms of different ages using microarrays showing comparable results to the life span studies (Lund et al. 2002; Golden and Melov 2004).

D. melanogaster

The life expectancy of the fruit fly *D. melanogaster* is relatively short (3months) compared to mammals, which is beneficial for aging research using this model. In addition, *D. melanogaster* exhibits an interesting feature. The life history of the fly is

divided into distinct morphological stages – the embryo, larval, and pupae stages where growth and development take place, and the mature adult stage, which is used for aging studies. The adult stage is almost entirely post-mitotic making aging research in *D. melanogaster* a viable tool for investigating solely post-mitotic aging features (Helfand and Rogina 2003). Life span studies in fruit fly mutants for example only measure expanded adult stages and do not take into account a prolonged larval or pupae stage, which may be comparable to the dauer diapause of *C.elegans*. Consequentially, like in yeast and nematodes, aging of the fruit fly is again evaluated by the mean life span of a cohort of animals. These studies revealed some non-genetic mechanisms regulating the life span of *D. melanogaster* which are mild stressors, ambient temperature, physical activity, the reproductive status, and the dietary status, and genetic mechanisms including antioxidant enzymes, the insulin signaling pathway, repair mechanisms, and chromatin structure (Helfand and Rogina 2003). Additionally, like in C. elegans, gene expression studies (Pletcher et al. 2002; Landis et al. 2004; Kim et al. 2005; Girardot et al. 2006) of different aged flies are performed and, in addition to the studies in the nematode, different parts of the fly are investigated separately such as head.

M. musculus

Due to the longer life expectancy of mice (2-3years) compared to yeast, nematodes and flies, investigations of prolonged life span are rare in *M. musculus*. However, some long-lived mutant mouse models exist (Brown-Borg et al. 1996; Flurkey et al. 2001; Liang et al. 2003) and are of interest in aging research (Amador-Noguez et al. 2004). Most of these long-lived mutant mice exhibit knockouts in insulin signaling-related genes. Additionally, treatments such as dietary restriction (DR) are tested for their life expanding feature (Fernandes et al. 1976), and at least the life prolonging effect of DR could be confirmed in mice. In contrast to the above described model systems, it is quite easy to extract different organs and even various cell types from the same organ from mice. An additional advantage of the mouse model compared to the other animal models is that aging processes in the mouse are more comparable to that of human. Therefore, the number of studies investigating changes in genome-wide gene expression of different aged mice in a variety of organs and tissues constantly increases (Lee et al. 1999; Lee et al. 2000; Cao et al. 2001; Jiang et al. 2001; Amador-Noguez et al. 2004; Bahar et al. 2006; Chelvarajan et al. 2006; Dhahbi et al. 2006; Fu et al. 2006; Higami et al. 2006; Edwards et al. 2007; Misra et al. 2007; Zahn et al. 2007). The results of these

studies are very heterogeneous, which makes it difficult to correlate the findings. The study of Zahn et al. (2007) investigated and compared the aging of 16 different mouse tissues. But even this fairly comprehensive comparison showed minor overlaps of genetic regulation between different tissues.

H. sapiens

Humans exhibit a maximum life expectancy of more than 100 years and the possibilities to do life span studies are of course minor. However, the fact that the rate of mortality of humans increases until age 90, but reaches a plateau for age 90+ makes this group of very old humans an interesting example for human longevity. In addition, most of these people overcome a variety of age-related diseases also indicating their increased probability for increased longevity or life span. This group of long-lived humans is used in a variety of studies to investigate human longevity in order to analyse the aging process (Franceschi et al. 2007). Interestingly, for instance polymorphic variants of sirtuin 3 (SIRT3), v-Ha-ras Harvey rat sarcoma viral oncogene homolog 1 (HRAS1), insulin-like growth factor 2 (IGF2), insulin (INS), and tyrosine hydroxylase (TH) are associated with human longevity. It is important to remember that these genes are the human homologues of genes that appear to play an important role in life-span extension in the animal models.

In contrast to the animal model systems, whole genome gene expression analyses in human have some drawbacks, which concern mainly the accessibility of samples. Normally, samples are collected during surgery or upon death of a patient in a hospital, which leads to non-standardized conditions between samples. Another drawback especially for aging studies is the variance in the age of patients and in their way of living. Concerning the age, aging studies in human either compare various patients of varying ages and calculate an age coefficient for e.g. the expression of a certain gene or compare different age groups to calculate e.g. expression ratios but these groups then exhibit a variance of several years. Nevertheless, many gene expression arrays have been performed to investigate human aging (Lu et al. 2004; Rodwell et al. 2004; Welle et al. 2004; Fraser et al. 2005; Giresi et al. 2005; Melk et al. 2005; Segev et al. 2005; Tan et al. 2005; Lener et al. 2006; Zahn et al. 2006). Comparable to the mouse studies, the results of these studies are very heterogeneous. However, results of the human and mouse whole genome gene expression studies will be discussed and compared in some detail in chapter *1.2.3 Gene expression microarrays and aging*.

As most studies independent of the model system used, are driven by the quest to understand the nature of human aging it is of major interest to find evolutionary conserved age-related processes (Warner 2005; Lepperdinger et al. 2008). In the still quite young field of aging genetics, three processes were found to date that seem to be evolutionary conserved across distant species. These are the histone deacetylases rpd3/Sir2 pathway, which plays at least a role in yeast, nematode and fly longevity, and the insulin/IGF-like signaling pathway and dietary restriction, which are additionally shown to be involved in the aging process of mammals (Helfand and Rogina 2003; Houthoofd and Vanfleteren 2007; Kaeberlein et al. 2007).

1.1.3 Human skin aging

The human aging studies in this work are focused on skin aging. Therefore, the special features of skin aging will be highlighted in the following paragraphs.

With age, human skin becomes wrinkled up, saggy and its laxity increases. The reasons for these obvious changes can be attributed to both biological and environmental factors. Therefore, skin aging research is divided in intrinsic and extrinsic skin aging (Jenkins 2002; Yaar et al. 2002).

Extrinsic skin aging

Extrinsic skin aging describes the aging caused by external influences (Marionnet et al. 2003). It is mostly caused by exposure to sunlight. UV radiation in sunlight damages the cells and leads to an altered expression of different genes. Photo-damaged skin is characterized by some typical changes like a loss of elasticity, increased roughness, dryness, irregular pigmentation and deep wrinkling (Jenkins 2002; Yaar et al. 2002). The visible changes in skin structure and function can be attributed mostly to changes of the extracellular components, which are collagen fibres, the elastic fibre network and glycosaminoglycans (Jenkins 2002). However, extrinsic skin aging just superimposes underlying processes and can therefore not be described without implicating intrinsic skin aging.

Intrinsic skin aging

Intrinsic or endogenous skin aging is caused by genetics, hormonal and metabolic processes (Rittie and Fisher 2002). The skin loses its structural und functional characteristics. The thickness of epidermis decreases by 10-50% and a clear flattening of the dermal-epidermal junction occurs resulting in a decrease of contact by approximately 35% (Moragas et al. 1993). Melanocytes and Langerhans cells decrease and undergo morphological alterations (Wulf et al. 2004). In addition, a general atrophy of the extracellular matrix appears, accompanied by a decrease in cellularity especially of the fibroblasts (Varani et al. 2001). There are reduced levels and disintegration of collagen and elastic fibres (Braverman and Fonferko 1982a). The vessels become abnormally thin (Braverman and Fonferko 1982b) and the subcutaneous fat atrophies as well. As a result, the skin appears thin, finely wrinkled, smooth, dry, unblemished, sallow and pale, with some loss of elasticity.

1.2 Whole genome microarray analyses

1.2.1 Molecular methods employed for gene expression analyses

Whole genome cDNA and messenger RNA amplification from limited number of cells depend on both whole genome PCR (Adjaye et al. 2005) and RNA polymerase amplification (Wang et al. 2000). However, there are significant limitations and shortcomings in cDNA and mRNA amplification technologies that should be kept in mind when designing studies that depend on these technologies.

In both cases the two main concerns are: (i) the representation of all transcripts present in the starting material in the final amplified material (i.e. loss of transcripts) and (ii) the preservation of the relative abundances of the different transcripts. Many amplification technologies have a normalizing effect on transcript abundance that becomes particularly noticeable with increasing amplification. To correct this in a study, it is important that comparing material is prepared using the same method and independently verified by semi-quantitative PCR or Real-Time PCR.

A limitation of cDNA microarray technology is the large amount of total RNA (20-50µg) required to produce an adequate signal. This is a particular issue with low-

abundance transcripts. For targets derived from samples offering just a few cells, some form of amplification process needs to be incorporated into the procedure. The ability to apply expression profiling to smaller samples including single cells would be beneficial for both basic research and clinical molecular diagnostics. However, since the total RNA content of a single mammalian cell is in the range 20-40pg and only 0.5-1.0pg of this is mRNA, any attempt at single cell profiling must be capable of dealing with a total of 10^5-10^6 mRNA molecules. Therefore amplification is unavoidable. In the last years, commercial available arrays and protocols were introduced, e.g. (Lockhart et al. 1996; Kuhn et al. 2004), which include amplification steps in the standard protocols.

1.2.2 Advantages and disadvantages of whole genome studies

The strength of whole genome gene expression studies is obviously the ability to compare the global expression patterns of different samples, for instance investigating the gene expression of different cell types or organs, changes in gene expression due to a treatment or gene knockout, or simply due to a period of time – aging. Data on whole genome gene expression changes enable the examination of patterns of regulation, which are hard to discover by investigating the expression of a single gene or a certain group of genes. Therefore, whole genome studies provide a first insight to understand complex biological processes.

But, the design, execution, and analysis of these studies are nontrivial (Page et al. 2007). Single gene studies are mostly hypothesis driven which implies that the researcher has a certain expectation. Whole genome studies, however, investigate many to all genes expressed in the sample, which leads to a high amount of results that is produced without background knowledge of the researcher. Without the use of statistical methods analysing these data it could be interpreted with the bias of the researchers interest (Page et al. 2007). Additionally, changes in gene expression of many of the investigated genes are minor, null, or the gene might be perturbed by an input other than the investigated question making those genes susceptible to technical differences (Page et al. 2007). Ultimately, findings achieved by microarray analyses have to be independently confirmed by robust methods like for instance Real-Time PCR (Vanguilder et al. 2008).

1.2.3 Gene expression microarrays and aging

Aging-related studies using the strength of whole genome microarrays constantly emerge since the first microarray-based studies were published in the late 90's. In the following paragraphs, of those, studies investigating the aging process in mouse and human will be shortly highlighted and discussed.

In mice, the first transcriptional profiles were generated in a limited number of mouse tissues such as muscle (Lee et al. 1999) and brain (Lee et al. 2000). Since then, transcriptional profiles of diverse organs and cells such as liver (Cao et al. 2001; Amador-Noguez et al. 2004; Fu et al. 2006), brain (Jiang et al. 2001; Fu et al. 2006), cardiomyocytes (Bahar et al. 2006), macrophages (Chelvarajan et al. 2006), heart (Dhahbi et al. 2006; Fu et al. 2006), adipose tissue (Higami et al. 2006), skeletal muscle (Edwards et al. 2007), and lungs (Misra et al. 2007) have been studied. In all of these studies, various tissues derived from mice of varying ages and strains were analysed on varying platforms. A consequence of this is the noticeable differential expression in age-regulated target genes. Nonetheless, there is conservation of common biological processes related to aging, independent of tissue, strain, array platform etc. These processes include stress/immune responses, cell cycle, and different metabolisms (e.g. energy, protein). A recent study (Zahn et al. 2007) now investigated and compared the transcriptional aging profiles of 16 mouse tissues, including adrenals, bone marrow, cerebellum, cerebrum, eye, gonads, heart, hippocampus, kidney, liver, lung, muscle, spinal cord, spleen, striatum, and thymus. Although this study eliminated many possible sources of error the overlap of conserved age-related processes did not increase.

In human, despite the already mentioned difficulties associated with the execution of these studies, numerous studies have been conducted, investigating aging in brain (Lu et al. 2004; Fraser et al. 2005), blood (Tan et al. 2005), eye (Segev et al. 2005), kidney (Rodwell et al. 2004; Melk et al. 2005), muscle (Welle et al. 2004; Giresi et al. 2005; Zahn et al. 2006), and skin (Lener et al. 2006). In contrast to mouse, some of the human studies lack in presenting possible age-related processes. However, the available data suggests that stress/immune responses, cell cycle, and metabolism are conserved.

In addition to biological similarities, the above-described studies reveal an important aspect regarding gene expression microarrays and aging. Changes in gene expression on the transcriptional level are quite small during the aging process

compared to other biological questions. For instance, a ratio cut-off for transcriptional regulation set to 2-fold normally leads to a list of less than 100 significantly age-regulated genes. Therefore, some of the discussed studies set their cut-offs to smaller ratios or they only calculated statistical significant regulation for target genes, which can lead to significant ratios close to 1. This leads to higher numbers of age-regulated target genes of some hundreds to more than a thousand.

1.3 Aim of this work

The study is aimed at investigating the aging process by the use of whole genome microarray analyses. The main focus is to understand the molecular and signal transduction mechanisms involved in endogenous human skin aging by performing microarray studies on:

- Intrinsic skin-aging models using hormone-treated sebocytes and skin fibroblasts corresponding to females of 20 and 60 years of life.
- Human skin biopsies of young (18-30 years) and old (65-95 years) males and females.

In addition, the transcriptional profiles of young (8-10 weeks) and aged (17-19 months) mice will be investigated in brain, heart, and kidney in order to find potentially conserved mechanisms in mammalian aging.

The array-derived data will be analysed for the regulation of single target genes, GO-annotated biological processes and cellular compartments, and Kegg-annotated pathways.

The changes in gene expression of selected genes will be validated by Real-Time PCR and the correlation of corresponding protein expression will be tested by Western blotting for a relevant gene. Additionally, age-related changes in the level of radical oxygen species (ROS) will be determined by measuring the lipid hydroperoxidation in the mouse tissues, and sections of mouse tissues will be prepared to search for obvious structural alterations between the young and aged mice.

2. Material and Methods

2.1 Model systems

2.1.1 Cell cultures

To understand the molecular mechanisms of endogenous skin aging and the influence of hormones, human SZ95 sebocyte cells and human skin fibroblasts were maintained at hormone-substituted defined conditions, which correspond to average serum levels for females and males from 0 to 60 years of life (Zouboulis 2000). Three hours in culture represent one year of life, whereas hormone levels were kept unchanged at the level of 20 years in control experiments. Detailed information on the performed cell culture was published before (Makrantonaki et al. 2006). RNA samples used corresponded to the following; female 20 years (F20), female 60 years (F60), and untreated cells as control (C).

The immortalized human sebocyte line SZ95 was established and characterized. It shows a stable morphologic, phenotypic and functional characteristic of normal human sebocytes (Zouboulis et al. 1999).

2.1.2 Human skin biopsies

Prof. Dr. Zouboulis (Hautklinik und Immunologisches Zentrum, Städtisches Klinikum Dessau) collected skin biopsies from patients of different ages and gender with approval of the ethics commission. The biopsies were taken from the sun-protected inner side of the upper arm to avoid extrinsic skin aging phenotypes. Patients were grouped into four groups - young males, old males, young females and old females. Altogether, 7 biopsies of each group were collected except for old females where just 5 were collected. The ages within the groups varied for young males between 18 and 32 years, for old males between 73 and 97 years, for young females between 18 and 30 years and for old females between 67 and 74 years of life.

2.1.3 Mice

Healthy wild-type female C57BL6 mice were housed in a room with controlled photoperiod and temperature. Animals were given free access to water and pelleted diet. Mice were sacrificed by cervical dislocation; tissues were collected and either flash frozen in liquid nitrogen and stored at -80°C or placed in 1x phosphate buffered saline (PBS) with 4% paraformaldehyde (PFA) over night at 4°C for preparing sections. Brain, heart and kidney were first collected from 10 young (10-12 weeks) and 9 aged (~14 months) mice on two different days without synchronizing the exact daytime. Afterwards the same tissues were collected from another 10 young (8-10 weeks) and 11 aged (17-19 months) mice. This time all mice were sacrificed at the same day alternating young and aged mice.

In a follow-up experiment heart and kidney were collected at 3 different time points during one day (12a.m., 8a.m. and 4p.m.) to investigate the impact of changes in gene expression in a 24hrs period. Two biological replicates per time point were collected.

2.2 RNA analyses

2.2.1 Total RNA isolation

All methods used for tissue homogenization and RNA isolation resulted in good quality total RNA (see *3.1.2 RNA quality control*). Below the methods used are described. All RNA samples were stored in a freezer at -80°C.

Using the NucleoSpin® RNA/Protein Kit

Whole mouse tissues (brain, heart and kidney) were homogenized in 350µl buffer RP1 (Macherey-Nagel, Düren, Germany) and 3.5µl β-mercaptoethanol (Merck, Darmstadt, Germany) using the TissueLyser and 5mm Stainless Steel Beads (Qiagen, Hilden, Germany) and homogenising 2 times for 30s and with a frequency of 30/s. The RNA isolation from the homogenates was performed using the NucleoSpin® RNA/Protein Kit (Macherey-Nagel) and following the manufacturers protocol.

Using Trizol and the RNeasy® Mini Kit

Whole mouse tissues (brain, heart and kidney) were homogenized in 1ml Trizol (Invitrogen, Carlsbad, CA, USA) using the TissueLyser and 5mm Stainless Steel Beads (Qiagen) and homogenising 2 times for 1min with a frequency of 30/s. Homogenized samples were then incubated for 5min at room temperature (RT). After addition of 200µl chloroform, vortex mixing, incubation for 2min at RT and centrifugation with 12000g at 4°C for 15min the water phase was transferred to a new tube. 500µl isopropanol were added and the mixture was incubated for 10min at RT and afterwards centrifuged with 8000g at 4°C for 5min. The supernatant was discarded and the pellet washed with 1ml of 75% ethanol, vortexed, and centrifuged with 8000g at 4°C for 5min. The supernatant was then discarded again and the pellet was air dried for 10min and afterwards re-suspended in 100µl RNase-free water (dH_2O) by pipetting up and down and centrifugation with 3000g at 4°C for 4min.

100µg Trizol-extracted RNA in a volume of 100µl was then purified with the RNeasy® Mini Kit (Qiagen). The procedure was performed following the manufacturers protocol including the also described DNase I on column treatment step to get rid of trace amounts of genomic DNA.

Using the RNeasy® Mini Kit

Human skin biopsies were homogenized in ~400µl of RLT buffer (Qiagen) using the Polytron PT3000 with a Polytron-Aggregate® homogenizer (Kinematika, Littau, Switzerland). The homogenizer was sequentially pre-treated with 3% H_2O_2 (Merck), 70% ethanol and dH_2O to get rid of possible RNase contamination. Each sample was homogenized for 1min then cooled on ice for 1min and again homogenized for 1min. After each sample the homogenizer was washed by treatment with dH_2O, 70% ethanol and dH_2O sequentially.

RNA isolation from the homogenates was performed using the RNeasy® Mini Kit (Qiagen) including DNase I on column treatment to get rid of trace amounts of genomic DNA following the manufacturers protocol.

2.2.2 RNA and cDNA quantification

The quantity of RNA and DNA was determined using the NanoDrop (NanoDrop Technologies, Wilmington, DE, USA). 1µl of sample was applied to the NanoDrop and

measured. If the concentration exceeded measurable values the samples were either concentrated by speed vac centrifugation or diluted by adding dH_2O, respectively.

2.2.3 Agarose gel electrophoresis

Agarose gel electrophoresis and ethidium bromide staining enabled the visualizing of RNA and DNA for quality control. By mixing 0.5-1.5g of agarose (Life Technologies, Paisley, Scotland) and 50ml of 1x TAE, gels of 1-3% were obtained. 1µl of ethidium bromide (10mg/ml; Invitrogen) was added directly to the gel and mixed before solidifying. To assign the length of the amplicons the GeneRuler^{TM} 1kb DNA ladder (Fermentas, St. Leon-Rot, Germany) was used. Prior to loading of samples, a third of the volume of 6x loading buffer (Fermentas) was added to the samples. Gels were run in an electrophoresis chamber with 50V for 30 to 60min. Nucleotides were visualized with UV light using the AlphaImager^{TM} (Alpha Innotech, San Leandro, CA, USA).

2.2.4 Reverse transcription

Using Superscript II

For reverse transcription using Superscript II (Invitrogen), 1.0µl (1µg/µl) RNA was added to 1.0µl of 50µM Oligo-dT primer plus 8.0µl of dH_2O. The mixture was spun briefly, heated to 70°C for 5min and cooled on ice. 10.0µl of master mix were added including the following components per reaction: 4.0µl of 5x RT buffer, 2.0µl of 0.1M DTT, 2.0µl of (10mM) dNTP, 1.0µl (200U/µl) Superscript II and 1.0µl of dH_2O. After pulse spinning, incubation was carried out at 42°C for 1.5hrs.

Using M-MLV reverse transcriptase

For reverse transcription using M-MLV reverse transcriptase (Promega, Madison, WI, USA), 2.0µl (1µg/µl) RNA was added to 0.5µl of Oligo-dT primer (1µg/µl; Invitek, Berlin, Germany) plus 7.5µl of dH_2O. The mixture was spun briefly, heated to 70°C for 3min and cooled on ice. 15.0µl of master mix were added including the following components per reaction: 5.0µl of 5x reaction buffer (Promega), 0.5µl of (25mM) dNTP, 0.1µl of M-MLV reverse transcriptase (200U/µl; Promega) and 9.4µl of dH_2O. After pulse spinning, incubation was carried out at 42°C for 1hr and then stopped at 65°C for 10min.

2.2.5 Real-time polymerase chain reaction (Real-Time PCR)

Real-Time PCR was performed in 96-Well Optical Reaction Plates (Applied Biosystems, Foster City, CA, United States). The PCR mix in each well included 10µl of SYBR®Green PCR Master Mix (Applied Biosystems), 5µl dH_2O, 1.5µl each of the forward and reverse primers (5pmol/µl; Invitek) and 2µl of single strand cDNA (2.5ng/µl) in a final reaction volume of 20µl. Triplicate amplifications were carried out per gene with three wells as negative controls without template. *GAPDH* and *ACTB* were amplified along with the target genes as endogenous controls for normalization. The PCR reaction was carried out on the ABI PRISM 7900HT Sequence Detection System (Applied Biosystems) using the following program, stage 1: 50°C for 2min, stage 2: 95°C for 10min, stage 3: 95°C for 15s and 60°C for 1min, for 40 cycles and, stage 4: 95°C for 15s, 60°C for 15s and 95°C for 15s. The last heating step in stage 4 was performed with a ramp rate of 2% in order to enable the generation of a dissociation curve of the product.

The output data generated by the Sequence Detection System 2 software were transferred to Excel (Microsoft, Redmond, WA, USA) for analysis. The differential mRNA expression of each gene was calculated with the comparative Ct (threshold cycle) method recommended by the manufacturer.

2.2.6 ENSEMBL chip hybridisation

The ENSEMBL chip was previously described (Adjaye et al. 2004). Three independent labelling reactions per aRNA sample derived from a T7-RNA amplification approach were carried out using 6µg aRNA per reaction. ENSEMBL chip hybridisation was performed for sebocytes (F20, F60 and C) and for fibroblasts (F20, F60 and C).

Labelling reaction

Direct incorporation of Cy3 during reverse transcription was carried out in a 20µl reaction volume using 1µg of a random hexamer primer. The RNA/primer mix was incubated at 70°C for 5min, held at room temperature for 10min and then cooled on ice for 2min. The following reagents were then added: 4µl first-strand buffer, 2µl 0.1M DTT, 0.5µl dNTP mix (25mM for each of dATP, dGTP, dCTP and 10mM dTTP), 1µl of 1.0mM Cy3-dUTP (Amersham, Piscataway, NJ, USA) and 1µl (200U/µl) Superscript

II (Invitrogen). The labelling reaction was carried out at 42°C for 1.5hrs and stopped with 4µl of 0.5M EDTA. The input RNA was hydrolysed by the addition of 2µl of 2.5M NaOH and incubated at 37°C for 15min followed by neutralization with 10µl HEPES free acid (2M, pH5.5). Labelled cDNAs (three replicates per treatment) were purified from unincorporated Cy-dyes using Microcon YM-30 purification columns (Millipore, Billerica, MA, USA). All labelled cDNAs were routinely analysed on a Fuji scanner (FL8-8000) to ascertain dye incorporation and the size-range of cDNAs. After concentrating cDNAs by evaporation in a Speedvac, labelled targets were re-suspended in 20µl of hybridisation buffer (10µg polydA and 20µg Human Cot1 DNA, Invitrogen; DIG-Easy Hybridisation mix, Roche, Mannhein, Germany).

Sample hybridisation

After thorough re-suspension, the cDNA was denatured by heating at 95°C for 5min followed by 20min at 42°C to enable the blocking reagents to anneal to repetitive sequences within the target cDNAs. The hybridisation mixture was placed on the blocked array under a 24x60mm coverslip (Menzel-Gläser, Braunschweig, Germany). To maintain humidity inside the chamber, 20µl of 3x SSC was added to the reservoir wells. The chamber was then tightly sealed and slides were incubated at 42°C for 18hrs in a water bath. Slides were washed twice in 0.2x SSC/0.1% SDS and then twice in 0.2x SSC. Washes were carried out at room temperature with 10min durations per wash. Finally, the slides were dried by centrifugation at 1100rpm for 10min. Fluorescence images were captured using an Affymetrix 428 scanner (Affymetrix, Santa Clara, CA, USA) with appropriate gains on the photo multiplier tube to obtain the highest intensity without saturation.

Data analysis

A 16-bit TIFF image was generated for each channel for image analyses. Image analysis was carried out by placing the centre of each spot manually (grid-finding step) using the software AIDA (Raytest, Straubenhardt, Germany) and then by quantifying in a pre-defined neighbourhood around this spot centre using a two-dimensional Gaussian distribution (quantification step). In order to verify whether a given gene was significantly expressed, its signal was compared to a signal distribution derived from negative controls. In the array design, ~3,362 empty spot positions were distributed on the array. After quantification, a small, non-zero intensity was assigned to each empty

spot reflecting the amount of background signal on the array. Since these positions were spread uniformly over the array, the distribution of signals reflects a global background distribution for the experiment and indicates if cDNA signals were at or above the background level of expression. For each cDNA, the relative proportion of empty positions on the array was counted that were smaller than the observed intensity (background-tag, BG). Background-tags from replicated experiments for the same cDNA were averaged. Thus, high values (close to one) indicated that the cDNA was expressed in the sample tested whereas low values reflected noise. cDNAs were considered 'expressed' when their average background-tag was above 0.9, a threshold consistent with the limit of visual detection of the spots.

2.2.7 Illumina bead chip hybridisation

Biotin-labelled cRNA was produced by means of a linear amplification kit (Ambion, Austin, TX, USA) using 300ng of quality-checked total RNA as input. Chip hybridisations, washing, Cy3-streptavidin staining, and scanning were performed on an Illumina BeadStation 500 platform (Illumina, San Diego, CA, USA) using reagents and following protocols supplied by the manufacturer. cRNA samples were hybridised on Illumina mouse-6 (different mouse tissues) and human-8 (human skin biopsies) BeadChips. The following samples were hybridised in biological triplicate; synchronised young and aged mouse tissues and human skin biopsies, and in biological duplicate; unsynchronised young and aged mouse tissues and kidneys collected at three different time points within a 24hrs period. All basic expression data analysis was carried out using the manufacturers software BeadStudio 1.0 (Illumina). Raw data were background-subtracted and normalised using the 'rank invariant' algorithm, by which negative intensity values may arise. Normalized data were then filtered for significant expression on the basis of negative control beads. Selection for differentially expressed genes was performed on the basis of arbitrary thresholds for fold changes plus statistical significance according to an Illumina custom model (Kuhn et al. 2004).

2.2.8 Pathway analysis

Differentially expressed genes were further filtered according to Gene Ontology (GO) terms or mapped to KEGG pathways using DAVID (http://david.abcc.ncifcrf.gov) and FatiGO+ (http://babelomics.bioinfo.cipf.es/fatigoplus/cgi-bin/fatigoplus.cgi). For analysis, Entrez Gene IDs (ENSEMBL data) or GenBank accession numbers (Illumina data) represented by the corresponding chip oligonucleotides were used as input. DAVID is very useful in identifying significant pathways and GOs, whereas FatiGO+ was used to visualize regulated genes in significant regulated pathways by analysing up- and down-regulated genes in parallel. Figure 2.1 shows a typical output from FatiGO+ and DAVID analyses used for this work.

A

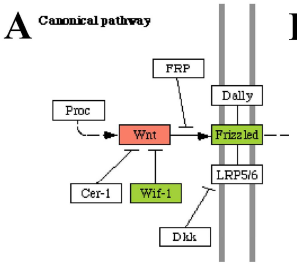

B

Category	Term	Count	%	PValue
GOTERM_CC_ALL	cytoplasm	82	25.71%	2.2E-05
GOTERM_CC_ALL	intracellular	146	45.77%	1.4E-04
GOTERM_CC_ALL	membrane-bound organelle	115	36.05%	2.3E-04
GOTERM_CC_ALL	intracellular membrane-bound organelle	114	35.74%	3.4E-04
GOTERM_CC_ALL	organelle	126	39.50%	5.1E-04
GOTERM_CC_ALL	intracellular organelle	125	39.18%	7.6E-04
GOTERM_CC_ALL	endoplasmic reticulum	19	5.96%	1.4E-03
GOTERM_CC_ALL	early endosome	4	1.25%	7.9E-03
GOTERM_CC_ALL	endosome	6	1.88%	1.1E-02
GOTERM_CC_ALL	cytosol	11	3.45%	3.8E-02
GOTERM_CC_ALL	extracellular region	49	15.36%	5.8E-02
GOTERM_CC_ALL	mitochondrion	20	6.27%	6.4E-02
GOTERM_CC_ALL	MHC protein complex	4	1.25%	6.7E-02

Figure 2.1 Sample output of pathway and GO analyses.

The figure shows typical output results of the (A) FatiGO+ and (B) DAVID analyses. The FatiGO+ output shows in part a Kegg pathway, where genes with significantly increased expression with age are coloured in red, genes with decreased expression in green and other genes stay uncoloured. The DAVID output shows as an example the result for significantly regulated GOs cellular compartment. The count is the number of genes annotated for the corresponding term in the target gene list, the percentage indicates the same number as the percent of input genes and the PValue reveals the significance of the finding.

2.3 Protein analyses

2.3.1 Protein isolation

Whole mouse tissues were homogenized in 500µl lysis buffer (25% glycerol, 0.42M NaCl, 1.5mM $MgCl_2$, 0.2mM EDTA, 20mM HEPES) and with addition of 5µl protease inhibitor using the TissueLyser and 5mm Stainless Steel Beads (Qiagen) and

homogenising 2 times for 1min and with a frequency of 30/s. After addition of another 5µl protease inhibitor homogenized samples were kept over night at -80°C. Samples were then mixed thoroughly by vortexing 4 times for 20s and cooling on ice for 10-15min after each step. Afterwards samples were centrifuged with 12000g at 4°C for 15min. The supernatant was then transferred to a fresh tube and stored at -80°C.

2.3.2 Protein quantification (Bradford)

Protein samples were quantified using the Bradford method. 10x bovine serum albumin (BSA, 1µg/µl; Sigma-Aldrich, Munich, Germany) was used as a standard and the samples were diluted 1:5 in 1x PBS before use in the assay. Standards and samples were brought to 50µl by adding dH_2O. For the samples 1µl of sample was mixed with 49µl of dH_2O. The standards were mixed in 7 different dilutions to enable a standard curve. The volume of 10x BSA was 0, 2, 4, 6, 8, 10 and 12µl mixed with the volume of dH_2O needed to get the final volume of 50µl. Bradford solution (Bio-Rad Protein Assay; Bio-Rad, Hercules, CA, USA) was diluted 1:5 with 1x PBS and 950µl of the diluted Bradford solution were added to each standard and sample. The mixtures were incubated with light for 5min at RT. Afterwards they were transferred to 1ml cuvettes (Sarstedt, Nümbrecht, Germany) and measured using the Ultrospec 3100 pro (GE Heathcare, Munich, Germany) and the Bradford programme provided by the photometer.

2.3.3 SDS-PAGE gel electrophoresis

Protein gels were poured in Bio-Rad protein chambers. To get good separation for the target protein a 10% gel was used. A 10% resolving gel was prepared by sequentially adding 2.45ml of dH_2O, 1.25ml of resolving buffer (see appendix I), 50µl of 10% SDS, 1.25ml of 40% acrylamid (Rotiphorese® Gel 40; Carl Roth, Karlsruhe, Germany), 25µl APS (Ammoniumperoxodisulfate; Carl Roth) and 2.5µl TEMED (Carl Roth) followed by well mixing and transfer to the chamber. For the time of solidifying, the gel was covered with isopropanol to get an even edge. After solidifying the isopropanol was discarded and a 5% stacking gel was prepared by sequentially adding 1.5ml of dH_2O, 0.6ml of stacking buffer (see appendix I), 25µl of 10% SDS, 0.3ml of 40% acrylamid,

25µl APS and 5µl TEMED followed by well mixing, transfer to the chamber and applying a comb.

21µg of protein were loaded by mixing 7µl of protein (~3µg/µl) with 3.5µl of 3x loading buffer (see appendix I). Prior use genomic DNA in the protein samples was disrupted by pipetting up and down 5 times with a BD Microlance™ 3 injection needle (Becton Dickinson, Madrid, Spain). The samples and 10µl prestained protein marker (New England Biolabs, Beverly, MA, USA) were heated to 95°C for 5min and afterwards cooled on ice for 1min before loading. The gel was run in 1x running buffer (see appendix I) with 110V until the loading buffer front did pass the whole gel. Gels were then used for western blotting.

2.3.4 Western blotting

Proteins were transferred from the gel to an Amersham Hybond™ ECL™ nitrocellulose membrane (GE Helthcare) by building up a blot in the following order; filter paper, membrane, gel, filter paper. The blot was then covered with cellular material from both sides and placed in the transfer chamber (Bio-Rad). The blot was run in ice cooled 1x transfer buffer (see appendix II) with a constant 350mA for 1hr. After blotting the protein quality was checked by Ponceau Red staining of the membrane using Ponceau S Solution (Sigma-Aldrich). The membrane was shortly washed with dH_2O and then blocked with blocking solution (see appendix II) by shaking for 5min at RT and then over night at 4°C.

After short washing with 1xTBST primary antibody was applied to the membrane by shaking 1hr at RT in 0.5gBSA dissolved in 10ml 1x TBST plus 2µl primary antibody. Afterwards the membrane was again shortly washed with 1x TBST and then extensively washed by shaking 4 times for 5min in 1x TBST. The secondary antibody was then applied by shaking 1hr at RT in 10ml blocking solution plus 2µl secondary antibody. Afterwards the membrane was again shortly washed with 1x TBST and then extensively washed by shaking 4 times for 5min in 1x TBST.

250µl of detection reagent 1 and 250µl of detection reagent 2 (GE Healthcare) were mixed in a tube and kept in the dark until use. The membrane was placed on foil and the mixture was dispensed on the membrane. The membrane was directly covered with foil by avoiding air bubbles and incubated for 1min. The liquid was then disposed from the membrane and the membrane was placed in a Hypercassette™ (Amersham). In

a dark room BioMAx XAR film (Kodak, Stuttgart, Germany) was exposed for 20-60s to the membrane and directly developed using the Curix 60 develop maschine (Agfa, Cologne, Germany).

2.4 Metabolite analyses

2.4.1 Lipid hydroperoxide (LPO) measurement

Lipid hydroperoxides were extracted from biological duplicates of young and aged mouse brain, heart and kidney using the Lipid Hydroperoxide (LPO) Assay Kit (Calbiochem, Merck) - following the manufacturers protocol. Whole tissues were homogenized in 500µl dH_2O using the TissueLyser and 5mm Stainless Steel Beads (Qiagen) and homogenising 2 times for 1min and with a frequency of 30/s. After completion of the protocol the absorbance at 500nm of each standard and sample was measured using the Ultrospec 3100 pro (GE Heathcare) and Chloroform:Methanol mixture as a blank. Results were calculated using a standard curve of the standards measured as indicated by the manufacturer.

2.5 Histology

2.5.1 Section preparation

Freshly sampled mouse tissues (brain, heart, and kidney) were fixed in 1x PBS with 4% PFA over night at 4°C. Tissues were then washed 2 times for 10min in 1x PBS at RT. An ascending alcohol series was performed to extract water from the tissues. The single steps were 1hr in 25% ethanol in 1x PBS, 1hr in 50% ethanol in 1x PBS and 1hr in 70% ethanol in dH_2O. The tissues were stored for 1 week maximum at 4°C.

Tissues were embedded in paraffin (Leica Microsystems, Wetzlar, Germany) using the semi-enclosed tissue processor TP1020 (Leica Microsystems). The used programme included the following steps:

1. 90% ethanol	2hrs
2. 95% ethanol	2hrs
3. 100% ethanol	2hrs
4. 100% ethanol	2hrs
5. 100% ethanol	2hrs
6. UltraClear (J.T. Baker, Griesheim, Germany)	15min
7. UltraClear	15min
8. UltraClear	30min
9. UltraClear + paraffin (1:1)	3hrs
10. Paraffin	3hrs

Steps 3-10 were carried out under vacuum for brain and kidney and without vacuum for heart. The final embedment in paraffin was performed using the EC 350 paraffin embedding center (Microm, Walldorf, Germany). The solidified paraffin-embedded tissues were then stored at 4°C. Tissues were cut with a thickness of 5µm using the HM 355 S electronic motorised microtome (Microm) and placed on SuperFrost® Plus glass slides (Menzel-Gläser). The sections were air dried at 37°C over night and afterwards stored at 4°C.

2.5.2 Hematoxylin Eosin staining

Tissue sections were stained at RT with hematoxylin (Microm) and eosin-Y (Microm) using glass cuvettes for all steps. To get rid of the paraffin the slides were incubated for 20min in UltraClear. Afterwards a descending alcohol series was performed including the following steps:

1. 100% ethanol	5min
2. 90% ethanol	5min
3. 70% ethanol	5min
4. dH_2O	5min

The slides were then stained with hematoxylin for 3min followed by a short wash in tap water. Afterwards slides were washed in constantly flowing tap water for 10min in which the water was completely poured away several times. After a short wash in dH_2O

the slides were stained with eosin-Y for 3min and then again shortly washed in dH_2O. For conservation performing an ascending alcohol series dehydrated the slides including the following steps:

1. 70% ethanol	5min
2. 90% ethanol	5min
3. 100% ethanol	5min
4. UltraClear	5min
5. UltraClear	5min

Finally the slides were fixed with 3-4 drops Entellan (Merck), covered with a coverslip, air-dried and stored at RT.

3. Results

3.1 Global data analysis

3.1.1 Global gene expression analysis

I provide experimental data at the molecular level based on a genomics approach to investigate changes in gene expression during human skin aging *in vitro* and *in vivo* and additionally during mouse brain, heart and kidney aging. To identify and further analyse genes, pathways and biological processes altered with age in human and mouse, RNA was isolated from (i) hormone-treated human sebocyte and fibroblast cell cultures, (ii) skin biopsies of young (18-30 years) and old (>60 years) male and female healthy volunteers and (iii) whole brain, heart and kidney of young (8-10 weeks) and aged (17-19 months) female mice. Whole-genome gene expression analysis employing the ENSEMBL Chip for the *in vitro* experiments and the Illumina Bead Chip for the *in vivo* experiments was then used to profile the transcriptomes of these samples. The different platforms were used, because the newer Illumina platform was installed after the *in vitro* part of this work was finished.

Data reproducibility is demonstrated by sample correlation and clustering for the *in vivo* human and mouse studies (Figure 3.1). As expected the clustering of mouse samples shows a slightly better correlation for the biological replicates (0.95-1.00) than human samples (0.67-0.97). Furthermore, replicates in cell culture showed even better correlations (data not shown). These differences reflect the best possibilities to assure the same conditions for each biological replicate in cell cultures followed by keeping laboratory mice and than *in vivo* derived human samples, which are not only different in the corresponding life style exhibited by the volunteers but also vary in their exact age even in the defined age groups.

The three mouse tissues show the expected separation from each other (<0.50). However, the separation of the two age groups for each tissue is not explicit. In detail, young brain (0.98-0.99) and aged brain (0.97-1.00) replicates show good correlations and also the correlation of young and aged samples is good (0.95-0.99), which causes the effect of not being able to clearly separate young brain from aged brain samples.

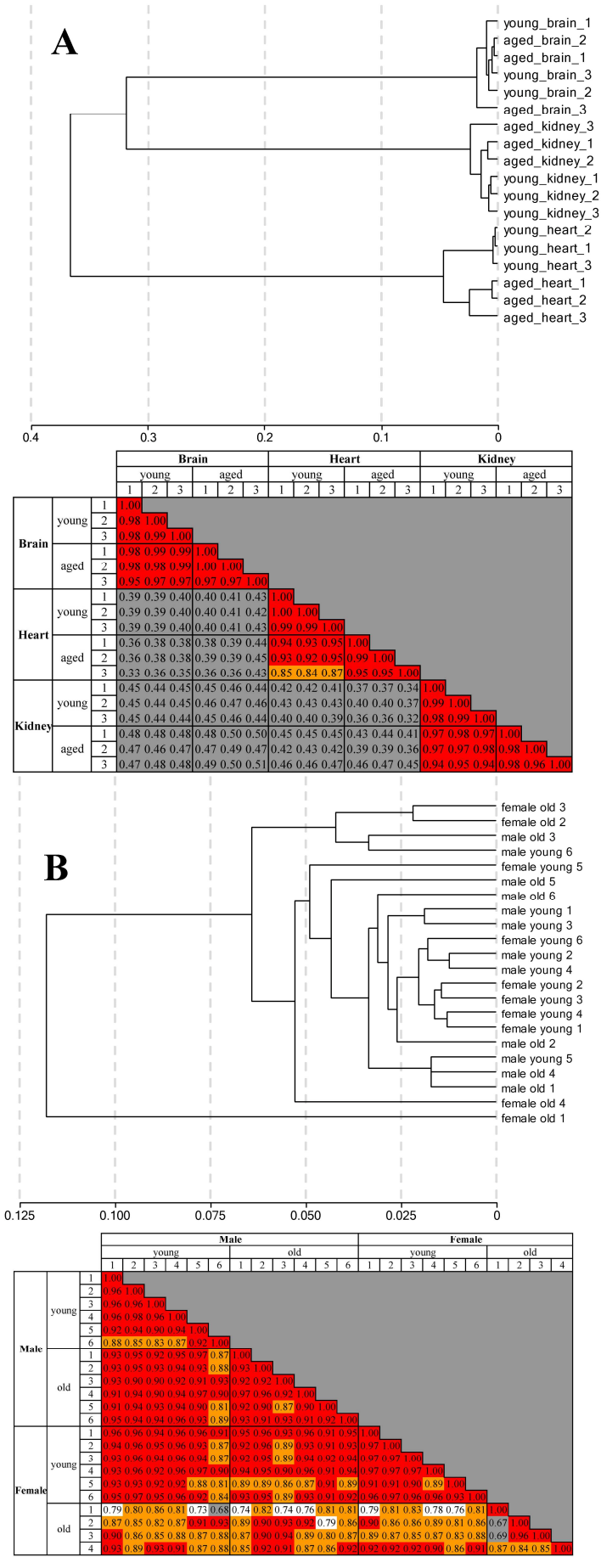

Figure 3.1 Clustering of samples and correlation factors for mouse and human *in vivo* experiments.

The figure shows the sample clustering and the corresponding correlation coefficients derived from whole genome gene expression analyses for (A) young and aged mouse whole brain, heart and kidney and (B) young and old male and female human skin biopsies. Correlation factors are coloured as follows: red = 0.90 – 1.00, orange = 0.80 – 0.90, white = 0.70 – 0.80 and grey < 0.70.

Young heart (0.99-1.00) and aged heart (0.95-0.99) replicates show better correlations than young compared to aged samples (0.84-0.95), but one of the aged samples exhibits slight variations. Finally, young kidney (0.98-0.99) and aged kidney (0.96-0.98) replicates show slightly better correlations than young compared to aged samples (0.94-0.98), leading to a good separation of the three young to two aged samples, whereas the last aged sample exhibits a higher variation compared to the others.

For the human skin biopsies, the clustering of the samples shows a good correlation for most of the replicates (>0.90). The correlation coefficients for replicates of the 6 young (0.83-0.98) and 6 old (0.87-0.97) males and the 6 young females (0.89-0.97) show in most cases good correlations. Additionally, the transcriptional difference between young and old males is minor (0.81-0.97) and even the correlation of all males to the young females is high (0.84-0.97). However, 3 of the 4 old females exhibit slightly lower correlation with each other (0.67-0.96) as well as with young females and all males (0.68-0.94). Old female number 1 shows the worst correlation with the rest (0.67-0.87). These differences could either reflect biological heterogeneity between samples or technical variations during the whole process of sample collection, RNA isolation and hybridisation.

3.1.2 RNA quality control

To ensure RNA integrity, all samples (cells or tissues) were directly frozen in liquid nitrogen and stored at -80°C until use. During the experiments RNAs were continuously cooled on ice. Used RNA samples were quality controlled throughout the whole process. After the RNA isolation from tissues or cell cultures, the quality of total RNA was checked by visually evaluating the 1 to 2 ratio of the dominant ribosomal RNAs using agarose gel electrophoresis and by measuring a 260/280nm ratio of around 2 using the NanoDrop. Amplified RNA for chip hybridisation was also checked using agarose gel electrophoresis and NanoDrop measurement. The RNA had to show a smear with a maximum peak at ~1kb on the gel and a 260/280nm ratio of more than 2 in the measurement. Amplified RNAs for use of the ENSEMBL chip were additionally evaluated for Cy3-dUTP incorporation using the Fuji scanner FL8-8000. Examples for RNA quality control gel pictures are shown in Figure 3.2.

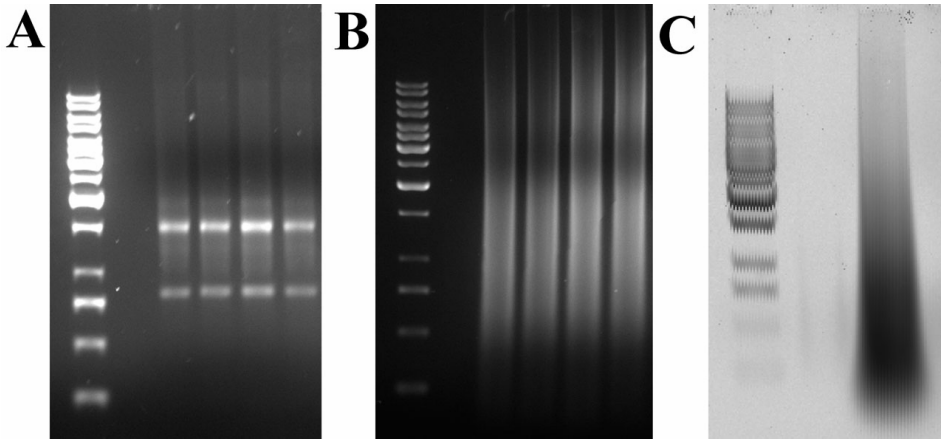

Figure 3.2 RNA quality control gel pictures.

The figure shows sample gel pictures of RNAs used in the experiments. (A) Total RNA after isolation from tissues, displaying the typical two ribosomal RNA bands (18s and 28s) with an intensity ratio of 1 to 2, (B) aRNA displaying the typical smear with a maximum at ~1kb and (C) Cy3-dUTP incorporation in aRNA for the use of ENSEMBL chips.

3.1.3 Target gene lists

Normalized data were analysed for significant (Illumina: detection >0.99 for at least one group and p-value <0.05; ENSEMBL: BGtag >0.90 for at least one group and p-value <0.05) changes in gene expression between the two age groups in the different *in vitro* and *in vivo* experiments with fold-ratios of 1.3 and above (more detailed target gene lists can be found in appendix III). Ratios in this work are normally presented logarithmic to base 2. The total number of target genes for all experiments are shown in Table 3.1.

Table 3.1 Number of target genes for all *in vitro* and *in vivo* aging experiments.

Data set	Fold-ratio > 1.3			Fold-ratio > 2.0		
	up	down	total	up	down	total
			in vitro experiments			
Sebocytes	437	461	898	2	24	26
Fibroblasts	201	170	371	50	121	171
			in vivo experiments			
Human skin female	286	584	870	18	102	120
Human skin male	213	170	383	17	32	49
Mouse brain	581	247	828	46	8	54
Mouse heart	569	421	990	127	68	195
Mouse kidney	1112	432	1544	302	37	339

For the chosen criteria, I found regulated genes in all experiments ranging from 371 in human fibroblasts to 1544 in mouse kidney. In most cases just a few genes show changes in gene expression of more than 2-fold and nearly no gene exhibits gene activation or inactivation, measured by a detection of more than 0.99 in the one age-group and a low detection of less than 0.8 in the other age-group. For further analysis, these target gene lists were divided in genes with increased and decreased expression with age.

3.1.4 Pathway analyses

The age-related gene lists (corresponding Gene accession as input) were analysed using the Gene Annotation Tools – DAVID (http://niaid.abcc.ncifcrf.gov/) and FatiGO+ (http://babelomics.bioinfo.cipf.es/fatigoplus/cgi-bin/fatigoplus.cgi) to identify altered pathways and Gene Ontologies (GOs). Detailed lists of significant age-regulated GOs (Biological Process) and Kegg pathways derived from the DAVID analyses are presented in appendix IV (PValue <0.05) or in context.

3.1.5 Array data confirmation by Real-Time PCR

To validate the data derived from whole genome expression analyses using the ENSEMBL and Illumina chips, selected significantly regulated target genes were confirmed using Real-Time PCR. The results of the array confirmation are shown in Table 3.2.

The table shows logarithmic ratios to base 2 for both arrays (ENSEMBL: sebocyte data; Illumina: mouse data) and the corresponding logarithmic ratios derived from the Real-Time PCR experiments. Positive ratios indicate increased expression and negative ratios decreased expression with age. The super- and subscript numbers next to the ratios show the positive and negative standard deviation, respectively.

All genes analysed were confirmed for significant regulation in the same direction; meaning increased or decreased expression with age. However, some genes show differences in the magnitude of regulation between the array and Real-time PCR results. These differences could be accounted for by the different sensitivities of the two approaches.

Table 3.2 Array data confirmation by Real-Time PCR.

Name	Accession	Definition	Ratio	
			Array	PCR
		ENSEMBL (human sebocytes)		
		female		
CCM1	NM_194455	cerebral cavernous malformations 1	$-0.62^{+0.24}_{-0.29}$	$-1.07^{+0.22}_{-0.22}$
DHCR7	NM_001360	7-dehydrocholesterol reductase	$-0.87^{+0.17}_{-0.19}$	$-3.26^{+0.20}_{-0.20}$
FDFT1	NM_004462	farnesyl-diphosphate farnesyltransferase 1	$-0.54^{+0.21}_{-0.24}$	$-1.65^{+0.17}_{-0.17}$
LYPLA1	NM_006330	lysophospholipase I	$-0.43^{+0.19}_{-0.22}$	$-1.41^{+0.15}_{-0.15}$
MVD	NM_002461	mevalonate (diphospho) decarboxylase	$-1.19^{+0.18}_{-0.20}$	$-2.78^{+0.13}_{-0.13}$
TJP2	NM_004817	tight junction protein 2 (zona occludens 2)	$-0.71^{+0.43}_{-0.62}$	$-1.52^{+0.20}_{-0.20}$
		male		
CCM1	NM_194455	cerebral cavernous malformations 1	$-0.85^{+0.33}_{-0.42}$	$-1.18^{+0.27}_{-0.27}$
DHCR7	NM_001360	7-dehydrocholesterol reductase	$-0.39^{+0.22}_{-0.26}$	$-1.55^{+0.44}_{-0.44}$
FDFT1	NM_004462	farnesyl-diphosphate farnesyltransferase 1	$-0.43^{+0.13}_{-0.15}$	$-0.57^{+0.03}_{-0.03}$
LYPLA1	NM_006330	lysophospholipase I	$-1.44^{+0.24}_{-0.29}$	$-1.04^{+0.29}_{-0.29}$
MVD	NM_002461	mevalonate (diphospho) decarboxylase	$-0.05^{+0.16}_{-0.18}$	$-1.08^{+0.22}_{-0.22}$
TJP2	NM_004817	tight junction protein 2 (zona occludens 2)	$-0.97^{+0.36}_{-0.49}$	$-1.04^{+0.11}_{-0.11}$
		Illumina (mouse tissues)		
		brain		
Casp1	NM_009807	caspase 1	$0.81^{+0.28}_{-0.34}$	$0.77^{+0.13}_{-0.13}$
Fcer1g	NM_010185	Fc receptor, IgE, high affinity I, gamma polypeptide	$0.76^{+0.09}_{-0.09}$	$1.15^{+0.03}_{-0.03}$
Inmt	NM_009349	indolethylamine N-methyltransferase	$0.74^{+0.26}_{-0.32}$	$0.74^{+0.03}_{-0.03}$
Psmb8	NM_010724	proteosome (prosome, macropain) subunit, beta type 8	$1.04^{+0.29}_{-0.37}$	$0.71^{+0.03}_{-0.03}$
		heart		
C3	NM_009778	complement component 3	$1.42^{+0.19}_{-0.22}$	$3.35^{+0.06}_{-0.06}$
Col3a1	NM_009930	procollagen, type III, alpha 1	$-1.21^{+0.31}_{-0.40}$	$-1.18^{+0.31}_{-0.31}$
Hmgn3	NM_175074	high mobility group nucleosomal binding domain 3	$-0.60^{+0.13}_{-0.15}$	$-0.95^{+0.17}_{-0.17}$
Mmp3	NM_010809	matrix metalloproteinase 3	$2.57^{+0.35}_{-0.46}$	$1.99^{+0.33}_{-0.33}$
		kidney		
Fcer1g	NM_010185	Fc receptor, IgE, high affinity I, gamma polypeptide	$1.34^{+0.30}_{-0.38}$	$1.11^{+0.11}_{-0.11}$
Inmt	NM_009349	indolethylamine N-methyltransferase	$-2.22^{+0.60}_{-1.03}$	$-1.88^{+0.21}_{-0.21}$
Irf8	NM_008320	interferon regulatory factor 8	$0.65^{+0.27}_{-0.34}$	$0.80^{+0.25}_{-0.25}$
Psmb8	NM_010724	proteosome (prosome, macropain) subunit, beta type 8	$0.81^{+0.30}_{-0.38}$	$1.12^{+0.53}_{-0.53}$
Tyrobp	NM_011662	TYRO protein tyrosine kinase binding protein	$1.50^{+0.27}_{-0.34}$	$0.98^{+0.03}_{-0.03}$

3.2 Human skin aging

3.2.1 Genetic changes in age-dependent hormone-treated cell cultures

Human sebocytes and skin fibroblasts were cultured in defined hormone substituted conditions corresponding to young (20 years) and old (60 years) female individuals. Global gene expression analyses were performed using the ENSEMBL chip, which contains spots for more than 15000 genes.

As shown in Table 3.1, 898 genes were significantly regulated in human sebocytes and 371 genes in skin fibroblasts for the chosen criteria. Of these, 437 genes exhibited increased and 461 decreased expression in sebocytes and 201 genes showed increased and 170 decreased expression in fibroblasts with age. The most regulated genes are presented in Tables X.1 and X.2 in appendix III. In addition, DAVID pathway and Gene Ontology analyses provided results for significantly regulated Kegg pathways and GOs for up- and down-regulated genes in fibroblasts and sebocytes. These results are shown in Tables X.8 and X.9 in appendix IV.

Up-regulated expression in fibroblasts correlates with increases in the Kegg pathways ribosome (11) and glutathione metabolism (4) and with increased biological processes referring for instance to biosynthesis (27) – especially protein (19) and macromolecule (20) biosynthesis and to RNA related processes such as RNA processing (11), metabolism (11) and splicing (5). For down-regulated genes in fibroblasts, no significantly regulated Kegg pathways were found. Significantly down-regulated biological processes in fibroblasts were for instance cell growth and/or maintenance (52), intracellular signaling cascade (16), cell proliferation (17) and protein related processes like protein metabolism (37), modification (21), targeting (5) and transport (9).

In sebocytes, the Kegg pathway aminoacyl-tRNA biosynthesis was up-regulated (5) and the pentose phosphate pathway down-regulated (4). Up-regulated biological processes referred for instance to apoptosis (17), metabolism (196), cell cycle (29), cell proliferation (40) and cell growth and/or maintenance (109). Cell cycle (32), cell proliferation (42) and cell growth and/or maintenance (105) were also in the list of down-regulated processes. In addition, development (51) and lipid related processes like lipid biosynthesis (10) and metabolism (19) were down-regulated in sebocytes.

Table 3.3 List of overlapping genes regulated in skin fibroblasts and sebocytes with age.

Name	ImageID	Description	Ratio	
			Fibro.	Sebo.
		up in fibroblasts and sebocytes		
EDD	358125	UBIQUITIN--PROTEIN LIGASE EDD	1.76	0.43
GBP1	1678893	INTERFERON-INDUCED GUANYLATE-BINDING PROTEIN 1	1.06	0.69
ALS2CR2	730342	AMYOTROPHIC LATERAL SCLEROSIS 2 (JUVENILE)	0.90	0.48
STC2	130057	STANNIOCALCIN 2 PRECURSOR	0.77	0.46
P15RS	357968	CDNA FLJ10656 FIS	0.70	0.52
ZNF644	134300	DJ924G13.1	0.69	0.56
MACF1	3619787	ACTIN CROSS-LINKING FAMILY PROTEIN 7	0.65	0.49
DKFZP564G2022	278707	HYPOTHETICAL 20.5 KDA PROTEIN.	0.63	0.52
ARHGEF12	265359	RHO GUANINE NUCLEOTIDE EXCHANGE FACTOR (GEF) 12	0.61	0.43
NUMB	202342	NUMB PROTEIN HOMOLOG	0.51	0.45
		down in fibroblasts and sebocytes		
GNAO1	1734348	GUANINE NUCLEOTIDE-BINDING PROTEIN G(O), ALPHA SUBUNIT 1	-1.91	-0.73
MGC2494	2271174	UNKNOWN	-1.51	-0.51
TPD52L2,PIK3R1	125046	TUMOR PROTEIN D54	-1.46	-0.59
PLK3	52216	CYTOKINE-INDUCIBLE SERINE/THREONINE-PROTEIN KINASE	-0.84	-0.44
HLA-G	2125838	HLA CLASS I HISTOCOMPATIBILITY ANTIGEN, A-1 ALPHA CHAIN PRECURSOR	-0.80	-1.31
FLJ10420	172028	CDNA FLJ13483 FIS	-0.53	-0.63
		up in fibroblasts and down in sebocytes		
MYO1C	5562766	MYOSIN IC	1.38	-0.89
BBP	202408	BETA-AMYLOID BINDING PROTEIN PRECURSOR.	0.81	-0.86
NOSIP	322613	ENOS INTERACTING PROTEIN; CGI-25 PROTEIN	0.72	-0.47
MMP2	323656	72 KDA TYPE IV COLLAGENASE PRECURSOR	0.70	-0.43
RAB1B	301716	PUTATIVE SMALL GTP-BINDING PROTEIN	0.65	-0.54
TXN2	259104	THIOREDOXIN, MITOCHONDRIAL PRECURSOR	0.55	-0.53
TTC11	229553	CGI-135 PROTEIN	0.54	-0.44
FASLG	4849770	TUMOR NECROSIS FACTOR LIGAND SUPERFAMILY MEMBER 6	0.53	-0.42
		down in fibroblasts and up in sebocytes		
TYROBP	152679	TYRO PROTEIN TYROSINE KINASE-BINDING PROTEIN PRECURSOR	-2.31	0.68
DKFZP586L0724	825282	CDNA FLJ13640 FIS	-2.13	0.67
KIAA1279	172289	KIAA1279 PROTEIN (FRAGMENT)	-2.87	0.57
FLJ10826	34187	OVARC1001341 PROTEIN	-1.76	0.57
FLJ32731	142851	---	-1.75	0.65
DDEF2	741382	DEVELOPMENT- AND DIFFERENTIATION-ENHANCING FACTOR 2	-1.49	0.63
TCF12	53051	TRANSCRIPTION FACTOR 12	-1.32	0.57
FLJ14753	740067	DC27	-1.07	0.54
CSE1L	122814	IMPORTIN-ALPHA RE-EXPORTER	-0.99	0.45
CAV2	110467	CAVEOLIN-2	-0.74	0.52
PODXL	201837	PODOCALYXIN-LIKE PROTEIN 1 PRECURSOR	-0.47	0.48

Table 3.3 shows genes that exhibited significant regulation in both fibroblasts and sebocytes with age. In total, 35 genes were found matching this criterion. Of these, 16 showed the same trend in fibroblasts and sebocytes – 10 were up-regulated and 6 were down-regulated in both experiments. The other 19 genes were regulated differentially in fibroblasts and sebocytes, with 8 genes showing up-regulation in fibroblasts and down-regulation in sebocytes and 11 genes showing down-regulation in fibroblasts and up-regulation in sebocytes.

Table 3.4 presents biological processes significantly regulated in both fibroblasts and sebocytes. The full DAVID output (p-value <0.1) was used for the pathway and biological process overlap analysis in contrast to the output lists in appendix IV (p-value <0.05) to also identify processes close to the threshold. Cellular physiological process, cell growth and/or maintenance, RNA metabolism and RNA processing were overrepresented in all 4 target gene lists. Many other processes were present in 3 target

gene lists. Just 2 processes were found to be up-regulated in fibroblasts and sebocytes and only one process was found to be down-regulated in both. Finally, 5 processes showed up-regulation in sebocytes and down-regulation in fibroblasts.

Table 3.4 List of overlapping biological processes regulated in fibroblasts and sebocytes with age.

Term	Fibroblasts		Sebocytes	
	up	down	up	down
CELLULAR PHYSIOLOGICAL PROCESS	57	59	131	125
CELL GROWTH AND/OR MAINTENANCE	48	52	109	105
RNA METABOLISM	11	8	24	14
RNA PROCESSING	11	8	15	12
METABOLISM	87	-	196	175
BIOSYNTHESIS	27	-	33	33
MACROMOLECULE BIOSYNTHESIS	20	-	24	29
CELLULAR PROCESS	-	77	180	165
MACROMOLECULE METABOLISM	-	41	102	88
CELL PROLIFERATION	-	17	40	42
TRANSCRIPTION FROM POL II PROMOTER	-	9	20	33
INTRACELLULAR PROTEIN TRANSPORT	-	8	11	11
PROTEIN METABOLISM	37	37	92	-
PROTEIN TRANSPORT	9	9	21	-
MRNA METABOLISM	7	7	10	-
MRNA PROCESSING	6	7	8	-
PHYSIOLOGICAL PROCESS	133	-	281	-
PROTEIN BIOSYNTHESIS	19	-	20	-
MUSCLE DEVELOPMENT	-	4	-	8
PROTEIN MODIFICATION	-	21	46	-
INTRACELLULAR SIGNALING CASCADE	-	16	31	-
PROTEIN AMINO ACID PHOSPHORYLATION	-	10	22	-
INTRACELLULAR TRANSPORT	-	10	19	-
REGULATION OF TRANSCRIPTION FROM POL II PROMOTER	-	6	12	-

3.2.2 Gene expression in young and old sun-protected skin biopsies

Human skin biopsies were collected from young (18-30 years) and old (>60 years) male and female volunteers. Whole genome gene expression analyses were performed using the Illumina array platform.

As shown in Table 3.1, 870 genes were significantly regulated in female skin and 383 genes in male skin for the chosen criteria. Of these, 286 genes exhibited increased and 584 decreased expression in females and 213 genes showed increased and 170 decreased expression in males with age. The most regulated genes are presented in Tables X.3 and X.4 in appendix III. In addition, DAVID pathway and Gene Ontology analyses provided results for significantly regulated Kegg pathways and GOs for up-

and down-regulated genes in female and male skin. These results are shown in Tables X.10 and X.11 in appendix IV.

Up-regulated expression in female skin biopsies correlates with increases in 5 Kegg-annotated metabolisms – for example glycerophospholipid metabolism (5) and 1- and 2-methylnaphthalene degradation (3) and with increased biological processes referring for instance to metabolism (126) – especially protein (61), macromolecule (82), DNA (15) and carboxylic acid (12) metabolism, and to biosynthesis (31) and cell organization and biogenesis (31). For down-regulated genes in female skin, Kegg pathways ribosome (36), cell communication (19) and WNT signaling pathway (18) were found. Significantly down-regulated biological processes in female skin were for instance development (97) – especially ectoderm (19), epidermis (16), tissue (22) and organ (26) development, macromolecule (55) and protein (53) biosynthesis, cell adhesion (36) and the signaling pathways WNT receptor (15), frizzled (5) and notch (5).

In male skin biopsies, the only significantly up-regulated Kegg pathway was arginine and proline metabolism (4) and no pathway was down-regulated. Up-regulated biological processes referred for instance to several metabolisms like phosphorus (18), protein (46) and membrane lipid (5) metabolism, and as well to phosphorylation (16), protein modification (27) and programmed cell death (11), whereas down-regulated processes referred for instance to development (26) and to several regulation related processes such as regulation of transcription (29) and regulation of metabolism (30).

Table 3.5 lists genes that exhibited significant regulation in both male and female skin biopsies with age. In total, 43 genes were common in the target lists of significant regulated genes in males and females. 41 of these genes showed increased (16) or decreased (25) expression independent of gender. Only 2 genes showed different regulation with increased expression in male and decreased expression in female skin biopsies.

Table 3.5 List of overlapping genes regulated in male and female skin biopsies with age.

Name	Accession	Description	Ratio	
			Male	Female
SIRT6	NM_016539.1	sirtuin (silent mating type information regulation 2 homolog) 6 (S. cerevisiae)	1.29	1.72
CPT1B	NM_152246.1	carnitine palmitoyltransferase 1B (muscle), transcript variant 3	0.96	1.12
CDC42BPA	NM_014826.3	CDC42 binding protein kinase alpha (DMPK-like), transcript variant A	0.56	0.97
ALDH4A1	NM_003748.2	aldehyde dehydrogenase 4 family, member A1, transcript variant P5CDhL	1.05	0.94
CYHR1	NM_032687.2	cysteine/histidine-rich 1	0.44	0.74
OPLAH	NM_017570.1	5-oxoprolinase (ATP-hydrolysing)	0.41	0.70
PET112L	NM_004564.1	PET112-like (yeast)	0.50	0.69
VWCE	NM_152718.1	von Willebrand factor C and EGF domains	0.82	0.69
GRINA	NM_000837.1	glutamate receptor, ionotropic, N-methyl D-asparate-associated protein 1 (glutamate binding), transcript variant 1	0.59	0.64
FLJ20920	NM_025149.3	hypothetical protein FLJ20920	0.55	0.60
CINP	NM_032630.2	cyclin-dependent kinase 2-interacting protein	0.59	0.60
PGLS	NM_012088.2	6-phosphogluconolactonase	0.49	0.57
ASS	NM_000050.3	argininosuccinate synthetase, transcript variant 1	0.46	0.57
TRIM50B	NM_198924.2	tripartite motif-containing 50B	0.44	0.54
NOL3	NM_003946.3	nucleolar protein 3 (apoptosis repressor with CARD domain)	0.46	0.52
TAF10	NM_006284.2	TAF10 RNA polymerase II, TATA box binding protein (TBP)-associated factor, 30kDa	0.50	0.45
OR52N2	NM_001005174.1	olfactory receptor, family 52, subfamily N, member 2	*0.40*	*-0.40*
LGR4	NM_018490.1	leucine-rich repeat-containing G protein-coupled receptor 4	-0.40	-0.42
PRRX2	NM_016307.3	paired related homeobox 2	-0.51	-0.48
ACY1L2	NM_001010853.1	aminoacylase 1-like 2	-0.48	-0.56
TGFBI	NM_000358.1	transforming growth factor, beta-induced, 68kDa	-0.38	-0.58
ENTPD7	NM_020354.2	ectonucleoside triphosphate diphosphohydrolase 7	-0.59	-0.59
FGFR1OP2	NM_015633.1	FGFR1 oncogene partner 2	*0.42*	*-0.59*
ABCG1	NM_004915.3	ATP-binding cassette, sub-family G (WHITE), member 1, transcript variant 4	-0.42	-0.62
SLC35F1	NM_001029858.1	solute carrier family 35, member F1	-0.70	-0.63
SDCCAG33	NM_005786.3	serologically defined colon cancer antigen 33	-0.44	-0.69
COL8A2	NM_005202.1	collagen, type VIII, alpha 2	-0.54	-0.70
PTGFRN	NM_020440.2	prostaglandin F2 receptor negative regulator	-0.44	-0.72
OCA2	NM_000275.1	oculocutaneous albinism II (pink-eye dilution homolog, mouse)	-1.22	-0.79
KIT	NM_000222.1	v-kit Hardy-Zuckerman 4 feline sarcoma viral oncogene homolog	-0.51	-0.88
SLC22A15	NM_018420.1	solute carrier family 22 (organic cation transporter), member 15	-0.47	-1.00
MRC2	NM_006039.2	mannose receptor, C type 2	-0.96	-1.01
MIB1	NM_020774.2	mindbomb homolog 1 (Drosophila)	-0.50	-1.03
NKD1	NM_033119.3	naked cuticle homolog 1 (Drosophila)	-0.92	-1.05
AXIN2	NM_004655.2	axin 2 (conductin, axil)	-0.58	-1.12
COL1A2	NM_000089.3	collagen, type I, alpha 2	-1.13	-1.63
TMEM46	NM_001007538.1	transmembrane protein 46	-1.39	-1.74
COL3A1	NM_000090.2	collagen, type III, alpha 1 (Ehlers-Danlos syndrome type IV, autosomal dominant)	-1.05	-1.93
MATN4	NM_003833.2	matrilin 4, transcript variant 1	-1.41	-1.95
MATN4	NM_030590.1	matrilin 4, transcript variant 2	-1.88	-1.99
CPZ	NM_001014447.1	carboxypeptidase Z, transcript variant 1	-1.69	-2.08
COL1A1	NM_000088.2	collagen, type I, alpha 1	-1.38	-2.33
WIF1	NM_007191.2	WNT inhibitory factor 1	-1.76	-2.48

Table 3.6 lists Kegg pathways, biological processes and cellular compartments significantly regulated in both male and female skin biopsies. The full DAVID output (p-value <0.1) was used for the pathway and biological process overlap analysis in contrast to the lists in appendix IV (p-value <0.05) to also identify processes close to the threshold. In most cases, where overlaps between regulated GOs and pathways in males and females were observed, these also showed the same trend – meaning either up or down-regulated in both sexes. The only overlapping pathway is the WNT signaling pathway with decreased gene expression for males (4) and females (18). Up-regulated biological processes are related to metabolism whereas down-regulated processes to developmental processes. For cellular compartment, the mitochondrion showed up-regulation and extracellular matrix and collagen down-regulation.

Table 3.6 List of overlapping pathways and GOs regulated in male and female skin biopsies with age.

Term	Male		Female	
	up	down	up	down
Kegg pathway				
WNT SIGNALING PATHWAY	-	4	-	18
GO – BP				
macromolecule metabolism	55	-	82	156
protein metabolism	46	-	61	133
cellular macromolecule metabolism	42	-	59	128
cellular protein metabolism	42	-	59	125
cellular physiological process	117	94	151	-
development	-	26	-	97
cell adhesion	-	10	-	36
anion transport	-	5	-	15
inorganic anion transport	-	5	-	15
Wnt receptor signaling pathway	-	4	-	15
phosphate transport	-	5	-	13
frizzled signaling pathway	-	3	-	5
cell maturation	-	3	-	4
nerve ensheathment	-	3	-	3
metabolism	94	-	126	-
biopolymer modification	27	-	32	-
protein modification	27	-	32	-
cellular lipid metabolism	10	-	11	-
negative regulation of programmed cell death	5	-	-	9
GO – CC				
cytoplasm	46	-	73	138
extracellular matrix	-	10	-	24
extracellular matrix (sensu Metazoa)	-	9	-	23
collagen	-	3	-	6
fibrillar collagen	-	3	-	3
mitochondrion	12	-	26	-
intracellular membrane-bound organelle	-	56	92	-
organelle lumen	-	8	13	-

GO = gene ontology; BP = biological process; CC = cellular compartment

3.2.3 Analogous gene expression of in vitro and in vivo skin samples

The results of the cell culture experiments with human sebocytes and skin fibroblasts were compared to the results of the skin biopsies experiments by investigating overlaps in target gene lists and age-regulated Kegg pathways and biological processes. Figure 3.3 presents Venn diagrams showing the overlap of target gene lists of fibroblasts and sebocytes with male and female skin biopsies, respectively.

The diagrams show that 5 genes were common between fibroblasts and male skin and 17 between fibroblasts and female skin. No gene was found to be common in fibroblasts, male and female skin. Sebocytes overlap with 2 genes (*SIRT6* and *PGLS*)

with both male and female skin, with 6 genes only with male and with 28 genes only with female skin. The 5 and 6 genes common between male skin and fibroblasts/sebocytes overlap in one gene (*TCF12*) and also the 17 and 28 genes common between female skin and fibroblasts/sebocytes overlap in one gene (*MMP2*).

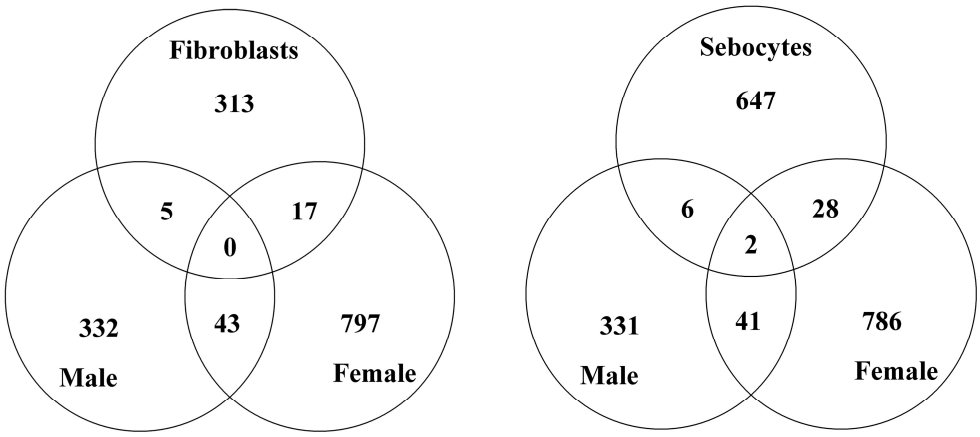

Figure 3.3 Venn diagrams visualizing the overlap of the *in vitro* and *in vivo* skin aging results.
The two Venn diagrams show the overlap of target gene lists of fibroblasts and sebocytes with male and female skin biopsies. The total number of target genes does not correlate with the numbers presented in Table 3.1, because some novel genes and transcript variants of the same gene were skipped from the lists for this analysis.

Table 3.7 List of overlapping biological processes regulated in the *in vitro* and *in vivo* experiments.

Term	Male		Female		Fibroblasts		Sebocytes	
	up	down	up	down	up	down	up	down
cellular physiological process	117	94	151	-	57	59	131	125
macromolecule metabolism	55	-	82	156	-	41	102	88
protein metabolism	46	-	61	133	37	37	92	-
protein transport	10	-	15	-	9	9	21	15
metabolism	94	-	126	-	87	-	196	175
biosynthesis	-	-	31	68	27	-	33	33
macromolecule biosynthesis	-	-	17	55	20	-	24	29
cellular process	-	111	-	-	-	77	180	165
protein modification	27	-	32	-	-	21	46	-
protein biosynthesis	-	-	16	53	19	-	20	-
physiological process	-	-	170	-	133	-	281	-
development	-	26	-	97	-	-	-	51
protein amino acid phosphorylation	16	-	-	-	-	10	22	-
programmed cell death	11	-	-	-	-	-	17	15
apoptosis	10	-	-	-	-	-	17	15
negative regulation of programmed cell death	5	-	-	9	-	-	7	-

In addition, no Kegg pathways were found to overlap between the *in vitro* and *in vivo* experiments. Table 3.7 shows the overlap of biological processes, which were significantly regulated in at least 3 of the 8 target gene lists and additionally in at least one *in vitro* and one *in vivo* experiment.

Processes regulated in 5 or more target gene lists were global processes like metabolism, biosynthesis and cellular biological process. Furthermore, the processes regulated in 3 or 4 target gene lists were either quite global processes like physiological process or they showed different regulation in the different experiments with age, e.g. protein amino acid phosphorylation.

3.3 Mouse aging (brain, heart & kidney)

3.3.1 Synchronizing the sample collection

Before I start to describe the aging of mouse tissues, I present here the necessity of daytime synchronised sample collection and the possibly problems which otherwise could occur – a process referred to as circadian rhythm.

Table 3.8 Circadian rhythm genes regulated in mouse brain, heart and kidney.

Gene	Ratio		
	Brain	**Heart**	**Kidney**
Arntl	-	3.26	6.20
Nfil3	-	1.98	2.01
Nr1d2	-	0.77	-
Clock	0.18	-	-
Per2	-	-	-1.64
Per3	-0.46	-	-2.27
Nr1d1	-1.07	-1.53	-1.90
Nr1d1	-	-1.64	-1.91
Per1	-	-1.69	-
Nr1d2	-1.46	-2.87	-
Dbp	-1.27	-4.76	-5.62

In a first mouse experiment, brain, heart and kidney of young (10-12 weeks) and aged (~15 months) mice were collected and the RNAs were hybridised in duplicate using the Illumina platform. The correlation of these samples is shown in Figure 3.4 A and B. The young and aged mice were sacrificed on different days and the analysis of the data revealed that the most significantly regulated process for all three tissues was the

circadian rhythm, which is responsible for awake-sleep control and other daytime-related processes. Table 3.8 and Figure 3.5 present the regulation of circadian rhythm-related genes in the three different tissues.

A

			Brain				Heart				Kidney			
			young		aged		young		aged		young		aged	
			1	2	1	2	1	2	1	2	1	2	1	2
Brain	young	1	1.00											
		2	0.99	1.00										
	aged	1	0.99	0.98	1.00									
		2	0.98	0.97	0.99	1.00								
Heart	young	1	0.39	0.38	0.41	0.43	1.00							
		2	0.42	0.40	0.44	0.45	0.99	1.00						
	aged	1	0.36	0.34	0.38	0.41	0.98	0.95	1.00					
		2	0.38	0.36	0.40	0.43	0.97	0.94	0.98	1.00				
Kidney	young	1	0.49	0.48	0.50	0.49	0.42	0.44	0.39	0.40	1.00			
		2	0.50	0.49	0.50	0.49	0.40	0.43	0.37	0.38	0.97	1.00		
	aged	1	0.51	0.50	0.52	0.52	0.45	0.47	0.43	0.43	0.96	0.96	1.00	
		2	0.50	0.50	0.51	0.50	0.42	0.44	0.39	0.40	0.96	0.97	0.97	1.00

B

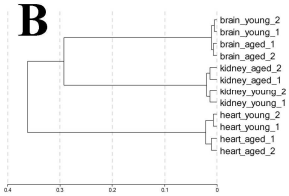

C

		8a.m.		4p.m.		12a.m.	
		1	2	1	2	1	2
8a.m.	1	1.00					
	2	0.96	1.00				
4p.m.	1	0.95	0.98	1.00			
	2	0.94	0.98	0.98	1.00		
12a.m.	1	0.97	0.97	0.98	0.97	1.00	
	2	0.96	0.96	0.96	0.95	0.98	1.00

Figure 3.4 Clustering of samples and correlation factors for synchronization experiments.
The figure shows (B) the sample clustering and (A) the corresponding correlation factors derived from whole genome gene expression analyses for young and aged mouse brain, heart and kidney and (C) correlation factors for mouse kidney samples collected at 3 different time points within a 24hrs period. Correlation factors are coloured as follows: red = 0.90 – 1.00 and grey < 0.70.

Since the exact time points of sample collection for the young and aged samples was unknown, additional heart and kidney samples of 5 months old mice were collected at three different time points (12a.m., 8a.m. and 4p.m.) on the same day to test the regulation of circadian rhythm genes within a 24hrs period. The kidney samples were also hybridised to test global gene regulations, the correlation of these data is shown in Figure 3.4 C.

The expression of three circadian rhythm genes (*Arntl*, *Dbp* and *Nr1d1*) was tested by Real-Time PCR using RNA from heart and kidney tissues over a 24hrs period. The results are presented in Figure 3.6 A. The test revealed that circadian rhythm-related genes exhibit high changes in gene expression during one day, e.g. a 16.5-fold change of *Dbp* expression between 8a.m. and 4p.m. in kidney.

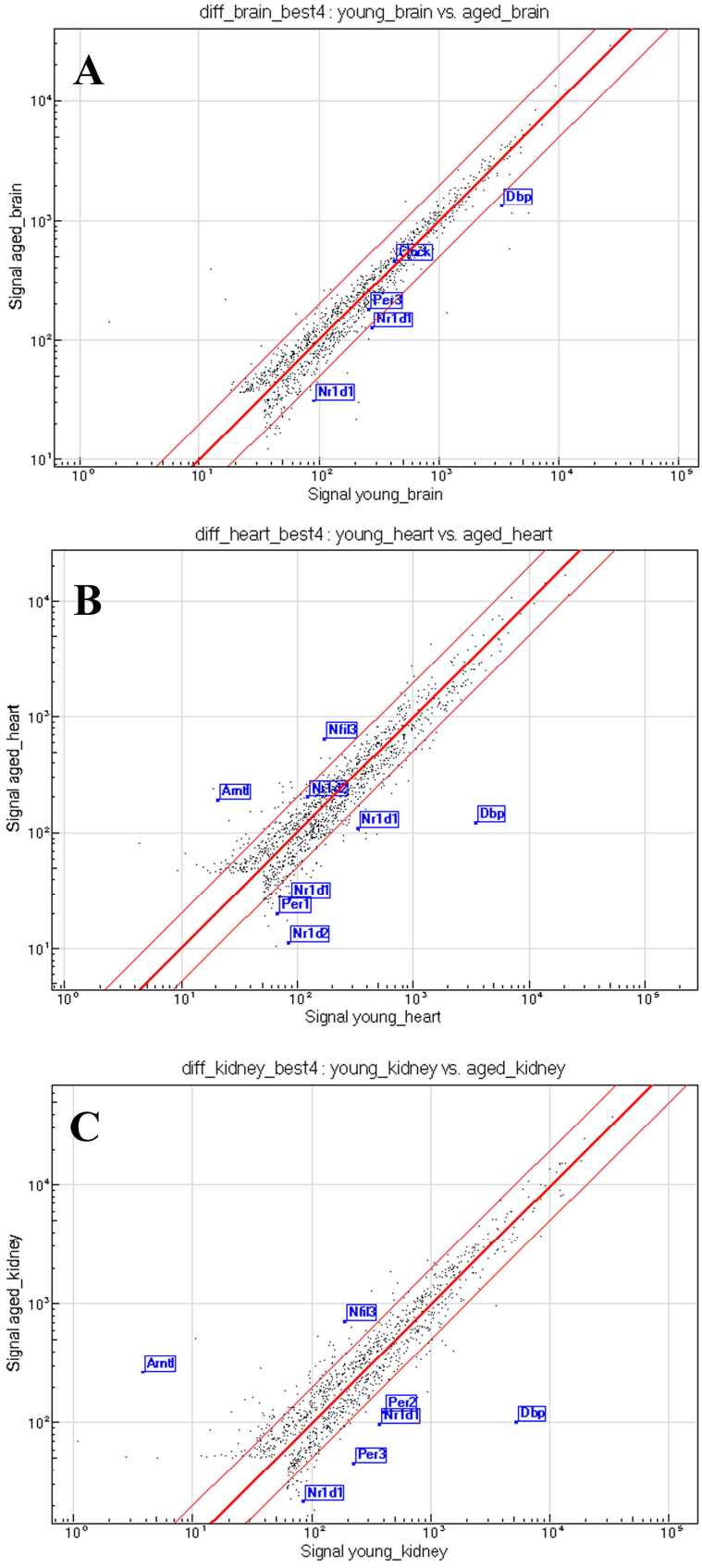

Figure 3.5 Scatter plots highlighting the regulation of circadian rhythm genes. The figure presents the scatter plots of significantly age-regulated genes in (A) brain, (B) heart and (C) kidney. All circadian rhythm genes are highlighted with blue spots and the corresponding gene names.

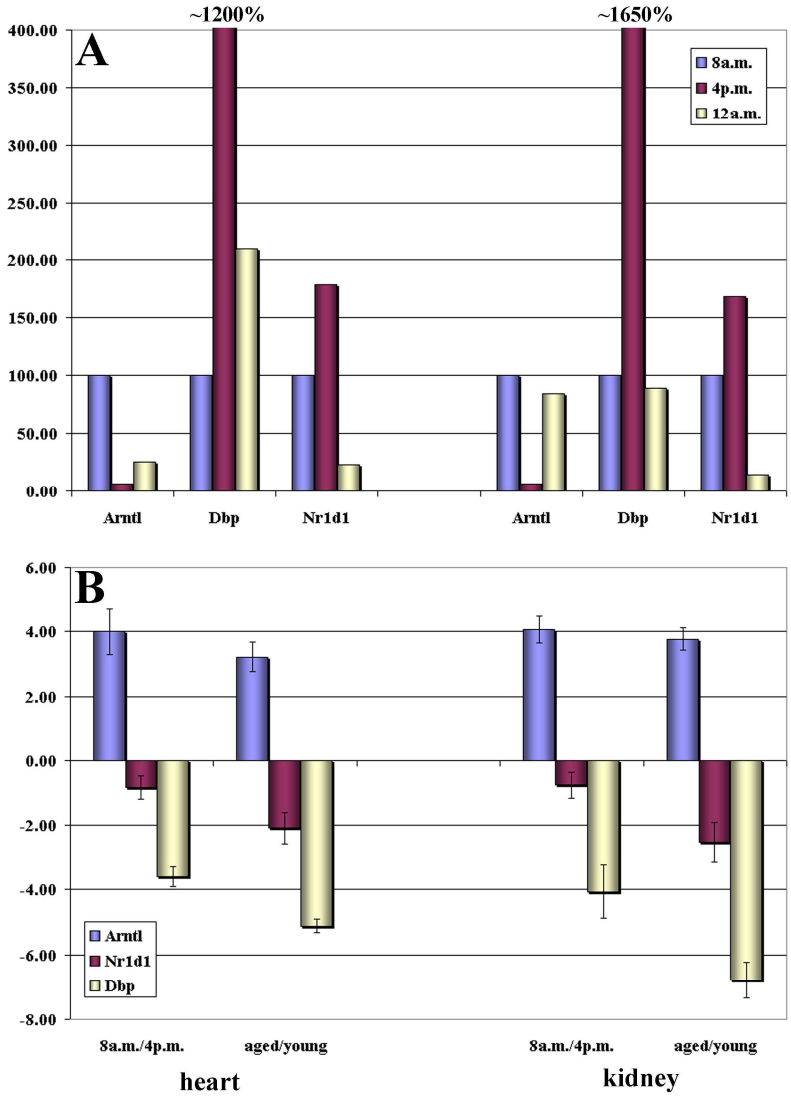

Figure 3.6 Real-Time PCR experiments investigating circadian rhythm gene expression.

(A) Gene expression of three circadian rhythm genes (*Arntl*, *Dbp* and *Nr1d1*) in mouse heart and kidney during a 24hrs period (8a.m., 4p.m. and 12a.m.). The ratio of expression is presented as the percentage of expression compared to expression at 8a.m. (B) Comparison of gene expression ratios for the three circadian rhythm genes between 8a.m. over 4p.m. and aged over young (unsynchronised aging experiment). The histogram shows that the genes exhibit similar ratios in the two experiments indicating a circadian rhythm artefact in the aging experiments introduced by unsynchronised sample collection.

To test, whether the changes in circadian rhythm gene expression in the aging experiment could be an artefact of unsynchronised sample collection they were compared to the changes in gene expression in the daytime experiments. Since it was known that the aging samples were not collected in the night the time points 8a.m. and 4p.m. were chosen. Figure 3.6 B shows that the ratios of 8a.m. over 4p.m. and aged

over young exhibit high similarity indicating a collection of the young tissues around 4p.m. and the aged tissues around 8a.m. and therefore a possible circadian rhythm artefact in the aging data.

Table 3.9 Most-regulated genes in a 16hrs period in mouse kidney.

Name	Accession	Description	Ratio	
			12a.m.-8a.m.	8a.m.-4p.m.
		Increased expression 12a.m.-8a.m.		
Dbp	NM_016974	D site albumin promoter binding protein	3.66	-
Per2	NM_011066	period homolog 2 (Drosophila)	3.58	-3.23
Angptl4	NM_020581	angiopoietin-like 4	3.02	-
Slc25a25	NM_146118	---	2.27	-0.84
Per3	NM_011067	period homolog 3 (Drosophila)	2.03	-0.91
Lin7a	XM_193582	lin 7 homolog a (C. elegans)	1.91	-
Per3	NM_011067	period homolog 3 (Drosophila)	1.85	-
Usp2	NM_198091	ubiquitin specific protease 2, transcript variant 2	1.72	-1.09
1500041J02Rik	NM_026424	RIKEN cDNA 1500041J02 gene	1.70	-
Nfib	AK034793	nuclear factor I/B	1.65	-
		Decreased expression 12a.m.-8a.m.		
Arntl	NM_007489	aryl hydrocarbon receptor nuclear translocator-like	-2.40	-
Fkhl18	NM_010226	forkhead-like 18 (Drosophila)	-2.17	-
Loxl4	AK014773	lysyl oxidase-like 4	-1.93	-
Cyp26b1	NM_175475	cytochrome P450, family 26, subfamily b, polypeptide 1	-1.73	-
3830422K02Rik	NM_173767	RIKEN cDNA 3830422K02 gene	-1.49	-
Npas2	NM_008719	neuronal PAS domain protein 2	-1.37	-
Ndrl	NM_008681	N-myc downstream regulated-like	-1.34	-
2810441C07Rik	NM_172415	RIKEN cDNA 2810441C07 gene	-1.22	-
Ccl4	NM_013652	chemokine (C-C motif) ligand 4	-1.22	0.89
Cdkn1a	NM_007669	cyclin-dependent kinase inhibitor 1A (P21)	-1.13	-
		Increased expression 8a.m.-4p.m.		
AW049829	NM_153571	expressed sequence AW049829	-	1.46
F5	AK050205	coagulation factor V	-	1.28
Rasd1	NM_009026	RAS, dexamethasone-induced 1	-	1.27
1810054O13Rik	NM_026436	RIKEN cDNA 1810054O13 gene	-	1.26
1810059H22Rik	---	---	-	1.13
Tbxas1	NM_011539	thromboxane A synthase 1, platelet	-0.53	1.08
Ell2	NM_138953	elongation factor RNA polymerase II 2	-1.07	1.05
Sult5a1	NM_020564	sulfotransferase family 5A, member 1	-	1.00
Tyrobp	NM_011662	TYRO protein tyrosine kinase binding protein	-	0.92
Rpl36	NM_018730	ribosomal protein L36	-	0.91
		Decreased expression 8a.m.-4p.m.		
Per2	NM_011066	period homolog 2 (Drosophila)	3.58	-3.23
Car3	NM_007606	carbonic anhydrase 3	-	-2.26
Rorc	NM_011281	RAR-related orphan receptor gamma	-	-2.14
Sgk	NM_011361	serum/glucocorticoid regulated kinase	-	-2.04
6330514A18Rik	NM_183152	RIKEN cDNA 6330514A18 gene	-	-1.76
D030032G01Rik	AK050903	---	-	-1.60
sty	U21209	---	-	-1.56
Cml3	NM_053097	camello-like 3	1.59	-1.51
Kcna6	NM_013568	potassium voltage-gated channel, shaker-related, subfamily, member 6	-	-1.46
Cry2	NM_009963	cryptochrome 2 (photolyase-like)	1.63	-1.43

As mentioned above, the kidney samples of the daytime experiment were hybridised onto the Illumina platform to test additional changes in gene expression apart from circadian rhythm genes during the day. This test revealed that 374 genes were regulated between 12a.m. and 8a.m. with 116 exhibiting increased and 258 decreased expression, and 537 genes were regulated between 8a.m. and 4p.m. with 327 exhibiting increased and 210 decreased expression. The magnitude of changes in gene expression is in the same range expected for aging experiments. The most regulated genes during daytime

in kidney are presented in Table 3.9. In the case that a gene was also significantly regulated in the other part of the day the corresponding ratio is also presented.

Since these results indicated that high numbers of target genes in the aging experiment could be circadian rhythm artefacts, new aging samples were collected with synchronised sample collection on the same day. In the following chapters, the aging process will be discussed using the synchronised samples named as young and aged mouse samples. Wherever the unsynchronised samples are used for comparison analysis the samples will be named synchronised and unsynchronised.

3.3.2 Physical and morphological differences of young and aged mice

Upon the sample collection, the young and aged mice were visually compared for significant differences. Two morphological differences were observed, which are also presented in Figure 3.7.

First, the fur of young mice looked shiny and smooth, whereas with age it became rough and dry and some mice had lost a significant part of their fur. Secondly, most of the aged mice were very fat compared to the young mice. The young mice mostly had no or very small fat deposits compared to the aged mice with quite huge fat deposits.

Figure 3.7 Morphological differences of young and aged mice.

The figure shows morphological differences of (A) aged and (B) young mice. With age, the fur of mice gets rough and dry and most of the older mice show significant increases in fat deposits.

3.3.3 Age-dependent gene expression in mouse brain, heart and kidney

Whole mouse tissues (brain, heart and kidney) were collected from young (10-12 weeks) and aged (17-19 months) female C57BL6 mice. Whole genome gene expression analyses were performed using the Illumina array platform.

As shown in Table 3.1, 828 genes were significantly regulated in mouse brain, 990 genes in heart and 1544 genes in kidney for the chosen criteria. Of these, 581 genes exhibited increased and 247 decreased expression in brain, 569 increased and 421 decreased in heart and 1112 genes showed increased and 432 decreased expression in kidney with age. The most regulated genes are presented in Tables X.5, X.6 and X.7 in appendix III. In addition, DAVID pathway and Gene Ontology analyses provided results for significantly regulated Kegg pathways and GOs for up- and down-regulated genes in brain, heart and kidney. These results are shown in Tables X.12, X.13 and X.14 in appendix IV.

Up-regulated expression in mouse brain correlates with increases in the Kegg pathways antigen processing and presentation (15), type I diabetes mellitus (11), cell adhesion molecules (14) and complement coagulation cascades (9) and with increased biological processes referring to many immune and inflammation-related processes such as antigen processing (16) and presentation (18), immune response (48), inflammatory response (14) and phagocytosis (7) but also to transport (77) and cell organization and biogenesis (52). For down-regulated genes in brain, no Kegg pathways were found. Significantly down-regulated biological processes in brain were for instance cellular physiological process (115), cytoskeleton organization and biogenesis (12), localization (45), development (32) and cell differentiation (17).

In heart, 7 Kegg pathways were up-regulated including like in brain, antigen processing and presentation (18), type I diabetes mellitus (13), cell adhesion molecules (20) and complement coagulation cascades (9) and additionally glutathione metabolism (10), metabolism of xenobiotics by cytochrome P450 (12) and starch and sucrose metabolism (7). Up-regulated biological processes referred as in brain to immune and inflammation-related processes like immune response (60), antigen processing (17) and presentation (19) and inflammatory response (16) and in addition to transport (87). For down-regulated genes in heart, Kegg pathways ECM-receptor interaction (13), focal adhesion (16), cell communication (12) and benzoate degradation via CoA ligation (4) were found. Significantly down-regulated biological processes in heart were

metabolism-related processes like protein (66), phosphorus (25) and macromolecule (78) metabolism, and also cell adhesion (28), protein modification (37) and phosphate transport (6).

In kidney, many Kegg pathways were up-regulated including like in brain and heart antigen processing and presentation (13), type I diabetes mellitus (9) and cell adhesion molecules (20) and additionally for instance T cell (20) and B cell (15) receptor signaling pathway, focal adhesion (22) and apoptosis (11) whereas five metabolism-related pathways were down-regulated including glutathione metabolism (5). Up-regulated biological processes referred again to immune and inflammation-related processes like immune response (66), lymphocyte activation (18) and inflammatory response (18) and additionally to death (42) and apoptosis (37). Metabolism (174) – especially for instance carboxylic acid (28), nitrogen compound (21) and lipid (26) metabolism as well as transport (76) and localization (80) were down-regulated in kidney.

Table 3.10 List of overlapping genes regulated in mouse brain, heart and kidney with age.

Name	Accession	Description	Ratio		
			brain	heart	kidney
Igk-C	XM_132633	---	2.66	1.31	3.58
Slp	NM_011413	sex-limited protein	2.12	2.48	1.89
Slp	NM_011413	sex-limited protein	2.05	1.96	2.03
C4	NM_009780	complement component 4 (within H-2S)	1.77	1.98	1.95
Cd52	NM_013706	CD52 antigen	1.72	1.28	1.44
Fcrl3	NM_144559	Fc receptor-like 3	1.68	1.75	1.68
C3	NM_009778	complement component 3	1.63	1.42	1.39
Lyzs	NM_017372	lysozyme	1.45	0.96	2.28
Bcl2a1a	NM_009742	B-cell leukemia/lymphoma 2 related protein A1a	1.39	1.70	1.94
Irak3	NM_028679	interleukin-1 receptor-associated kinase 3	1.23	0.78	0.87
Igh-1a	XM_354704	---	1.13	3.89	7.33
Psmb8	NM_010724	proteosome (prosome, macropain) subunit, beta type 8	1.04	0.86	0.81
Ii	NM_010545	Ia-associated invariant chain	0.99	1.16	0.95
Bcl2a1b	NM_007534	B-cell leukemia/lymphoma 2 related protein A1b	0.98	1.01	1.84
Rmcs1	NM_207105	response to metastatic cancers 1	0.97	1.30	0.94
Serpina3n	NM_009252	serine (or cysteine) proteinase inhibitor, clade A, member 3N	0.92	2.80	1.37
Ctss	NM_021281	cathepsin S	0.86	0.79	1.88
Ms4a6d	NM_026835	membrane-spanning 4-domains, subfamily A, member 11	0.86	0.84	3.15
Casp1	NM_009807	caspase 1	0.81	0.78	1.16
Temt	NM_009349	thioether S-methyltransferase	0.74	2.13	-2.22
Cd68	NM_009853	CD68 antigen	0.72	0.67	1.50
Ifi205	NM_172648	interferon activated gene 205	0.70	0.96	0.64
Icam1	NM_010493	intercellular adhesion molecule	0.68	0.98	0.61
Fcgr3	NM_010188	Fc receptor, IgG, low affinity III	0.65	0.61	1.30
C1qa	NM_007572	complement component 1, q subcomponent, alpha polypeptide	0.64	0.73	1.18
C1qg	NM_007574	complement component 1, q subcomponent, gamma polypeptide	0.64	0.62	1.16
Tcrb-V8.2	---	---	-0.66	0.99	1.41
Itm2a	NM_008409	integral membrane protein 2A	-0.66	-0.79	-0.73

Table 3.11 List of overlapping pathways and GOs regulated in mouse brain, heart and kidney with age.

Term	Brain		Heart		Kidney	
	up	down	up	down	up	down
Kegg pathways						
TYPE I DIABETES MELLITUS	11	-	13	-	9	5
ANTIGEN PROCESSING AND PRESENTATION	15	-	18	-	13	-
CELL ADHESION MOLECULES (CAMS)	14	-	20	-	20	-
NATURAL KILLER CELL MEDIATED CYTOTOXICITY	9	-	-	-	19	-
COMPLEMENT AND COAGULATION CASCADES	9	-	9	-	-	-
FOCAL ADHESION	-	-	-	16	22	-
GLUTATHIONE METABOLISM	-	-	10	-	-	5
GO – BP						
cellular physiological process	207	119	256	174	387	221
localization	84	45	92	59	131	80
establishment of localization	84	44	92	59	128	79
regulation of programmed cell death	16	9	15	11	28	-
protein metabolism	67	-	85	66	125	-
cellular macromolecule metabolism	65	-	83	64	117	-
intracellular signaling cascade	26	-	33	22	52	-
programmed cell death	19	10	20	-	39	-
apoptosis	18	10	20	-	37	-
regulation of apoptosis	15	9	14	-	27	-
vesicle-mediated transport	12	-	14	12	26	-
regulation of protein metabolism	12	-	11	8	14	-
response to biotic stimulus	55	-	66	-	78	-
defense response	51	-	63	-	74	-
immune response	48	-	60	-	66	-
positive regulation of biological process	24	-	28	-	42	-
death	21	-	23	-	42	-
cell death	20	-	23	-	41	-
antigen presentation	18	-	19	-	14	-
antigen processing	16	-	17	-	9	-
inflammatory response	14	-	16	-	18	-
humoral immune response	14	-	13	-	12	-
regulation of organismal physiological process	13	-	11	-	21	-
behavior	13	-	12	-	19	-
humoral defense mechanism (sensu Vertebrata)	12	-	10	-	9	-
immune cell activation	10	-	11	-	21	-
hemopoietic or lymphoid organ development	9	-	12	-	20	-
hemopoiesis	9	-	10	-	15	-
endocytosis	9	-	9	-	17	-
chemotaxis	7	-	9	-	13	-
transport	77	36	87	53	-	76
phosphate transport	5	4	-	6	-	6
ion transport	-	15	-	20	-	23
metal ion transport	-	8	-	11	-	13
inorganic anion transport	-	5	-	7	-	9
GO – CC						
intracellular organelle	146	79	163	105	251	-
cytoplasm	122	-	118	61	141	105
extracellular region	77	-	98	57	125	-
extracellular space	71	-	91	47	115	-
plasma membrane	51	-	60	-	94	-
cytosol	18	-	14	-	20	-
vacuole	13	-	13	-	13	-
lysosome	13	-	11	-	13	-
lytic vacuole	13	-	11	-	13	-
cell surface	11	-	9	-	20	-
immunological synapse	9	-	12	-	11	-
actin cytoskeleton	8	-	10	-	16	-
endosome	7	-	6	-	8	-

GO = gene ontology; BP = biological process; CC = cellular compartment

Table 3.10 shows genes that exhibited significant regulation with age in all three mouse tissues – brain, heart and kidney. In total, 28 genes were common in the target lists of

significant regulated genes in brain, heart and kidney. 26 of these genes showed increased (25) or decreased (1) expression independent of tissue. Only 2 genes showed different regulation, *Temt* with increased expression in brain and heart and decreased expression in kidney and *Tcrb-V8.2* with increased expression in heart and kidney and decreased expression in brain.

In addition to target gene comparisons, commonly regulated Kegg pathways and GOs were investigated by comparing the output lists. Table 3.11 shows Kegg pathways with significant regulation in at least 2 of the 3 tissues and furthermore biological processes and cellular compartments with similar regulation in all three tissues. Five Kegg pathways exhibited increased expression in 2 or 3 tissues, whereas focal adhesion and glutathione metabolism showed different trends of regulation in heart and kidney. For biological processes, localization exhibited up- and down-regulation in all 3 tissues, many immune and inflammation-related processes showed increased expression and some transport-related processes decreased expression. Finally, only cellular compartments exhibiting up-regulation in all three tissues were found including for instance intracellular organelle, extracellular region and lysosome.

In an additional approach to identify potential candidates for typical aging genes in the three tissues investigated, the target gene lists for brain, heart and kidney aging were compared to the target gene lists of the unsynchronised aging experiments of the corresponding tissue. In brain, 13 genes were overlapping in the two experiments, in heart 50 genes and in kidney 89 genes. Most of these overlapping genes also exhibited the same trend of regulation with age (Figure 3.8). Detailed information of these genes is presented in Tables 3.12, 3.13 and 3.14.

Table 3.12 List of overlapping genes regulated in synchronised and unsynchronised brain samples.

Name	Accession	Description	Ratio	
			synch.	unsynch.
Slp	NM_011413	sex-limited protein	2.12	1.24
Lyzs	NM_017372	lysozyme	1.45	1.19
Psmb8	NM_010724	proteosome (prosome, macropain) subunit, beta type 8	1.04	0.92
Gfap	NM_010277	glial fibrillary acidic protein	0.90	0.80
Casp1	NM_009807	caspase 1	0.81	0.76
Fcer1g	NM_010185	Fc receptor, IgE, high affinity I, gamma polypeptide	0.76	0.63
Temt	NM_009349	thioether S-methyltransferase	0.74	-0.68
H2-Ab1	NM_010379	histocompatibility 2, class II antigen A, beta 1	0.69	0.61
2810046M22Rik	NM_026621	RIKEN cDNA 2810046M22 gene	0.65	-0.74
C1qa	NM_007572	complement component 1, q subcomponent, alpha polypeptide	0.64	0.60
Mtap7	AK008182	microtubule-associated protein 7	0.60	-0.82
Rras2	NM_025846	related RAS viral (r-ras) oncogene homolog 2	-0.74	-0.68
F830002E14Rik	AK089567	---	-1.63	-2.29

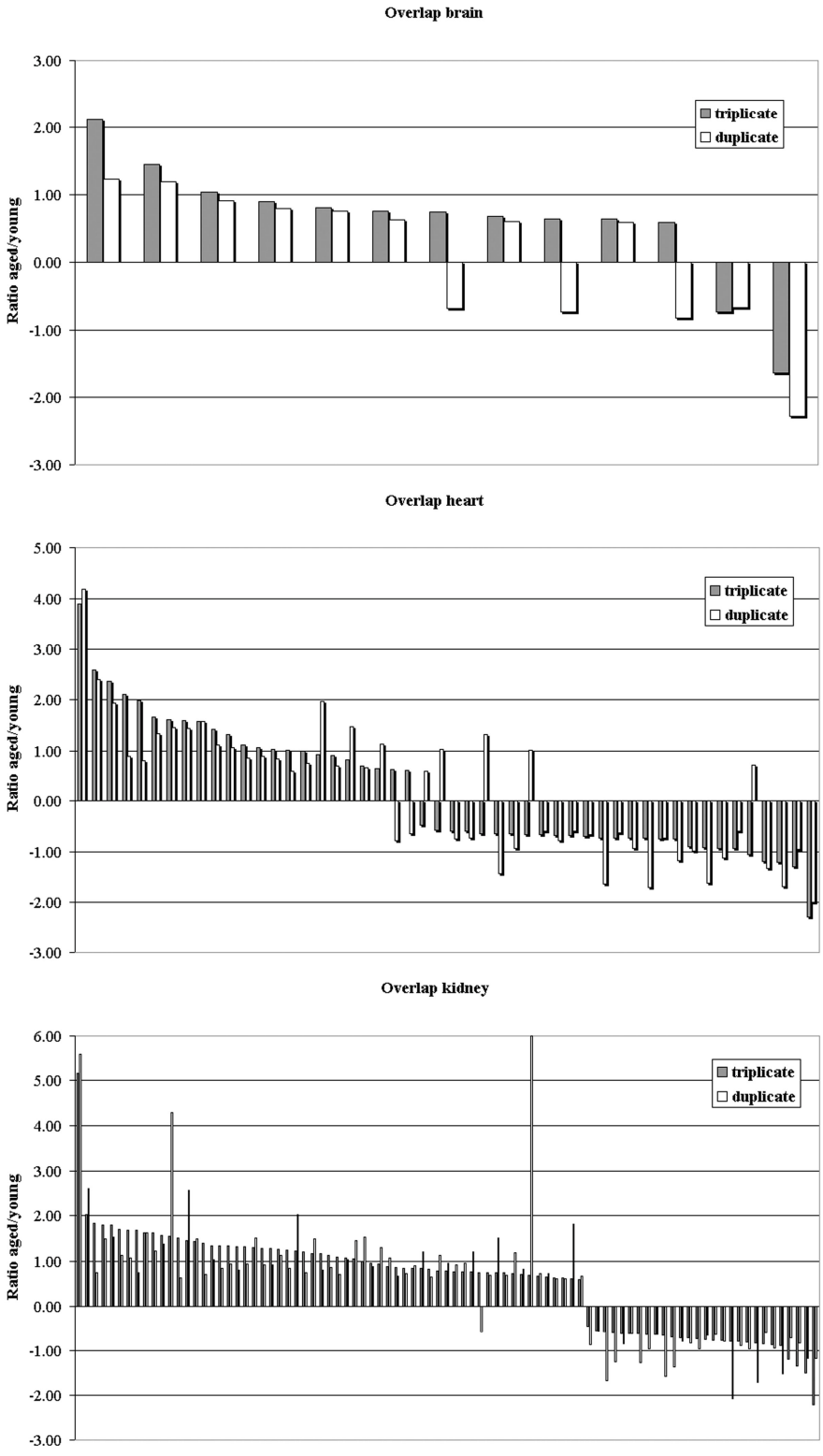

Figure 3.8 Overlapping target genes of synchronised and unsynchronised aging samples.

The histograms show that the overlapping target genes between the two different aging experiments with synchronised (in triplicate) and unsynchronised (in duplicate) sample collection exhibit in most cases the same trend of regulation – increased or decreased expression with age.

Table 3.13 List of overlapping genes regulated in synchronised and unsynchronised heart samples.

Name	Accession	Description	Ratio	
			synch.	unsynch.
Igh-1a	XM_354704	---	3.89	4.19
Mmp3	NM_010809	matrix metalloproteinase 3	2.57	2.39
Cds1	NM_173370	CDP-diacylglycerol synthase 1	2.35	1.93
Tac1	NM_009311	tachykinin 1	2.11	0.89
Gsta2	NM_008182	glutathione S-transferase, alpha 2 (Yc2)	1.98	0.80
Mal	NM_010762	myelin and lymphocyte protein, T-cell differentiation protein	1.65	1.33
Retnla	NM_020509	resistin like alpha	1.60	1.45
Amy2	NM_009669	amylase 2, pancreatic	1.59	1.43
Abat	NM_172961	4-aminobutyrate aminotransferase	1.58	1.56
C3	NM_009778	complement component 3	1.42	1.11
Bdh	NM_175177	3-hydroxybutyrate dehydrogenase (heart, mitochondrial)	1.32	1.05
LOC244682	XM_146640	similar to contactin 5	1.11	0.86
Fcgr2b	NM_010187	Fc receptor, IgG, low affinity IIb	1.05	0.89
Neurl	NM_021360	neuralized homolog (Drosophila)	1.03	0.84
6330405H19	XM_358637	---	1.01	0.59
Hsd11b1	NM_008288	hydroxysteroid 11-beta dehydrogenase 1	0.99	0.76
Idb2	AK013239	inhibitor of DNA binding 2	0.92	1.96
Pparg	NM_011146	peroxisome proliferator activated receptor gamma	0.90	0.71
Slc16a6	NM_134038	solute carrier family 16 (monocarboxylic acid transporters), member 6	0.82	1.46
Ptpn11	NM_011202	protein tyrosine phosphatase, non-receptor type 11	0.70	0.67
1200008A14Rik	AK078433	RIKEN cDNA 1200008A14 gene	0.65	1.12
Gpihbp1	XM_128001	---	0.63	-0.79
Dnajc12	NM_013888	DnaJ (Hsp40) homolog, subfamily C, member 12	0.62	-0.65
Nfib	AK089127	nuclear factor I/B	-0.47	0.60
6720477C19Rik	---	---	-0.59	1.02
LOC194913	XM_110926	similar to ribosomal protein S2	-0.60	-0.76
Hmgn3	NM_175074	high mobility group nucleosomal binding domain 3, transcript variant 1	-0.60	-0.74
1200012P04Rik	AK004731	weakly similar to PLAKOPHILIN 2 [Homo sapiens]	-0.64	1.32
2300009N04Rik	---	---	-0.65	-1.42
Emilin2	NM_145158	elastin microfibril interfacer 2	-0.65	-0.93
9630007P13Rik	AK035818	---	-0.66	1.02
2010305C02Rik	AK008522	---	-0.67	-0.59
B230365C01Rik	AK046289	---	-0.67	-0.79
LOC243268	XM_144526	similar to NADH-ubiquinone oxidoreductase ESSS subunit, mitochondrial precursor	-0.68	-0.59
Rab6	NM_024287	RAB6, member RAS oncogene family	-0.70	-0.66
Prkwnk4	NM_175638	protein kinase, lysine deficient 4	-0.73	-1.63
Wfdc1	NM_023395	WAP four-disulfide core domain 1	-0.73	-0.62
Nono	NM_023144	non-POU-domain-containing, octamer binding protein	-0.74	-0.94
Mlf1	NM_010801	myeloid leukemia factor 1	-0.74	-1.71
2310075M15Rik	XM_283052	RIKEN cDNA 2310075M15 gene	-0.75	-0.73
Ppic	NM_008908	peptidylprolyl isomerase C	-0.75	-1.17
Lamb1-1	NM_008482	laminin B1 subunit 1	-0.91	-0.99
Chchd3	NM_025336	coiled-coil-helix-coiled-coil-helix domain containing 3	-0.91	-1.62
Sparc	NM_009242	secreted acidic cysteine rich glycoprotein	-0.94	-1.13
D430044G18Rik	NM_172628	RIKEN cDNA D430044G18 gene	-0.94	-0.59
C130075A20Rik	---	---	-1.05	0.72
Copg2as2	AK018238	coatomer protein complex, subunit gamma 2, antisense 2	-1.19	-1.33
Col3a1	NM_009930	procollagen, type III, alpha 1	-1.21	-1.69
D0H4S114	NM_053078	DNA segment, human D4S114	-1.30	-0.96
F830002E14Rik	AK089567	---	-2.28	-1.99

In brain, 10 of the 13 overlapping genes exhibited the same trend with 8 genes showing increased and 2 decreased expression with age, in heart, 43 of 50 genes exhibited the same trend with 21 genes showing increased and 22 decreased expression and, in kidney, 88 of 89 genes exhibited the same trend with 60 genes showing increased and 28 decreased expression. Table 3.14 which presents the results for kidney only shows the top 25 genes up- and down-regulated in the synchronised experiments. Genes exhibiting the same trend of regulation with age mostly also showed similar fold-changes of gene expression in all three tissues comparing the 2 data sets.

Table 3.14 List of overlapping genes regulated in synchronised and unsynchronised kidney samples.

Name	Accession	Description	Ratio	
			synch.	unsynch.
AU044919	XM_354705	---	5.15	5.59
Slp	NM_011413	sex-limited protein	2.03	2.62
Bcl2a1b	NM_007534	B-cell leukemia/lymphoma 2 related protein A1b	1.84	0.74
Aldh1a1	NM_013467	aldehyde dehydrogenase family 1, subfamily A1	1.81	1.49
Bcl2a1d	NM_007536	B-cell leukemia/lymphoma 2 related protein A1d	1.80	1.54
Cyp24a1	NM_009996	cytochrome P450, family 24, subfamily a, polypeptide 1	1.69	1.12
Cybb	NM_007807	cytochrome b-245, beta polypeptide	1.69	1.06
Fcrl3	NM_144559	Fc receptor-like 3	1.68	0.73
Cdkn1a	NM_007669	cyclin-dependent kinase inhibitor 1A (P21)	1.63	1.63
Cd68	NM_009853	CD68 antigen	1.62	1.22
Mpeg1	XM_129176	macrophage expressed gene 1	1.57	1.38
A430104N18Rik	---	---	1.55	4.29
Tyrobp	NM_011662	TYRO protein tyrosine kinase binding protein	1.50	0.63
Azgp1	NM_013478	alpha-2-glycoprotein 1, zinc	1.46	2.58
Ltc4s	NM_008521	leukotriene C4 synthase	1.44	1.48
Cp	NM_007752	ceruloplasmin	1.39	0.70
Fcer1g	NM_010185	Fc receptor, IgE, high affinity I, gamma polypeptide	1.34	1.02
AI132321	NM_178911	expressed sequence AI132321	1.33	0.83
Laptm5	NM_010686	lysosomal-associated protein transmembrane 5	1.33	0.94
Il6ra	AK020663	interleukin 6 receptor, alpha	1.32	0.80
LOC226691	XM_129595	similar to Ifi204 protein	1.32	0.94
Slc12a3	AK085430	solute carrier family 12, member 3	1.30	1.51
Cyp4b1	NM_007823	cytochrome P450, family 4, subfamily b, polypeptide 1	1.29	0.92
1200013B08Rik	NM_028773	RIKEN cDNA 1200013B08 gene	1.28	0.92
Coro1a	NM_009898	coronin, actin binding protein 1A	1.27	1.12
Gjb2	NM_008125	gap junction membrane channel protein beta 2	-0.60	-1.25
0610010D20Rik	NM_026152	RIKEN cDNA 0610010D20 gene	-0.62	-0.84
Asb9	NM_027027	ankyrin repeat and SOCS box-containing protein 9	-0.62	-0.61
E230024B12Rik	AK087605	hypothetical protein	-0.62	-1.26
B430216N15Rik	AK046642	hypothetical protein	-0.64	-0.97
5730438N18Rik	NM_027460	RIKEN cDNA 5730438N18 gene	-0.65	-0.64
Slc26a6	NM_134420	solute carrier family 26, member 6	-0.66	-1.58
Cirbp	NM_007705	cold inducible RNA binding protein	-0.69	-1.37
Slc30a2	XM_131731	solute carrier family 30 (zinc transporter), member 2	-0.71	-0.78
C730027J19Rik	NM_178758	RIKEN cDNA C730027J19 gene	-0.72	-0.82
Dlgh2	NM_011807	discs, large homolog 2 (Drosophila)	-0.74	-0.97
D630045J12Rik	XM_485743	---	-0.76	-0.66
Car14	AK009805	carbonic anhydrase 14	-0.77	-0.65
Susd2	NM_027890	sushi domain containing 2	-0.78	-0.79
1700018O18Rik	XM_131683	RIKEN cDNA 1700018O18 gene	-0.79	-2.08
1700013L23Rik	XM_130127	RIKEN cDNA 1700013L23 gene	-0.80	-0.90
AU018778	NM_144930	expressed sequence AU018778	-0.82	-0.96
Hmgcr	XM_127496	3-hydroxy-3-methylglutaryl-Coenzyme A reductase	-0.84	-1.72
4933417C16Rik	NM_172568	RIKEN cDNA 4933417C16 gene	-0.86	-0.60
Xpnpep2	NM_178074	X-prolyl aminopeptidase (aminopeptidase P) 2, membrane-bound	-0.86	-0.94
Rnf24	NM_178607	ring finger protein 24	-0.89	-1.53
Gadd45g	NM_011817	growth arrest and DNA-damage-inducible 45 gamma	-1.19	-0.72
Es22	NM_133660	esterase 22	-1.34	-0.84
9030611N15Rik	NM_134072	RIKEN cDNA 9030611N15 gene	-1.50	-1.18
Temt	NM_009349	thioether S-methyltransferase	-2.22	-1.18

3.3.4 Age-related post-transcriptional and structural changes

In addition to the RNA analyses, post-transcriptional and structural changes with age were investigated in mice using Western blots, Hematoxylin Eosin stained sections and LPO measurements. These are summarized and presented in Figure 3.9 and Table 3.15.

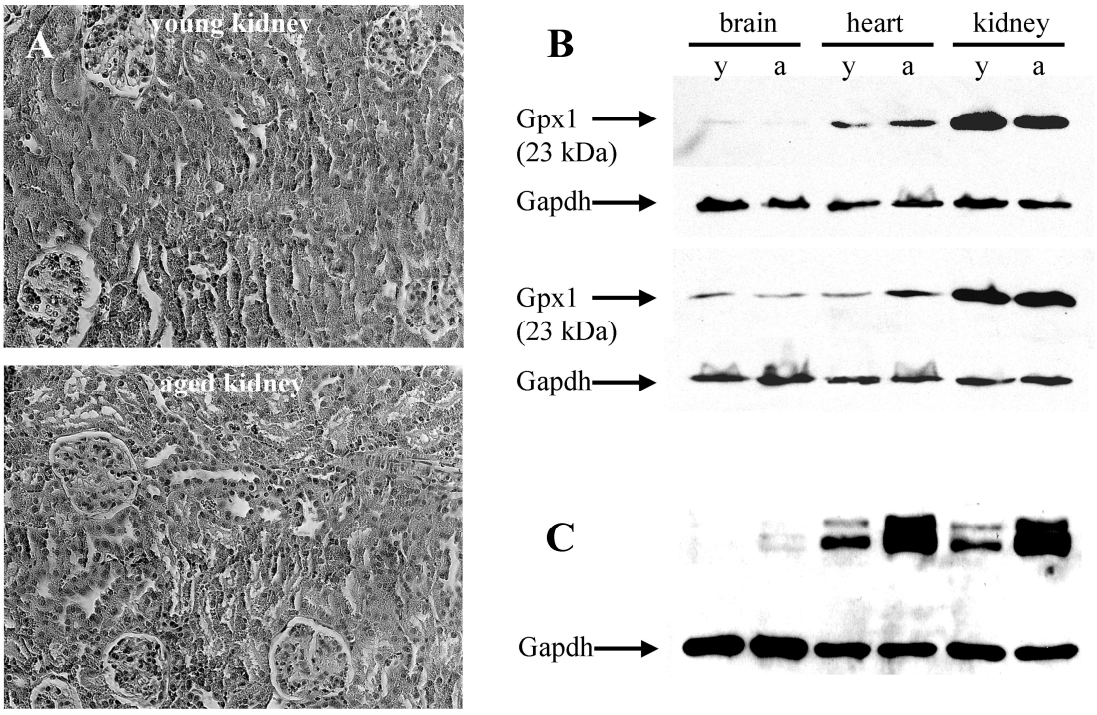

Figure 3.9 Investigations beyond the RNA levels.

(A) Hematoxylin Eosin stained sections of young and aged kidneys did not reveal any structural changes with age. The same results were observed for brain and heart sections (data not shown).

(B) Western blots for glutathione peroxidise 1 (Gpx1) using Gapdh as loading control revealed that changes in gene expression observed for this gene in heart are consistent with the protein expression levels. Gpx1 is up-regulated with age in heart and shows constant expression in brain and kidney. In the upper part of the figure equal concentrations of protein for brain, heart and kidney were loaded on the gel. In the lower part, twice the concentration was loaded for brain and heart compared to kidney.

(C) Western blots for Gapdh revealed that the functional version of this protein is constantly expressed independent of age. Interestingly, modified larger versions of the protein were detected which exhibited increased expression with age in all three tissues.

First, sections of young and aged brain, heart and kidney were prepared to investigate possible structural changes. Hematoxylin Eosin staining of these sections did not reveal any changes with age (Figure 3.9 A).

On the protein level, the protein expression of Gpx1 was investigated to compare the results with the corresponding gene expression (Figure 3.9 B). The increased gene expression of *Gpx1* in heart was confirmed by a similar increase on the protein level. For brain and kidney, no changes in expression were found on the RNA and on the protein level. Additionally, modified larger versions of the used loading control Gapdh were detected, which interestingly accumulate with age (Figure 3.9 C). Although this finding was very exciting the nature of these modifications was not further investigated.

Table 3.15 Results of the LPO measurement.

Tissue	**LPO in µM**	
	young	**aged**
Brain	b.d.l.	3.19 ± 0.05
Heart	b.d.l.	1.02 ± 0.02
Kidney	b.d.l.	1.71 ± 0.03

b.d.l. = below detection limit

Furthermore, lipid hydroperoxide (LPO) concentrations in tissue lysates of whole brain, heart and kidney were measured (Table 3.15). LPO are formed in the presence of radical oxygen species (ROS). Therefore, this measurement is indirectly investigating ROS levels in the tissues. In all three tissues, the LPO concentrations were below the detection limit of this method in the young tissues but detectable in the aged tissues. These results indicate increased ROS levels with age independent of the tissue.

3.4 Comparison of human and mouse aging

3.4.1 Correlation of age-regulated target genes

In order to find potential conserved age-regulated genes, processes, and pathways, the results of the human and mouse aging studies were first investigated for common age-related genes.

To detect genes with age-related regulation in all seven data sets, the overlapping target genes of the *in vitro* and *in vivo* human studies and of the mouse studies were compared using Venn analysis. Figure 3.10 shows that this analysis did not detect a single gene to be regulated in all 7 data sets. Furthermore, overlaps between two of the three target gene lists also revealed no resulting common genes.

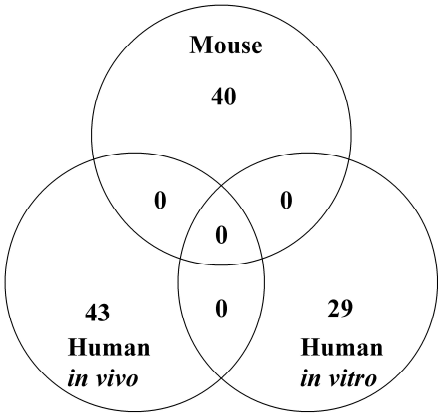

Figure 3.10 Venn diagram visualizing the overlap of common regulated target genes in the mouse *in vivo* and human *in vivo* and *in vitro* samples.

The figure shows the overlaps of age-regulated target genes of the *in vitro* and *in vivo* human studies and of the mouse studies. The used target gene lists represent the overlaps of target genes of the human sebocytes and fibroblast studies (Human *in vitro*; Table 3.3), of the male and female skin biopsies studies (Human *in vivo*; Table 3.5), and of the mouse brain, heart and kidney studies (Mouse; Table 3.10). The Venn diagram showed that there is no overlap between these three target gene lists.

For a more detailed picture, 4-way Venn diagram analyses were performed to investigate overlaps between the single human data sets and the three mouse data sets. The results presented in Figure 3.11 show that some target genes are common between the different human and mouse studies. In addition to the presented comparisons of the human data sets to all three mouse tissues, the resulted overlapping target genes with the

single mouse tissues were compared to the corresponding target lists. For instance, the four resulted overlaps of mouse brain with fibroblasts, sebocytes, male skin biopsies and female skin biopsies were also compared using 4-way Venn diagrams (data not shown). Finally, this whole analysis revealed that genes regulated in both the mouse and the human studies were present in a maximum of 4 different target gene lists. The genes present in 4 lists were *CASP1/Casp1* (Mouse brain, heart and kidney, and human female skin biopsies), *COL1A1/Col1a1* (Mouse heart and kidney, and human male and female skin biopsies), *LCP1/Lcp1* (Mouse brain, heart and kidney, and human sebocytes), *PGLS/Pgls* (Mouse kidney, human male and female skin biopsies, and sebocytes), and *TYROBP/Tyrobp* (Mouse brain and kidney, human sebocytes, and fibroblasts).

Figure 3.11 4-way Venn diagrams visualizing the detailed overlap of regulated target genes in the mouse *in vivo* and human *in vivo* and *in vitro* samples.

The figure shows the overlaps of age-regulated target genes of the three mouse tissues (brain, heart and kidney) with human male skin biopsies (A), female skin biopsies (B), fibroblasts (C), and sebocytes (D). The target gene lists used are partially presented in appendix III. The Venn diagrams show all possible overlaps of the target gene lists. The number in column 3 and row 3 represents for instance the overlap of all 4 lists.

3.4.2 Correlation of age-regulated Kegg pathways and Gene Ontologies (BP and CC)

In addition to the gene wise comparisons of human and mouse aging, the results of the human and mouse aging studies were investigated for common age-related Kegg pathways, biological processes and cellular compartments.

To detect Kegg pathways with age-related regulation in all seven data sets, the overlapping pathways of the *in vitro* and *in vivo* human studies and of the mouse studies were compared using Venn analysis. Figure 3.12 shows that the overlaps in the three different comparisons were minor with 3 in mouse, 1 in human *in vivo* and 0 in human *in vitro*, and that the 1 detected in human was different to the 3 detected in mouse.

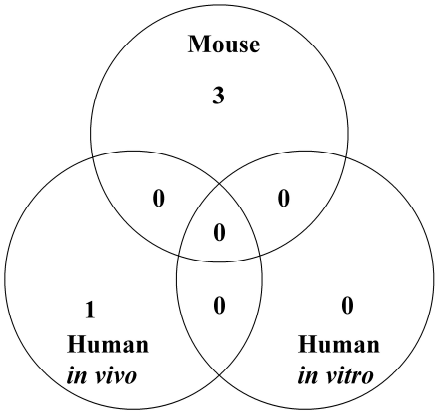

Figure 3.12 Venn diagram visualizing the overlap of common regulated Kegg pathways in the mouse *in vivo* and human *in vivo* and *in vitro* samples.

The figure shows the overlaps of age-regulated Kegg pathways of the *in vitro* and *in vivo* human studies and of the mouse studies. The used lists represent the overlaps of Kegg pathways of the human sebocytes and fibroblast studies (Human *in vitro*), of the male and female skin biopsies studies (Human *in vivo*; Table 3.6), and of the mouse brain, heart and kidney studies (Mouse; Table 3.11). The Venn diagram showed that there is no overlap.

For a more detailed picture, 4-way Venn diagram analyses were performed to investigate overlaps between the single human data sets and the three mouse data sets. The results presented in Figure 3.13 show that some Kegg pathways are common between the different human and mouse studies. In addition to the presented comparisons of the human data sets to all three mouse tissues, the resulted overlapping pathways with the single mouse tissues were compared to the corresponding target lists (data not shown). This analysis revealed that pathways regulated in both the mouse and the human studies were cell adhesion molecules (Mouse brain, heart and kidney, and

human female skin biopsies), focal adhesion (Mouse heart and kidney, and human male skin biopsies), glutathione metabolism (Mouse heart and kidney, and human fibroblasts) and 6 additional pathways, which were regulated in a single human and a single mouse study (Arginine and proline metabolism, alanine and aspartate metabolism, nitrogen metabolism, hematopoietic cell lineage, cell communication, and ECM receptor interaction).

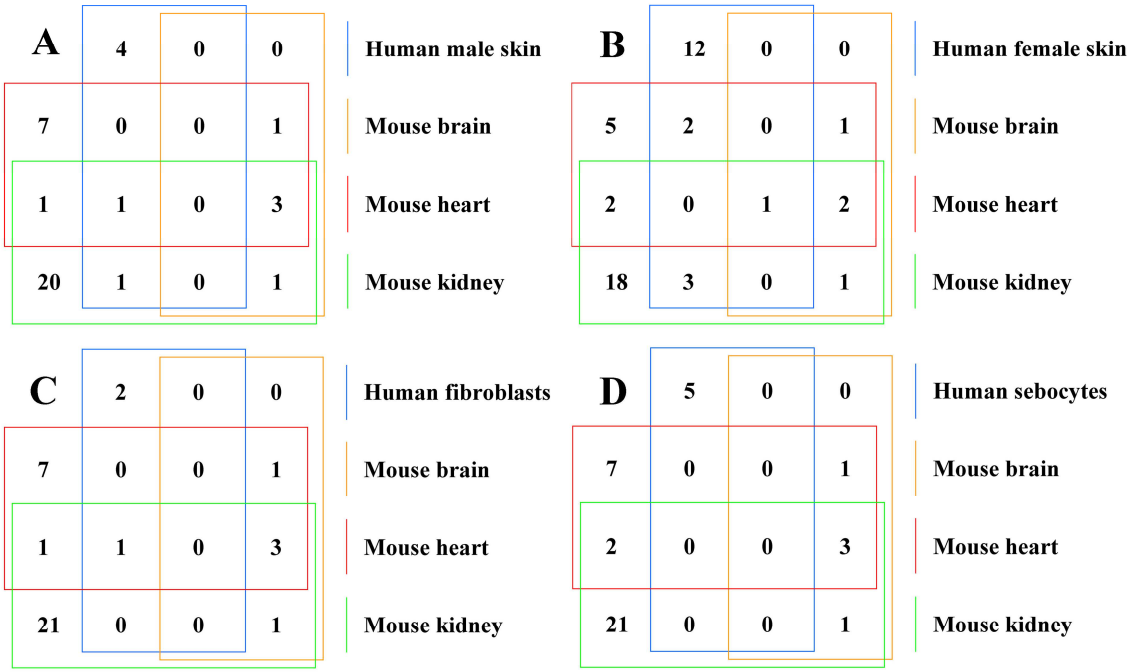

Figure 3.13 4-way Venn diagrams visualizing the detailed overlap of regulated Kegg pathways in the mouse *in vivo* and human *in vivo* and *in vitro* samples.

The figure shows the overlaps of age-regulated Kegg pathways of the three mouse tissues (brain, heart and kidney) with human male skin biopsies (A), female skin biopsies (B), fibroblasts (C), and sebocytes (D). The lists of Kegg pathways used are presented in appendix IV. The Venn diagrams show all possible overlaps of the lists of Kegg pathways. The number in column 3 and row 3 represents for instance the overlap of all 4 lists.

To detect biological processes with age-related regulation in all seven data sets, the overlapping biological processes of the *in vitro* and *in vivo* human studies and of the mouse studies were compared using Venn analysis. Figure 3.14 shows that 2 processes were present in all 7 data sets – these were cellular physiological process and protein metabolism. Furthermore, 3 additional processes were common between human *in vivo* and *in vitro* (macromolecule metabolism, metabolism, and protein modification), 5 between human *in vivo* and mouse (cell adhesion, cellular macromolecule metabolism,

development, inorganic anion transport, and phosphate transport) and 1 between human *in vitro* and mouse (intracellular signaling cascade).

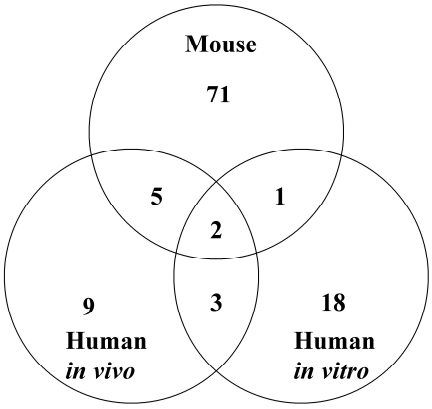

Figure 3.14 Venn diagram visualizing the overlap of common regulated biological processes in the mouse *in vivo* and human *in vivo* and *in vitro* samples.

The figure shows the overlaps of age-regulated biological processes of the *in vitro* and *in vivo* human studies and of the mouse studies. The used lists represent the overlaps of biological processes of the human sebocytes and fibroblast studies (Human *in vitro*; Table 3.4), of the male and female skin biopsies studies (Human *in vivo*; Table 3.6), and of the mouse brain, heart and kidney studies (Mouse; Table 3.11). The Venn diagram showed that there are some overlaps between these three lists.

For a more detailed picture, 4-way Venn diagram analyses were performed to investigate overlaps between the single human data sets and the three mouse data sets. The results presented in Figure 3.15 show that various biological processes are common between the different human and mouse studies. In addition to the presented comparisons of the human data sets to all three mouse tissues, the resulted overlapping pathways with the single mouse tissues were compared to the corresponding target lists (data not shown). This analysis revealed many processes regulated in both the mouse and the human studies. In addition to the above mentioned processes regulated in all 7 data sets, 4 were regulated in 6 – development (Mouse brain, heart and kidney, human male and female skin biopsies, and sebocytes), macromolecule metabolism, metabolism, and protein modification (Mouse heart and kidney, human male and female skin biopsies, sebocytes, and fibroblasts) – 14 processes were regulated in 5 – cell adhesion, cellular macromolecule metabolism, inorganic anion transport, phosphate transport, apoptosis, cell death, death, programmed cell death, morphogenesis, intracellular signaling cascade, cellular process, negative regulation of programmed cell

death, physiological process, and protein amino acid phosphorylation – and many other processes in 4 data sets.

Figure 3.15 4-way Venn diagrams visualizing the detailed overlap of regulated biological processes in the mouse *in vivo* and human *in vivo* and *in vitro* samples.

The figure shows the overlaps of age-regulated biological processes of the three mouse tissues (brain, heart and kidney) with human male skin biopsies (A), female skin biopsies (B), fibroblasts (C), and sebocytes (D). The lists of biological processes used are partially presented in appendix IV. The Venn diagrams show all possible overlaps of the lists of biological processes. The number in column 3 and row 3 represents for instance the overlap of all 4 lists.

To detect cellular compartments with age-related regulation in mouse and human only the results for the human *in vivo* studies and the mouse studies were investigated. The two lists of overlapping cellular compartments were compared using 2-way Venn analysis. Figure 3.17 shows that 1 compartment was present in the five analysed data sets – cytoplasm.

For a more detailed picture, 4-way Venn diagram analyses were performed to investigate overlaps between the two single human data sets and the three mouse data sets. The results presented in Figure 3.18 show that some cellular compartments are common between the different human and mouse studies. In addition to the presented comparisons of the human data sets to all three mouse tissues, the resulted overlapping

pathways with the single mouse tissues were compared to the corresponding target lists (data not shown).

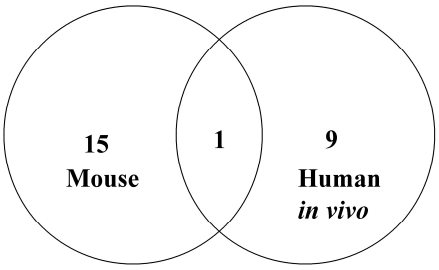

Figure 3.16 Venn diagram visualizing the overlap of common regulated cellular compartments in the mouse *in vivo* and human *in vivo* samples.

The figure shows the overlaps of age-regulated cellular compartments of the *in vivo* human studies and of the mouse studies. The used lists represent the overlaps of cellular compartments of the male and female skin biopsies studies (Human *in vivo*; Table 3.6) and of the mouse brain, heart and kidney studies (Mouse; Table 3.11). The Venn diagram showed that there is 1 overlap between the two lists, which is cytoplasm.

This analysis revealed that, in addition to the above mentioned cytoplasm regulated in all 5 data sets, no compartment was regulated in 4, but 8 were regulated in 3 – intracellular membrane-bound organelle, membrane-bound organelle, collagen, extracellular matrix, extracellular matrix (sensu metazoa), mitochondrion, golgi apparatus, and nucleus.

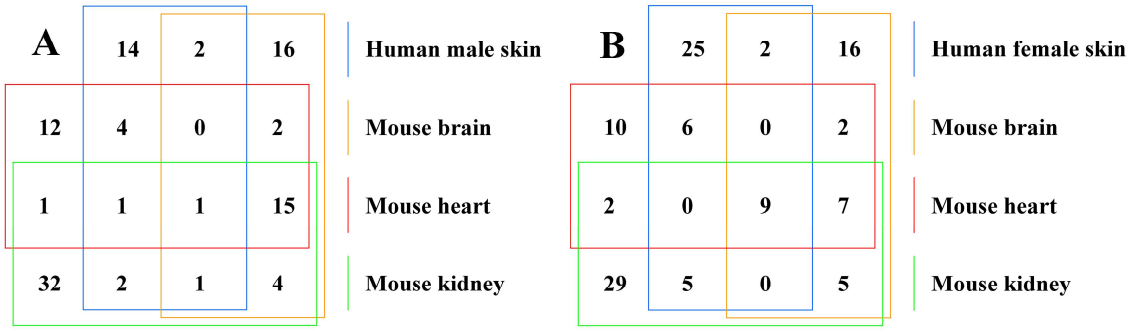

Figure 3.17 4-way Venn diagrams visualizing the detailed overlap of regulated cellular compartments in the mouse *in vivo* and human *in vivo* samples.

The figure shows the overlaps of age-regulated cellular compartments of the three mouse tissues (brain, heart and kidney) with human male skin biopsies (A), and female skin biopsies (B). The Venn diagrams show all possible overlaps of the lists of cellular compartments. The number in column 3 and row 3 represents for instance the overlap of all 4 lists.

3.4.3 Correlation of target genes to published data

Finally, the results of the described studies in this work were compared to published data by gene wise correlations. The target gene lists of the *in vitro* and *in vivo* human studies were compared to the target gene list of a study (Lener et al. 2006) investigating human skin aging by comparing foreskin samples of young (3-4 years) and old (68-72 years) patients using cDNA microarrays, which led to a target list of 102 age-regulated genes. The results of these comparisons are presented in Table 3.16.

Table 3.16 List of overlapping target genes in Lener et al. (2006) and the investigated human skin samples.

Lener et al. vs.	Fold change	
	Human data	Lener et al.
Male skin biopsies		
FLRT2	**0.70**	**0.50**
SMARCA1	**0.75**	**0.44**
ST14	**1.48**	**1.71**
Female skin biopsies		
CASP1	1.34	0.52
KRT2A	**0.65**	**0.44**
KRT6A	0.43	2.12
MXD1	0.66	1.80
SERPINB2	0.48	1.81
TGFA	0.64	1.96
WISP2	0.50	4.46
Fibroblasts		
FOSB	1.69	0.30
IGFBP3	1.98	0.47
MYC	**0.33**	**0.56**
Sebocytes		
ABLIM	**1.40**	**2.24**
FDFT1	0.69	1.88
KIAA1404	1.34	0.56
STAT3	0.72	2.12
THBS1	1.38	0.51
UGCG	0.63	1.83

The Table shows all the overlapping target genes between the different data sets. Genes showing the same trend of regulation in the two target gene lists are highlighted in bold. Although the comparison between Lener et al. and the male skin biopsies showed only 3 genes, these genes were all showing the same trend. In comparison, the other three data sets showed the same or higher numbers of overlapping target genes, but with only 1 gene the correlation of the trend of regulation was weak.

The target gene lists of the mouse studies were compared to the age-regulated target genes of the AGEMAP database (Zahn et al. 2007) investigating mouse aging in 9 different mouse tissues by calculating an age-coefficient using 4 different time points in life. The results of these comparisons are presented in Table 3.17.

Table 3.17 List of overlapping target genes in the AGEMAP database and the investigated mouse tissues (brain, heart, kidney).

AGEMAP vs.	Mouse data		
	Brain	**Heart**	**Kidney**
Adrenals	**Arfip2**	**1500015O10Rik**, BC022145, **Mcrs1**, *Nme4*	**3300001P08Rik**, **9030611N15Rik**, ***Nme4***
Cerebellum	*Pcolce2*	-	Ndn
Eye	**Asah2**, ***Lyzs***, ***Tap2***	6530402N02Rik, ***AI987712***, Acta2, ***Col1a2***, Cryab, Gstm2, ***Lyzs***, Rab6, **Rnf25**, **Serhl**, ***Tap2***, ***Tdrkh***	*AI987712*, Car2, ***Lyzs***, Slc5a10, ***Tap2***, ***Tdrkh***, **Trim46**, Trpm7
Gonads	***F11r***	***Col1a2***, **E430002G05Rik**, Rps14, ***Sparc***	**Ap2a2**, **Cd44**
Heart	-	***Col1a2***, Sec63	**Hmgcr**, **Slc39a4**
Lung	**Arid4a**, ***BC005662***, **Wasf2**	**Adamts2**, ***Catnb***, ***Col1a2***, Hba-a1, ***Igh-6***, Rp9h, ***Sparc***	A630082K20Rik, Anxa6, *Catnb*, **Cdkn1c**, Cyhr1, **Ell3**, ***Igh-6***
Spleen	**Tgfbr3**	***Igh-6***, ***Txndc5***	***Igh-6***, ***Txndc5***
Spinal Cord	***4930553M18Rik***, **A2m**, ***B2m***, ***C1qa***, **D14Ertd449e**, Enpp1, **Entpd5**, ***Ifitm3***, **Mt2**, *Opa1*, **Rpl27a**, **Rps20**	**2010315L10Rik**, ***B2m***, ***C1qa***, ***Ifitm3***, Nono	***C1qa***, Etv5, *Opa1*
Thymus	*4930553M18Rik*, *BC005662*, BC021395, Bcat1, **C630016B22Rik**, ***Csf1***, ***F11r***, ***Icsbp1***, **Myo1d**, **Ntrk2**, ***Pcolce2***, ***Rbpms***, Tcf19, Vil2	***2310004N11Rik***, **C130086A10**, Cutl2, Eef2, Gnai2, ***Jam2***, ***Klf7***, **Ninj1**, Pip5k1b, Prickle1, **Ptpn11**, Rab8a, **Rbm14**, ***Rbpms***, *Selpl*, Tubb5, ***Vcam1***	***2310004N11Rik***, 4732418C07Rik, Apob, Cfl1, ***Csf1***, Fbxo7, **Foxo1**, Grip1, Hgd, **Hip1**, ***Icsbp1***, Ilf2, ***Jam2***, ***Klf7***, Mocs1, **Nfkb1**, **Phgdh**, *Selpl*, **Tnfrsf12a**, ***Vcam1***

The Table shows all the overlapping target genes between the different data sets. Genes showing the same trend of regulation in the two target gene lists are highlighted in bold. Genes present in 2 or more of the determined overlaps are shown in italics.

4. Discussion

4.1 Global data analysis

The studies presented in this work are mainly aimed to highlight age-related changes in molecular processes on the transcriptional level in human and mouse by the use of whole genome microarray analysis. The human studies are focussed on aging processes in the skin, whereas the aging processes in mouse are analysed in whole tissues of brain, heart, and kidney. In both cases the age-related changes are defined as changes in gene expression between two different age groups. The *in vitro* models of human skin aging using sebocytes and fibroblasts compare female samples corresponding to the ages of 20 and 60 years of life. The *in vivo* skin biopsies from male and female patients include a young group ranging from 18 to 32 years and an old group ranging from 67 to 97 years. The mouse aging studies are based on young female mice with the age of 8-10 weeks and aged female mice with the age of 17-19 months.

With regards to the use of microarrays, two key aspects are of major importance before discussing the homologies and differences of age-related processes in the investigated human and mouse systems: the comparability of the data and the setting of threshold cut-offs.

Comparability

With regards to comparability, different factors have to be considered for the analyses carried out in this study, which are the use of different platforms (ENSEMBL and Illumina), different species (human and mouse), different sexes (male and female), and different cells/tissues (sebocytes, fibroblasts, skin, brain, heart, and kidney), and in addition technical and biological heterogeneity within the replicates.

The two microarray-platforms used in this study differ for instance in the number of genes represented. The human ENSEMBL chip contains cDNA tags for around 15000 genes, whereas the Illumina beadchip contains oligonucleotide tags for nearly all known human or mouse genes, respectively. Therefore, results obtained by using the Illumina beadchip may not be detectable by using the ENSEMBL chip. As the different platforms were used for different samples, it is not possible to compare the results of biologically identical experimentation and thus to critically address the

technical heterogeneity. Another possible source of error between the platforms is the employed and possible different nomenclature for the genes.

The use of different species, sexes, and cells/tissues leads to biological differences that may have a higher impact on gene expression compared to the investigated process, which in this case is aging. Species comparisons for instance are problematic because they do not completely share the same genome and even homologous genes may differ in their nomenclature. However, in the case of human and mouse at least most of the homologous genes share an identical name. But even homologous genes in different species may have varying impact on certain processes. The same problems exist for the investigation of different cells/tissues. Although, different tissues of the same species share the same genome the actual use of it may largely differ due to tissue-specific gene silencing and expression, and also the function of a gene can be different in different tissues. Gender differences do not show this high impact on gene expression but at least gender-specific genes on chromosomes X and Y may largely differ and as aging is a hormone-dependent process the aspect of different hormone levels may also account for transcriptional variations.

Another source of error are technical and biological heterogeneity within single experiments, e.g. mouse brain aging. Most technical variations can be eliminated by standardized experimentation. Ideally, always the same people should perform the cell cultures, sample collection, RNA isolations, and hybridisations and if possibly on the same day, which was realized for this work. Biological variations are easy to eliminate for cell culture and can be good controlled for mouse experiments. In mice, however, it is possible that some of the mice sleep, eat or drink shortly before they are sacrificed in contrast to the others, which may cause variations. In human, different life styles (e.g. alcohol and smoking) and environments (e.g. living in the city or the hinterland) may account for differential gene expression. In this work, it was additionally impossible to control the exact age of the two age-groups for the human skin biopsies study, causing even heterogeneity between biological replicates within the analysed process of aging.

A good example for a technical variation, which leads finally to a biological variation, is described in this work (*3.3.1 Synchronizing the sample collection*). The unsynchronised sample collection of tissues of young and aged mice leads to changes in the expression of genes involved in the control of the circadian clock. The problem emerges because the sample collections of two different biological groups, young and aged, are separated from each other, which consequently leads to the significant

biological finding of regulations in the circadian rhythm, which ultimately superimposes the aging processes.

Setting of relevant thresholds

The setting of thresholds is an artificial definition of certain parameters. In the case of microarrays two main values are of special interest: the expression of a gene in a single sample or a group of replicates and the differential expression of a gene in a comparison of two groups of samples. Therefore, the signal over noise has to be set to a threshold where the gene is defined as significantly expressed and the p-value of differential expression has to be set to a threshold where the change in gene expression is defined as significantly regulated. For this work, in the ENSEMBL chip analyses the same settings are used like in previous published studies (Adjaye et al. 2004; Makrantonaki et al. 2006) and in the Illumina beadchip analyses the default settings of the Illumina beadstudio 1.0 software are used as recommended by the manufacturer.

In addition to these two thresholds in most microarray studies a third parameter is set to a certain value that is the fold-change of expression between the two investigated sample groups. Many scientists argue that the threshold of fold-changes should be set at least to 2-fold to ensure significant findings. As this is an artificial value, however, this is not done in all the available published studies.

Microarray studies investigating the aging process in mice, for instance, have shown that the changes in gene expression with age are minor. In the first set of studies from 1999 to 2001 (Lee et al. 1999; Lee et al. 2000; Cao et al. 2001; Jiang et al. 2001) a cut-off for ratios of 1.7-2.1-fold was used, which led to up to 100 significantly regulated genes. Later studies used either a smaller cut-off ratio of 1.4-fold (Misra et al. 2007) or no cut-off ratio (Amador-Noguez et al. 2004; Fu et al. 2006; Edwards et al. 2007; Zahn et al. 2007) to define significantly regulated genes. These studies therefore presented larger lists of age-regulated genes of some hundreds to more than thousand.

In this work, a cut-off ratio of 1.3 was used with good reason. With the goal to find not only age-regulated genes but also biological processes and pathways target gene lists of more than 100 genes are needed to obtain significant results. To find for example conserved age-related processes the strategy to decrease the stringency may improve the chance to find them. It is of course important to validate those findings independently.

4.2 Human skin aging

In this work, human aging is investigated by age-related transcriptional changes in the skin. The *in vitro* and *in vivo* studies are both aimed at understanding and analysing the endogenous or intrinsic part of skin aging. Intrinsic skin aging is caused by genetics, hormonal and metabolic processes (Rittie and Fisher 2002). Consequently, as it is known that hormone levels decline with age (Roshan et al. 1999) the *in vitro* studies are based on hormonal treatments of cell cultures, which mimic the *in vivo* situation of 20 and 60 year-old females respectively (Makrantonaki et al. 2006). The *in vitro* studies include cultures of the immortalized human sebocyte line SZ95 (Zouboulis et al. 1999) and primary cultures of human skin fibroblasts. In addition, *in vivo* skin biopsies from the sun-protected inner side of the upper arm are used to avoid extrinsic effects which are mainly caused by UV-light (Marionnet et al. 2003).

The discussion on human skin aging will focus mainly on the results of the *in vivo* experiments and will include comparisons with the *in vitro* data. Nevertheless, some interesting details of the sebocyte and fibroblast data will be discussed in the following paragraphs.

***In vitro* sebocytes and fibroblasts**

The results of hormone-treated cell cultures revealed that there is a higher degree of gene regulation in sebocytes compared to fibroblasts. This result may be explained by the finding that the sebaceous gland acts as a target and source of hormones (Ohnemus et al. 2006) in contrast to dermal fibroblasts. However, recent studies have shown that hormones may influence a variety of human skin cells during the aging process including also dermal fibroblasts (Stevenson and Thornton 2007; Detti et al. 2008).

Sebocytes are highly specialised cells in the sebaceous glands that produce sebum, which supplies hairs and skin with lipids (Kanitakis 2002). As the skin becomes dry with age and as it was shown that sebaceous glands exhibit an age-related reduced secretory output, which leads to decreases in surface lipid levels (Pochi et al. 1979) it is of key interest whether lipid-related processes are influenced by the decline of hormones. In fact, the biological processes lipid biosynthesis and lipid metabolism are significantly down-regulated upon hormonal decline. Additionally, some of the key genes that are for instance involved in cholesterol biosynthesis (*DHCR7*, *FDFT1*, and

MVD) and fatty acid metabolism (*LYPLA1*) show decreased expression, which was also validated by Real-Time PCR. We have already published the sebocytes data (Makrantonaki et al. 2006).

In fibroblasts, due to the relative small number of age-regulated target genes only a few pathways and biological processes exhibit significant regulation. However, these findings give rise to an interesting hypothesis on what hormonal decline causes in fibroblasts. Genes involved in protein modifications are down-regulated in the investigated fibroblasts. It has been shown that protein modifying genes are likely to be regulated by hormones (Medvedova et al. 2003). This down-regulation could be a direct downstream effect of the decreased hormone levels. Two of these genes are for instance *SETD7*, a histone methyl transferase (Xiao et al. 2003), and *PLOD3*, a collagen lysyl hydroxylase (Ruotsalainen et al. 2001), both modifying lysine residues. In addition, free lysine residues can react with sugars and ultimately form advanced glycation end products (AGEs), which cannot be degraded by the cells. These AGEs are reported to accumulate with age (Lohwasser et al. 2006; Kuhla et al. 2007) and there is evidence that AGEs are formed in collagens (Monnier et al. 2005; Pageon and Asselineau 2005) and histones (Cervantes-Laurean et al. 1996; Wondrak et al. 2000). Furthermore, AGEs are a possible source of increased ROS levels (Verbeke et al. 2001), which could lead to an activation of ROS-regulating systems like glutathione metabolism, which is significantly up-regulated in the fibroblast data. Interestingly, protein biosynthesis is up-regulated, which could indicate an increased production of proteins due to the accumulation of glycated and therefore dysfunctional proteins. However, the increase in ROS and AGEs in the hormone-treated fibroblast is highly hypothetical and needs therefore further validation.

The comparison of regulated genes in sebocytes and fibroblasts shows no significant overlap in regulation of those genes. Although nearly 40 genes are regulated in both cell types the trend of regulation is only the same for about half of these genes. In addition, the overlap of biological processes exists mostly of global processes relevant for e.g. cell proliferation, cell maintenance and metabolism.

In vivo skin biopsies

The results of the analyses in human skin biopsies in males and females revealed a higher degree of regulation in the females compared to males, especially for genes down-regulated with age. Although there is not a definite argument to explain this

difference, the influence of varying hormone-levels in males and females, and additionally the sex-specific decline with age, might account for the observed variations (Dao and Kazin 2007). In this regard, it should also be kept in mind that the female volunteers did not exhibit synchronised period upon sample collection but that the group of old females were selected to be post-menopausal.

Analyses on the single gene level revealed only 43 overlapping genes between male (383) and female (870) skin aging. However, these overlapping genes exhibited high similarity in regulation and, as many of the other target genes were close to the threshold of a 1.3 fold-change, it is likely that many genes were missed out because of minor differences. In addition, the global picture of the analysis of regulations in biological processes and pathways showed that these were also mostly overlapping or were specific processes belonging to a similar cluster. The only up-regulated pathway in males, for instance, was the arginine and proline metabolism, and in females 5 of 6 up-regulated pathways were other specific metabolisms. Therefore, the discussion on human skin aging will be focussed on conserved mechanisms in male and female.

As expected, the overlapping genes also directly correlated with the observed overlap of biological processes, cellular compartments, and Kegg pathways. The analysis of cellular compartments showed for instance that extracellular matrix and especially collagen-related genes were down-regulated with age. In addition, related biological processes like cell adhesion validated this decrease with age. In the list of overlapping genes, 8 genes that contribute to the extracellular region were present and 7 of them exhibited decreased expression with age. In this context, it is important to mention that additional experiments performed by collaborators (publication on *in vivo* skin aging is in preparation) using different stainings on female skin sections revealed a loss of structure in both the dermis and the epidermis of female skin. Conserved down-regulated genes related to the extracellular matrix are the collagens *COL1A1*, *COL1A2*, *COL3A1*, and *COL8A2*, the collagen-binding factor *TGFBI*, matrilin 4 *MATN4*, and the extracellular receptor *KIT*. The loss of collagens in aged skin is an accepted fact (Uitto 2008). Interestingly, dehydroepiandrosterone (DHEA), the most abundantly produced human adrenal steroid, which exhibits significantly reduced levels with age (Nouveau et al. 2008), was shown to directly increase procollagen synthesis, and to inhibit collagen degradation (Shin et al. 2005). Therefore, the decrease in extracellular structure especially through reduced collagen synthesis may be a direct effect of decreased hormone-levels with age.

Another down-regulated group of biological processes were those related to transport. Overlapping transport-related genes were for instance the solute carriers *SLC22A15* and *SLC35F1*. In addition, 2 genes with important known skin-related transport functions were also down-regulated: First, *OCA2*, a transport gene involved in pigmentation (Sturm et al. 2001), which may indicate a contribution to the formation of e.g. age spots or a decrease in melanocytes cellularity; and secondly, *ABCG1*, a member of the ATP-binding cassette transporters, responsible for macrophage cholesterol and phospholipid transport and ultimately for cellular lipid homeostasis (Baldan et al. 2006). In contrast to the decreased expression of *ABCG1*, the analysis of biological processes revealed increased expression of cellular lipid metabolism. Although this was unexpected, as skin is getting dry with age, 2 lipid-related genes, *CPT1B* and *FLJ20920* validated the increased expression of lipid metabolism in males and females. However, the analysis of hormone-treated sebocytes, the specialised cells responsible for providing lipids to the skin, revealed decreased expression of lipid-related processes. Therefore, it is possible that the loss of lipids of aged skin is solely related to a loss of function of skin sebocytes.

Another interesting conserved gene, which showed increased expression with age, is *ALDH4A1*. This gene has a p53-dependent protective role against cellular stress and especially overexpression of the gene showed significantly lower intracellular ROS levels after treatment with hydrogen peroxide or UV compared to controls (Yoon et al. 2004). Additionally, this gene is like the 2 above-mentioned up-regulated genes *CPT1B* and *FLJ2090* located in the mitochondria, the only cellular compartment, which showed increased regulation of related genes with age. These findings indicate an expected increase of ROS in old skin compared to the young, which is also underscored by the observed potential increase of ROS in hormone-treated fibroblasts.

The only conserved Kegg pathway was the WNT signaling pathway, which exhibited decreased regulation with age. In addition to this, the GO-annotated biological processes WNT receptor signaling and the related frizzled signaling pathways were part of the conserved findings. The list of overlapping genes also revealed 4 genes of the WNT signaling pathway – *AXIN2*, *CPZ*, *NKD1*, and *WIF1*. The WNT signaling pathway is mainly discussed and investigated in cancer, stem cells (Brink et al. 2008), and differentiation, as it is essential during embryogenesis (Dreesen and Brivanlou 2007). Recently however, the WNT signaling pathway has raised some interest in aging

research, although its main contribution to the aging process remains unknown and controversially discussed (Carlson et al. 2008; DeCarolis et al. 2008).

Last but not least, the sirtuin *SIRT6* showed increased expression in males and females. Sirtuins were related to the aging process in many species. *Sir2* the *S. cerevisiae* homologue for instance is known to play a critical role in the regulation of life span of yeast (Lombard et al. 2008) and mice deficient in *Sirt6* exhibit shortened life span and a premature aging-like phenotype (Mostoslavsky et al. 2006). Recently, the gene was proposed to contribute to the propagation of a specialized chromatin state at mammalian telomeres, which in turn is required for proper telomere metabolism and function (Michishita et al. 2008). Since telomere shortening is one of the mechanisms previously related to the aging process, increased expression of this gene might be the cellular answer to shortened telomeres in old human skin.

Human skin aging conclusion

Overall, the overlap of age-related genes and mechanisms of the *in vivo* and the *in vitro* data was minor. The reason for this could be the use of different microarray platforms, but the overlap of the different cell types analysed on the same platform was also of minor significance. This indicates that the aging process of different cell types and of biopsies consisting of various cell types may largely differ. As mentioned above, the main feature of aging sebocytes may for instance be a loss in the specialised function of lipid production, which is not that important in e.g. skin fibroblasts. To investigate the observed differences it would be of benefit to analyse the single cell types of the skin *in vivo* to investigate cell-to-cell variations in the aging process.

In summary, the data on human skin aging reveals some known age-related processes like the decrease in collagens and also some new insights like the possible involvement of WNT signaling in human skin aging. Furthermore, the potential regulation of different mechanisms including the loss of structure in the extracellular matrix, telemore shortening, and the involvement of sirtuins, highlight the complexity of the aging process. In addition, the difference between sebocytes, fibroblasts and skin biopsies underscore the belief that aging is at least in part cell type specific.

4.3 Mouse aging

In this work, the process of aging in mouse is mainly studied by investigating transcriptional changes in brain, heart, and kidney with age. The analysis of the data shows that more genes exhibit age-related regulation in heart and kidney compared to the brain. A possible explanation of this is a better protective system in brain as its function is of major importance for the organism. The detailed investigation of genes, biological processes, and Kegg pathways reveals an increase in immune-related processes in all three tissues. As this finding is very prominent and as this study is mainly focussed on uncovering conserved age-related processes, the discussion on mouse aging will be limited to overlapping findings in brain, heart, and kidney.

It was previously shown that aging is accompanied by a significant decline of adaptive immunity – immunosenescence (Hakim and Gress 2007), and an activation of innate immunity – inflammaging (Franceschi 2007). Interestingly, the age-related genes overlapping in the three tissues investigated in this study all exhibit functions related to the immune system and are in most cases increased with age. In addition, the overlap of biological processes and pathways confirms the increase in immune-related mechanisms. Recently, the activation of the innate immune system during aging was discussed to be a downstream effect of activated NF-kB signaling (Salminen et al. 2008) and the impact of NF-kB signaling on different mouse and human tissues was identified by an extensive screen for age-related transcription factor motifs (Adler et al. 2007). The validation of increased ROS levels with age in all three tissues observed in this study and the finding that ROS and oxidative stress can activate the NF-kB pathway (Schreck et al. 1992) indicates activated NF-kB signaling in aged mice. Increased expression of the genes relevant to the NF-kB complex was not observed in this study. However, the eventual activation of NF-kB signaling is underscored by the fact that activation of NF-kB is independent of expressional changes of the NF-kB complex, but relies on its translocation from the cytoplasm to the nucleus (Gosselin and Abbadie 2003).

As mentioned above, nearly all the overlapping age-regulated genes in brain, heart and kidney exhibit increased expression with age. Including the finding that these genes are all related to the immune system leads to the expectation that they play key roles in innate immunity. The innate immune system comprises the cells and

mechanisms that defend the host from infection by other organisms in a non-specific manner. This means that the cells of the innate system recognize and respond to pathogens in a generic way. In contrast to the adaptive immune system, it does not confer long-lasting or protective immunity to the host. The major roles of the vertebrate innate immune system include:

- *Recruiting immune cells to sites of infection and inflammation, through the production of chemical factors, including specialized chemical mediators, called cytokines.*

Inflammation is produced by eicosanoids and cytokines, which are released by injured or infected cells. Common cytokines include interleukins that are responsible for communication between white blood cells, chemokines that promote chemotaxis, and interferons that have anti-viral effects. In the list of overlapping age-related genes, at least 5 genes are present that are involved in the inflammatory response – *Casp1*, *Cd48*, *Dock2*, *Icam1*, and *Irak3*.

Casp1 was identified by its ability to proteolytically cleave and activate the inactive precursor of interleukin-1. The expression of its human homologue and the subsequent release of IL-1beta and IL-18 significantly contribute for instance to intestinal inflammation (Siegmund 2002). Moreover, it was recently concluded that IL-1beta and IL-18 participate in fundamental inflammatory processes that increase during the aging process (Dinarello 2006). Also directly related to IL-1 are the interleukin-1 receptor associate kinases. The member *Irak3* regulates innate immunity through unknown mechanism (Su et al. 2007). *Cd48* is an interleukin (IL)-3-induced activating receptor on eosinophils, which may be involved in promoting allergic inflammation (Munitz et al. 2006). *Dock2* is a member of chemokines that promote chemotaxis, which has been shown to be of key importance for lymphocyte chemotaxis (Fukui et al. 2001). Most interestingly, *Icam1* is one of the molecules involved in inflammatory response that is overexpressed in senescent cells and aged tissues and, in addition, the role of the NF-kB signaling cascade is crucial in ICAM-1 activation (Kletsas et al. 2004).

- *Activation of the complement cascade to identify bacteria, to activate cells and to promote clearance of dead cells or antibody complex.*

The complement system is a biochemical cascade that attacks the surfaces of foreign cells. It contains over 20 different proteins and is named for its ability to 'complement' the killing of pathogens by antibodies. Complement is the major humoral component of the innate immune response. This response is activated by complement binding to antibodies that have attached to microorganisms or the binding of complement proteins to carbohydrates on the surface of microorganisms. One group of genes from the list of overlapping age-related genes, which is definitely involved in the complement cascade are the 5 complement components – *C1qa*, *C1qg*, *C3*, *C4*, and *Slp*/*C4a*. In addition, 2 antibodies are present in the list, which may also contribute to this mechanism – *Igh-1a* and *Igk-C*.

The detailed mechanisms of the complement cascade and the contribution of the single complement components would exceed the coverage of this discussion. An important aspect to this work are the findings that several complement components exhibit alterations in their gene expression with age (Plackett et al. 2004) and that these changes also contribute to age-related diseases like Alzheimer's disease (Zhou et al. 2008).

- *Identification and removal of foreign substances present in the organism by specialized white blood cells.*

Leukocytes (white blood cells) act like independent, single-cell organisms and are the cellular arm of the innate immune system. The innate leukocytes include the phagocytes (macrophages, neutrophils, and dendritic cells), mast cells, eosinophils, basophils, and natural killer cells. These cells identify and eliminate pathogens, either by attacking larger pathogens through contact or by engulfing and then killing microorganisms. The list of overlapping age-related genes includes at least 3 genes that are involved in the process of phagocytosis – *Cd68*, *Fcgr3*, and *Lyzs*.

Phagocytosis is an important feature of cellular innate immunity performed by cells called phagocytes that engulf pathogens. Fcgamma receptors like *Fcgr3* for instance have roles in many different parts of the immune system including phagocytosis (Nimmerjahn and Ravetch 2006). Lysozyme (*Lyzs*) serves as a non-specific innate opsonin by binding to the bacterial surface, and thus facilitating phagocytosis of the bacterium before opsonins from the acquired immune system arrive

at the scene (Gomez and Balcazar 2008). Finally, macrosialin (*Cd68*) was shown to have a specific function in macrophage-mediated phagocytosis (da Silva and Gordon 1999).

- *Activation of the adaptive immune system mediated by antigen presentation.*

The above-described leukocytes that contribute to the innate immune system are also important mediators in the activation of the adaptive immune system. This activation is accomplished by the presentation of antigens. The results of this study show that antigen processing and presentation is 1 of the 3 overlapping pathways that is significantly increased with age in all three tissues. At least 3 genes are present in the overlapping list of age-related target genes involved in this process – *Ctss*, *Ii*/*Cd74*, and *Rmcs1*/*H2-Ab1*.

These genes play a role in major histocompatibility complex (MHC) class II antigen presentation. *Rmcs1*/*H2-Ab1* is part of the MHC class II complex. The MHC class II-associated invariant chain (*Ii*) plays a critical role in the endocytic pathway, which is crucial in the MHC class II mediated antigen presentation (Rocha and Neefjes 2008). Furthermore, cathepsin S (*Ctss*) plays a major role in the degradation of the invariant peptide chain associated with the MHC and thus also affects antigen presentation (Gupta et al. 2008).

It should be kept in mind that the above-mentioned genes are not restricted to their described functions. Furthermore, as the innate and adaptive immune systems have overlapping functions it is likely that also the genes involved have several roles in immunity. An increase in the adaptive immune system for instance may contribute to autoimmunity. For example, a case-control study of rheumatoid arthritis identified an associated single nucleotide polymorphism in the *NCF4* gene, supporting a role in autoimmunity (Olsson et al. 2007). *Ncf4* is among the conserved age-related genes of this study. Additionally, certain autoimmune responses are known to increase with age (Yung and Julius 2008).

In summary, the analysis of transcriptional profiles of aging in the three mouse tissues, brain, heart, and kidney, highlights the importance of the immune system as a conserved mechanism in mouse aging and indicates the involvement of NF-kB signaling by the observed increased levels of ROS.

4.4 The basis of aging

This study was primarily aimed at identifying potential conserved aging mechanisms in mammalian species including different tissues. The final results revealed that the overlap of different transcriptional aging profiles is minor, which is also confirmed by others (Zahn et al. 2007). The analyses showed that even the profiles of more similar samples like male and female skin biopsies or the three different mouse tissues reveal just a few overlapping genes. However, these genes show at least the same trend of regulation. Furthermore, the comparison of the data to similar published data (Lener et al. 2006; Zahn et al. 2007) underscore the minor correlations of age-related target genes.

Interestingly, as described in the introduction of this work, microarray studies on human and mouse aging – although not elucidating conserved genes – provide conserved processes related to the aging process including stress/immune responses, cell cycle, and metabolism. This study validates the involvement of the immune system (mainly in mouse) and of metabolism. The inter-species overlap revealed for instance immune-related pathways like cell adhesion molecules and hematopoietic cell lineage, and metabolism-related pathways like glutathione metabolism and nitrogen metabolism. Many other specific metabolism-related pathways are additionally regulated in the single data sets. Furthermore, metabolism-related biological processes show significant inter-species regulation like protein metabolism and macromolecule metabolism. Especially the species-independent regulation of glutathione metabolism responsible for the regulation of constant levels of ROS (Figure 1.1) and the observed increase of ROS levels in the mouse tissues indicate that the rate of aging may be dependent on the ability of the organism to control a vital metabolism and especially constant levels of certain metabolites including ROS, which are constantly unbalanced by random perturbations during aging. This observation resulted in the submission of mouse data for publication discussing the concept of metabolic stability, life span and aging (Brink et al. 2008, under review).

Overall, the comparative studies in this work and the age-related gene expression studies introduced in the introduction highlight the difficulty in investigating the aging process at the transcriptional level. They reveal that the magnitude of changes in gene expression is minor with age. This leads to an increased impact of the setting of

thresholds to define age-related genes, which may additionally account for differences between different studies.

However, the age-related findings in mouse other than changes in gene expression like increased ROS and the accumulation of non-functional proteins indicate that the observed small changes in gene expression may be a reaction to processes like oxidative stress and decreased functionality of proteins or membranes caused by cross-links with e.g. sugars. The capacity of ROS to activate gene expression via NF-kB signaling for instance has been indicated before (Schreck et al. 1992). Unfortunately, due to a lack of material the increase of ROS levels could not be validated in the human skin.

In summary, this study is not sufficient to provide a defined conserved process that plays a key role in mouse and human aging. However, it confirms the observation that the immune system and general metabolism are significantly involved in the process of mammalian aging, and supports the concept that aging is not a single gene but rather a gene network-mediated process.

5. Conclusion

The studies conducted to investigate the age-regulated changes in gene expression of human male and female skin, and mouse brain, heart and kidney tissues in parallel confirm the general assumption that aging is a complex process. Furthermore, they show that analysing the aging process on the transcriptional level is a challenging task due to solely slight changes in transcriptional levels of age-related genes. The poor correlations of determined transcriptional regulation in different array-based studies are often discussed as a result of different platforms, tissues, species, age-groups and statistical parameters used for the data generation. However, the attempt to find novel conserved age-related processes between tissues and species by avoiding the other sources of error did not expand the list of certain genes, processes and pathways conserved in the aging process of mammals. But, aging processes underlying the specific species and tissues are highlighted by the array-derived data.

The aging studies on human skin biopsies identified known age-related processes like a reduction in the skin collagen structure but also potential new age-related processes like the involvement of WNT signaling in human skin aging. The analysis of hormone-treated skin cells (sebocytes and fibroblasts) revealed significant differences between these two skin cell types. The lipid-related processes crucial for the key function of sebocytes are significantly regulated in these cells, but mostly not affected in fibroblasts. These results underscore the potential that age-related transcriptional changes are cell type specific.

The aging studies on the three mouse tissues identified a conserved increase on the transcriptional level of immune-related genes, especially those of the innate immune system. In addition, measurements of LPO in the mouse tissues indicate elevated levels of ROS. Together these results suggest a ROS-mediated activity of NF-kB signaling responsible for enhanced inflammatory transcriptional activity in the tissues.

Overall, the results of this study confirm the conserved involvement of immune responses and of metabolism-related processes including regulating systems of ROS like glutathione metabolism in mammalian aging. In addition, the analyses conducted here validate the fluctuations observed in transcriptional aging profiles.

Finally, the age-dependent decreases in the collagen structure of human skin are a potential downstream effect of the decline in hormone levels with age and the age-

dependent activation of the innate immune system in mouse tissues is a potential downstream effect of the observed increase in ROS levels. These findings support the argument that transcriptional changes with age do not contribute to the driving forces of the process and that environmental factors are the main contributors. In addition, the finding that similar processes are age-regulated including different genes in varying tissues such as immune and metabolism-related genes, suggests that aging is not dependent on single genes but rather on a network of genes. However, it remains unclear, which mechanisms are responsible for the induction of the aging process.

References

Adjaye J., Herwig R., Herrmann D., Wruck W., Benkahla A., Brink T.C., Nowak M., Carnwath J.W., Hultschig C., Niemann H. & Lehrach H. (2004) Cross-species hybridisation of human and bovine orthologous genes on high density cDNA microarrays. BMC Genomics 5:83.

Adjaye J., Huntriss J., Herwig R., BenKahla A., Brink T.C., Wierling C., Hultschig C., Groth D., Yaspo M.L., Picton H.M., Gosden R.G. & Lehrach H. (2005) Primary differentiation in the human blastocyst: comparative molecular portraits of inner cell mass and trophectoderm cells. Stem Cells 23:1514-1525.

Adler A.S., Sinha S., Kawahara T.L., Zhang J.Y., Segal E. & Chang H.Y. (2007) Motif module map reveals enforcement of aging by continual NF-kappaB activity. Genes Dev 21:3244-3257.

Amador-Noguez D., Yagi K., Venable S. & Darlington G. (2004) Gene expression profile of long-lived Ames dwarf mice and Little mice. Aging Cell 3:423-441.

Artal-Sanz M. & Tavernarakis N. (2008) Mechanisms of aging and energy metabolism in Caenorhabditis elegans. IUBMB Life 60:315-322.

Avery N.C. & Bailey A.J. (2006) The effects of the Maillard reaction on the physical properties and cell interactions of collagen. Pathol Biol (Paris) 54:387-395.

Bahar R., Hartmann C.H., Rodriguez K.A., Denny A.D., Busuttil R.A., Dolle M.E., Calder R.B., Chisholm G.B., Pollock B.H., Klein C.A. & Vijg J. (2006) Increased cell-to-cell variation in gene expression in ageing mouse heart. Nature 441:1011-1014.

Baldan A., Tarr P., Lee R. & Edwards P.A. (2006) ATP-binding cassette transporter G1 and lipid homeostasis. Curr Opin Lipidol 17:227-232.

Braverman I.M. & Fonferko E. (1982a) Studies in cutaneous aging: I. The elastic fiber network. J Invest Dermatol 78:434-443.

Braverman I.M. & Fonferko E. (1982b) Studies in cutaneous aging: II. The microvasculature. J Invest Dermatol 78:444-448.

Brink T.C., Sudheer S., Janke D., Jagodzinska J., Jung M. & Adjaye J. (2008) The origins of human embryonic stem cells: a biological conundrum. Cells Tissues Organs 188:9-22.

Brown-Borg H.M., Borg K.E., Meliska C.J. & Bartke A. (1996) Dwarf mice and the ageing process. Nature 384:33.

Cao S.X., Dhahbi J.M., Mote P.L. & Spindler S.R. (2001) Genomic profiling of short- and long-term caloric restriction effects in the liver of aging mice. Proc Natl Acad Sci U S A 98:10630-10635.

Carlson M.E., Silva H.S. & Conboy I.M. (2008) Aging of signal transduction pathways, and pathology. Exp Cell Res 314:1951-1961.

Cervantes-Laurean D., Jacobson E.L. & Jacobson M.K. (1996) Glycation and glycoxidation of histones by ADP-ribose. J Biol Chem 271:10461-10469.

Chelvarajan R.L., Liu Y., Popa D., Getchell M.L., Getchell T.V., Stromberg A.J. & Bondada S. (2006) Molecular basis of age-associated cytokine dysregulation in LPS-stimulated macrophages. J Leukoc Biol 79:1314-1327.

Curran S.P. & Ruvkun G. (2007) Lifespan regulation by evolutionarily conserved genes essential for viability. PLoS Genet 3:e56.

da Silva R.P. & Gordon S. (1999) Phagocytosis stimulates alternative glycosylation of macrosialin (mouse CD68), a macrophage-specific endosomal protein. Biochem J 338 (Pt 3):687-694.

Dao H., Jr. & Kazin R.A. (2007) Gender differences in skin: a review of the literature. Gend Med 4:308-328.

Dawczynski J. & Strobel J. (2006) [The aging lens--new concepts for lens aging]. Ophthalmologe 103:759-764.

DeCarolis N.A., Wharton K.A., Jr. & Eisch A.J. (2008) Which way does the Wnt blow? Exploring the duality of canonical Wnt signaling on cellular aging. Bioessays 30:102-106.

Detti L., Saed G.M., Jiang Z.L., Kruger M.L. & Diamond M.P. (2008) The effect of estradiol on the expression of estrogen, progesterone, androgen, and prolactin receptors in human peritoneal fibroblasts. J Assist Reprod Genet 25:245-250.

Dhahbi J.M., Tsuchiya T., Kim H.J., Mote P.L. & Spindler S.R. (2006) Gene expression and physiologic responses of the heart to the initiation and withdrawal of caloric restriction. J Gerontol A Biol Sci Med Sci 61:218-231.

Dilman V.M., Revskoy S.Y. & Golubev A.G. (1986) Neuroendocrine-ontogenetic mechanism of aging: toward an integrated theory of aging. Int Rev Neurobiol 28:89-156.

Dinarello C.A. (2006) Interleukin 1 and interleukin 18 as mediators of inflammation and the aging process. Am J Clin Nutr 83:447S-455S.

Dreesen O. & Brivanlou A.H. (2007) Signaling pathways in cancer and embryonic stem cells. Stem Cell Rev 3:7-17.

Edwards M.G., Anderson R.M., Yuan M., Kendziorski C.M., Weindruch R. & Prolla T.A. (2007) Gene expression profiling of aging reveals activation of a p53-mediated transcriptional program. BMC Genomics 8:80.

Fernandes G., Yunis E.J. & Good R.A. (1976) Influence of diet on survival of mice. Proc Natl Acad Sci U S A 73:1279-1283.

Finkel T. & Holbrook N.J. (2000) Oxidants, oxidative stress and the biology of ageing. Nature 408:239-247.

Flurkey K., Papaconstantinou J., Miller R.A. & Harrison D.E. (2001) Lifespan extension and delayed immune and collagen aging in mutant mice with defects in growth hormone production. Proc Natl Acad Sci U S A 98:6736-6741.

Franceschi C. (2007) Inflammaging as a major characteristic of old people: can it be prevented or cured? Nutr Rev 65:S173-176.

Franceschi C., Bezrukov V., Blanche H., Bolund L., Christensen K., de Benedictis G., Deiana L., Gonos E., Hervonen A., Yang H., Jeune B., Kirkwood T.B., Kristensen P., Leon A., Pelicci P.G., Peltonen L., Poulain M., Rea I.M., Remacle J., Robine J.M., Schreiber S., Sikora E., Slagboom P.E., Spazzafumo L., Stazi M.A., Toussaint O. & Vaupel J.W. (2007) Genetics of healthy aging in Europe: the EU-integrated project GEHA (GEnetics of Healthy Aging). Ann N Y Acad Sci 1100:21-45.

Fraser H.B., Khaitovich P., Plotkin J.B., Paabo S. & Eisen M.B. (2005) Aging and gene expression in the primate brain. PLoS Biol 3:e274.

Fu C., Hickey M., Morrison M., McCarter R. & Han E.S. (2006) Tissue specific and non-specific changes in gene expression by aging and by early stage CR. Mech Ageing Dev 127:905-916.

Fukui Y., Hashimoto O., Sanui T., Oono T., Koga H., Abe M., Inayoshi A., Noda M., Oike M., Shirai T. & Sasazuki T. (2001) Haematopoietic cell-specific CDM family protein DOCK2 is essential for lymphocyte migration. Nature 412:826-831.

Girardot F., Lasbleiz C., Monnier V. & Tricoire H. (2006) Specific age-related signatures in Drosophila body parts transcriptome. BMC Genomics 7:69.

Giresi P.G., Stevenson E.J., Theilhaber J., Koncarevic A., Parkington J., Fielding R.A. & Kandarian S.C. (2005) Identification of a molecular signature of sarcopenia. Physiol Genomics 21:253-263.

Goh S.Y. & Cooper M.E. (2008) Clinical review: The role of advanced glycation end products in progression and complications of diabetes. J Clin Endocrinol Metab 93:1143-1152.

Golden T.R. & Melov S. (2004) Microarray analysis of gene expression with age in individual nematodes. Aging Cell 3:111-124.

Gomez G.D. & Balcazar J.L. (2008) A review on the interactions between gut microbiota and innate immunity of fish. FEMS Immunol Med Microbiol 52:145-154.

Gosselin K. & Abbadie C. (2003) Involvement of Rel/NF-kappa B transcription factors in senescence. Exp Gerontol 38:1271-1283.

Gupta S., Singh R.K., Dastidar S. & Ray A. (2008) Cysteine cathepsin S as an immunomodulatory target: present and future trends. Expert Opin Ther Targets 12:291-299.

Hakim F.T. & Gress R.E. (2007) Immunosenescence: deficits in adaptive immunity in the elderly. Tissue Antigens 70:179-189.

Harman D. (1956) Aging: a theory based on free radical and radiation chemistry. J Gerontol 11:298-300.

Harman D. (1972) The biologic clock: the mitochondria? J Am Geriatr Soc 20:145-147.

Hayflick L. (1965) The Limited in Vitro Lifetime of Human Diploid Cell Strains. Exp Cell Res 37:614-636.

Helfand S.L. & Rogina B. (2003) Genetics of aging in the fruit fly, Drosophila melanogaster. Annu Rev Genet 37:329-348.

Higami Y., Barger J.L., Page G.P., Allison D.B., Smith S.R., Prolla T.A. & Weindruch R. (2006) Energy restriction lowers the expression of genes linked to inflammation, the cytoskeleton, the extracellular matrix, and angiogenesis in mouse adipose tissue. J Nutr 136:343-352.

Houthoofd K. & Vanfleteren J.R. (2007) Public and private mechanisms of life extension in Caenorhabditis elegans. Mol Genet Genomics 277:601-617.

Jenkins G. (2002) Molecular mechanisms of skin ageing. Mech Ageing Dev 123:801-810.

Jiang C.H., Tsien J.Z., Schultz P.G. & Hu Y. (2001) The effects of aging on gene expression in the hypothalamus and cortex of mice. Proc Natl Acad Sci U S A 98:1930-1934.

Jiang J.C., Jaruga E., Repnevskaya M.V. & Jazwinski S.M. (2000) An intervention resembling caloric restriction prolongs life span and retards aging in yeast. Faseb J 14:2135-2137.

Kaeberlein M., Burtner C.R. & Kennedy B.K. (2007) Recent developments in yeast aging. PLoS Genet 3:e84.

Kaeberlein M., Powers R.W., 3rd, Steffen K.K., Westman E.A., Hu D., Dang N., Kerr E.O., Kirkland K.T., Fields S. & Kennedy B.K. (2005) Regulation of yeast replicative life span by TOR and Sch9 in response to nutrients. Science 310:1193-1196.

Kanitakis J. (2002) Anatomy, histology and immunohistochemistry of normal human skin. Eur J Dermatol 12:390-399; quiz 400-391.

Kim S.N., Rhee J.H., Song Y.H., Park D.Y., Hwang M., Lee S.L., Kim J.E., Gim B.S., Yoon J.H., Kim Y.J. & Kim-Ha J. (2005) Age-dependent changes of gene expression in the Drosophila head. Neurobiol Aging 26:1083-1091.

Kletsas D., Pratsinis H., Mariatos G., Zacharatos P. & Gorgoulis V.G. (2004) The proinflammatory phenotype of senescent cells: the p53-mediated ICAM-1 expression. Ann N Y Acad Sci 1019:330-332.

Kuhla B., Haase C., Flach K., Luth H.J., Arendt T. & Munch G. (2007) Effect of pseudophosphorylation and cross-linking by lipid peroxidation and advanced glycation end product precursors on tau aggregation and filament formation. J Biol Chem 282:6984-6991.

Kuhn K., Baker S.C., Chudin E., Lieu M.H., Oeser S., Bennett H., Rigault P., Barker D., McDaniel T.K. & Chee M.S. (2004) A novel, high-performance random array platform for quantitative gene expression profiling. Genome Res 14:2347-2356.

Landis G.N., Abdueva D., Skvortsov D., Yang J., Rabin B.E., Carrick J., Tavare S. & Tower J. (2004) Similar gene expression patterns characterize aging and oxidative stress in Drosophila melanogaster. Proc Natl Acad Sci U S A 101:7663-7668.

Lee C.K., Klopp R.G., Weindruch R. & Prolla T.A. (1999) Gene expression profile of aging and its retardation by caloric restriction. Science 285:1390-1393.

Lee C.K., Weindruch R. & Prolla T.A. (2000) Gene-expression profile of the ageing brain in mice. Nat Genet 25:294-297.

Lener T., Moll P.R., Rinnerthaler M., Bauer J., Aberger F. & Richter K. (2006) Expression profiling of aging in the human skin. Exp Gerontol 41:387-397.

Lepperdinger G., Berger P., Breitenbach M., Frohlich K.U., Grillari J., Grubeck-Loebenstein B., Madeo F., Minois N., Zwerschke W. & Jansen-Durr P. (2008) The use of genetically engineered model systems for research on human aging. Front Biosci 13:7022-7031.

Liang H., Masoro E.J., Nelson J.F., Strong R., McMahan C.A. & Richardson A. (2003) Genetic mouse models of extended lifespan. Exp Gerontol 38:1353-1364.

Lin S.J., Defossez P.A. & Guarente L. (2000) Requirement of NAD and SIR2 for life-span extension by calorie restriction in Saccharomyces cerevisiae. Science 289:2126-2128.

Lockhart D.J., Dong H., Byrne M.C., Follettie M.T., Gallo M.V., Chee M.S., Mittmann M., Wang C., Kobayashi M., Horton H. & Brown E.L. (1996) Expression monitoring by hybridization to high-density oligonucleotide arrays. Nat Biotechnol 14:1675-1680.

Lohwasser C., Neureiter D., Weigle B., Kirchner T. & Schuppan D. (2006) The receptor for advanced glycation end products is highly expressed in the skin and upregulated by advanced glycation end products and tumor necrosis factor-alpha. J Invest Dermatol 126:291-299.

Lombard D.B., Schwer B., Alt F.W. & Mostoslavsky R. (2008) SIRT6 in DNA repair, metabolism and ageing. J Intern Med 263:128-141.

Lu T., Pan Y., Kao S.Y., Li C., Kohane I., Chan J. & Yankner B.A. (2004) Gene regulation and DNA damage in the ageing human brain. Nature 429:883-891.

Lund J., Tedesco P., Duke K., Wang J., Kim S.K. & Johnson T.E. (2002) Transcriptional profile of aging in C. elegans. Curr Biol 12:1566-1573.

Makrantonaki E., Adjaye J., Herwig R., Brink T.C., Groth D., Hultschig C., Lehrach H. & Zouboulis C.C. (2006) Age-specific hormonal decline is accompanied by transcriptional changes in human sebocytes in vitro. Aging Cell 5:331-344.

Marionnet C., Bernerd F., Dumas A., Verrecchia F., Mollier K., Compan D., Bernard B., Lahfa M., Leclaire J., Medaisko C., Mehul B., Seite S., Mauviel A. & Dubertret L. (2003) Modulation of gene expression induced in human epidermis by environmental stress in vivo. J Invest Dermatol 121:1447-1458.

McClearn G.E. (1997) Biogerontologic theories. Exp Gerontol 32:3-10.

Medvedova L., Knopp J. & Farkas R. (2003) Steroid regulation of terminal protein glycosyltransferase genes: molecular and functional homologies within sialyltransferase and fucosyltransferase families. Endocr Regul 37:203-210.

Melk A., Mansfield E.S., Hsieh S.C., Hernandez-Boussard T., Grimm P., Rayner D.C., Halloran P.F. & Sarwal M.M. (2005) Transcriptional analysis of the molecular basis of human kidney aging using cDNA microarray profiling. Kidney Int 68:2667-2679.

Michishita E., McCord R.A., Berber E., Kioi M., Padilla-Nash H., Damian M., Cheung P., Kusumoto R., Kawahara T.L., Barrett J.C., Chang H.Y., Bohr V.A., Ried T., Gozani O. & Chua K.F. (2008) SIRT6 is a histone H3 lysine 9 deacetylase that modulates telomeric chromatin. Nature 452:492-496.

Misra V., Lee H., Singh A., Huang K., Thimmulappa R.K., Mitzner W., Biswal S. & Tankersley C.G. (2007) Global Expression Profiles from C57BL/6J and DBA/2J Mouse Lungs to Determine Aging-related Genes. Physiol Genomics

Monnier V.M., Mustata G.T., Biemel K.L., Reihl O., Lederer M.O., Zhenyu D. & Sell D.R. (2005) Cross-linking of the extracellular matrix by the maillard reaction in aging and diabetes: an update on "a puzzle nearing resolution". Ann N Y Acad Sci 1043:533-544.

Moragas A., Castells C. & Sans M. (1993) Mathematical morphologic analysis of aging-related epidermal changes. Anal Quant Cytol Histol 15:75-82.

Mostoslavsky R., Chua K.F., Lombard D.B., Pang W.W., Fischer M.R., Gellon L., Liu P., Mostoslavsky G., Franco S., Murphy M.M., Mills K.D., Patel P., Hsu J.T., Hong A.L., Ford E., Cheng H.L., Kennedy C., Nunez N., Bronson R., Frendewey D., Auerbach W., Valenzuela D., Karow M., Hottiger M.O., Hursting S., Barrett J.C., Guarente L., Mulligan R., Demple B., Yancopoulos G.D. & Alt F.W. (2006) Genomic instability and aging-like phenotype in the absence of mammalian SIRT6. Cell 124:315-329.

Munitz A., Bachelet I., Eliashar R., Khodoun M., Finkelman F.D., Rothenberg M.E. & Levi-Schaffer F. (2006) CD48 is an allergen and IL-3-induced activation molecule on eosinophils. J Immunol 177:77-83.

Nimmerjahn F. & Ravetch J.V. (2006) Fcgamma receptors: old friends and new family members. Immunity 24:19-28.

Nouveau S., Bastien P., Baldo F. & de Lacharriere O. (2008) Effects of topical DHEA on aging skin: a pilot study. Maturitas 59:174-181.

Ohnemus U., Uenalan M., Inzunza J., Gustafsson J.A. & Paus R. (2006) The hair follicle as an estrogen target and source. Endocr Rev 27:677-706.

Olsson L.M., Lindqvist A.K., Kallberg H., Padyukov L., Burkhardt H., Alfredsson L., Klareskog L. & Holmdahl R. (2007) A case-control study of rheumatoid arthritis identifies an associated single nucleotide polymorphism in the NCF4 gene, supporting a role for the NADPH-oxidase complex in autoimmunity. Arthritis Res Ther 9:R98.

Page G.P., Zakharkin S.O., Kim K., Mehta T., Chen L. & Zhang K. (2007) Microarray analysis. Methods Mol Biol 404:409-430.

Pageon H. & Asselineau D. (2005) An in vitro approach to the chronological aging of skin by glycation of the collagen: the biological effect of glycation on the reconstructed skin model. Ann N Y Acad Sci 1043:529-532.

Plackett T.P., Boehmer E.D., Faunce D.E. & Kovacs E.J. (2004) Aging and innate immune cells. J Leukoc Biol 76:291-299.

Pletcher S.D., Macdonald S.J., Marguerie R., Certa U., Stearns S.C., Goldstein D.B. & Partridge L. (2002) Genome-wide transcript profiles in aging and calorically restricted Drosophila melanogaster. Curr Biol 12:712-723.

Pochi P.E., Strauss J.S. & Downing D.T. (1979) Age-related changes in sebaceous gland activity. J Invest Dermatol 73:108-111.

Powers R.W., 3rd, Kaeberlein M., Caldwell S.D., Kennedy B.K. & Fields S. (2006) Extension of chronological life span in yeast by decreased TOR pathway signaling. Genes Dev 20:174-184.

Reverter-Branchat G., Cabiscol E., Tamarit J. & Ros J. (2004) Oxidative damage to specific proteins in replicative and chronological-aged Saccharomyces cerevisiae: common targets and prevention by calorie restriction. J Biol Chem 279:31983-31989.

Rittie L. & Fisher G.J. (2002) UV-light-induced signal cascades and skin aging. Ageing Res Rev 1:705-720.

Rocha N. & Neefjes J. (2008) MHC class II molecules on the move for successful antigen presentation. Embo J 27:1-5.

Rodwell G.E., Sonu R., Zahn J.M., Lund J., Wilhelmy J., Wang L., Xiao W., Mindrinos M., Crane E., Segal E., Myers B.D., Brooks J.D., Davis R.W., Higgins J., Owen

A.B. & Kim S.K. (2004) A transcriptional profile of aging in the human kidney. PLoS Biol 2:e427.

Roshan S., Nader S. & Orlander P. (1999) Review: Ageing and hormones. Eur J Clin Invest 29:210-213.

Ruotsalainen H., Vanhatupa S., Tampio M., Sipila L., Valtavaara M. & Myllyla R. (2001) Complete genomic structure of mouse lysyl hydroxylase 2 and lysyl hydroxylase 3/collagen glucosyltransferase. Matrix Biol 20:137-146.

Salminen A., Huuskonen J., Ojala J., Kauppinen A., Kaarniranta K. & Suuronen T. (2008) Activation of innate immunity system during aging: NF-kB signaling is the molecular culprit of inflamm-aging. Ageing Res Rev 7:83-105.

Schreck R., Albermann K. & Baeuerle P.A. (1992) Nuclear factor kappa B: an oxidative stress-responsive transcription factor of eukaryotic cells (a review). Free Radic Res Commun 17:221-237.

Segev F., Mor O., Segev A., Belkin M. & Assia E.I. (2005) Downregulation of gene expression in the ageing lens: a possible contributory factor in senile cataract. Eye 19:80-85.

Shin M.H., Rhie G.E., Park C.H., Kim K.H., Cho K.H., Eun H.C. & Chung J.H. (2005) Modulation of collagen metabolism by the topical application of dehydroepiandrosterone to human skin. J Invest Dermatol 124:315-323.

Siegmund B. (2002) Interleukin-1beta converting enzyme (caspase-1) in intestinal inflammation. Biochem Pharmacol 64:1-8.

Sinex F.M. (1964) Cross-Linkage and Aging. Adv Gerontol Res 21:165-180.

Stevenson S. & Thornton J. (2007) Effect of estrogens on skin aging and the potential role of SERMs. Clin Interv Aging 2:283-297.

Sturm R.A., Teasdale R.D. & Box N.F. (2001) Human pigmentation genes: identification, structure and consequences of polymorphic variation. Gene 277:49-62.

Su J., Xie Q., Wilson I. & Li L. (2007) Differential regulation and role of interleukin-1 receptor associated kinase-M in innate immunity signaling. Cell Signal 19:1596-1601.

Tan Q., Christensen K., Christiansen L., Frederiksen H., Bathum L., Dahlgaard J. & Kruse T.A. (2005) Genetic dissection of gene expression observed in whole blood samples of elderly Danish twins. Hum Genet 117:267-274.

Uitto J. (2008) The role of elastin and collagen in cutaneous aging: intrinsic aging versus photoexposure. J Drugs Dermatol 7:s12-16.

Vanguilder H., Vrana K. & Freeman W. (2008) Twenty-five years of quantitative PCR for gene expression analysis. Biotechniques 44:619-626.

Varani J., Spearman D., Perone P., Fligiel S.E., Datta S.C., Wang Z.Q., Shao Y., Kang S., Fisher G.J. & Voorhees J.J. (2001) Inhibition of type I procollagen synthesis by damaged collagen in photoaged skin and by collagenase-degraded collagen in vitro. Am J Pathol 158:931-942.

Verbeke P., Clark B.F. & Rattan S.I. (2001) Reduced levels of oxidized and glycoxidized proteins in human fibroblasts exposed to repeated mild heat shock during serial passaging in vitro. Free Radic Biol Med 31:1593-1602.

Wang E., Miller L.D., Ohnmacht G.A., Liu E.T. & Marincola F.M. (2000) High-fidelity mRNA amplification for gene profiling. Nat Biotechnol 18:457-459.

Warner H.R. (2005) Longevity genes: from primitive organisms to humans. Mech Ageing Dev 126:235-242.

Welle S., Brooks A.I., Delehanty J.M., Needler N., Bhatt K., Shah B. & Thornton C.A. (2004) Skeletal muscle gene expression profiles in 20-29 year old and 65-71 year old women. Exp Gerontol 39:369-377.

Wondrak G.T., Varadarajan S., Butterfield D.A. & Jacobson M.K. (2000) Formation of a protein-bound pyrazinium free radical cation during glycation of histone H1. Free Radic Biol Med 29:557-567.

Wulf H.C., Sandby-Moller J., Kobayasi T. & Gniadecki R. (2004) Skin aging and natural photoprotection. Micron 35:185-191.

Xiao B., Jing C., Wilson J.R., Walker P.A., Vasisht N., Kelly G., Howell S., Taylor I.A., Blackburn G.M. & Gamblin S.J. (2003) Structure and catalytic mechanism of the human histone methyltransferase SET7/9. Nature 421:652-656.

Yaar M., Eller M.S. & Gilchrest B.A. (2002) Fifty years of skin aging. J Investig Dermatol Symp Proc 7:51-58.

Yoon K.A., Nakamura Y. & Arakawa H. (2004) Identification of ALDH4 as a p53-inducible gene and its protective role in cellular stresses. J Hum Genet 49:134-140.

Yung R.L. & Julius A. (2008) Epigenetics, aging, and autoimmunity. Autoimmunity 41:329-335.

Zahn J.M., Poosala S., Owen A.B., Ingram D.K., Lustig A., Carter A., Weeraratna A.T., Taub D.D., Gorospe M., Mazan-Mamczarz K., Lakatta E.G., Boheler K.R., Xu X., Mattson M.P., Falco G., Ko M.S., Schlessinger D., Firman J., Kummerfeld S.K., Wood W.H., Zonderman A.B., Kim S.K. & Becker K.G. (2007) AGEMAP: A Gene Expression Database for Aging in Mice. PLoS Genet 3:e201.

Zahn J.M., Sonu R., Vogel H., Crane E., Mazan-Mamczarz K., Rabkin R., Davis R.W., Becker K.G., Owen A.B. & Kim S.K. (2006) Transcriptional profiling of aging in human muscle reveals a common aging signature. PLoS Genet 2:e115.

Zhou J., Fonseca M.I., Pisalyaput K. & Tenner A.J. (2008) Complement C3 and C4 expression in C1q sufficient and deficient mouse models of Alzheimer's Disease. J Neurochem

Zouboulis C.C. (2000) Human skin: an independent peripheral endocrine organ. Horm Res 54:230-242.

Zouboulis C.C., Seltmann H., Neitzel H. & Orfanos C.E. (1999) Establishment and characterization of an immortalized human sebaceous gland cell line (SZ95). J Invest Dermatol 113:1011-1020.

Zs-Nagy I. (1978) A membrane hypothesis of aging. J Theor Biol 75:189-195.

Publications

Brink TC, Demetrius L, Lehrach H, Adjaye J. Metabolic Stability, Life Span, and Aging. Mechanisms of Ageing and Development. **2008**. under review

Brink TC, Sudheer S, Janke D, Jagodzinska J, Jung M, Adjaye J. The Origins of Human Embryonic Stem Cells: A Biological Conundrum. Cells Tissues Organs. **2008**;188(1-2):9-22. Epub 2007 Dec 20.

Adjaye J, Herwig R, **Brink TC**, Herrmann D, Greber B, Sudheer S, Groth D, Carnwath JW, Lehrach H, Niemann H. Conserved molecular portraits of bovine and human blastocysts as a consequence of the transition from maternal to embryonic control of gene expression. Physiol Genomics. **2007** Oct 22;31(2):315-27. Epub 2007 Jun 26.

Babaie Y, Herwig R, Greber B, **Brink TC**, Wruck W, Groth D, Lehrach H, Burdon T, Adjaye J. Analysis of Oct4-dependent transcriptional networks regulating self-renewal and pluripotency in human embryonic stem cells. Stem Cells. **2007** Feb;25(2):500-10. Epub 2006 Oct 26.

Makrantonaki E, Adjaye J, Herwig R, **Brink TC**, Groth D, Hultschig C, Lehrach H, Zouboulis CC. Aging of human sebocytes in vitro induced by exposure to a defined hormone environment. Dermatology. **2006**;213(3):262-3.

Makrantonaki E, Adjaye J, Herwig R, **Brink TC**, Groth D, Hultschig C, Lehrach H, Zouboulis CC. Age-specific hormonal decline is accompanied by transcriptional changes in human sebocytes in vitro. Aging Cell. **2006** Aug;5(4):331-44. Epub 2006 Jun 29.

Adjaye J, Huntriss J, Herwig R, BenKahla A, **Brink TC**, Wierling C, Hultschig C, Groth D, Yaspo ML, Picton HM, Gosden RG, Lehrach H. Primary differentiation in the human blastocyst: comparative molecular portraits of inner cell mass and trophectoderm cells. Stem Cells. **2005** Nov-Dec;23(10):1514-25. Epub 2005 Aug 4.

Adjaye J, Herwig R, Herrmann D, Wruck W, Benkahla A, **Brink TC**, Nowak M, Carnwath JW, Hultschig C, Niemann H, Lehrach H. Cross-species hybridisation of human and bovine orthologous genes on high density cDNA microarrays. BMC Genomics. **2004** Oct 28;5(1):83.

Curriculum Vitae

Thore Brink

Appendix

I Buffers for SDS-PAGE gel electrophoresis

Resolving Buffer

1.5M Tris-HCl pH8.8:	180g Tris base (121g/mol)
	ad 900ml dH_2O
	adjust pH8.8 with 37% HCl (approx. 26ml)
	ad 1000ml dH_2O

Stacking Buffer

0.5M Tris-HCl pH6.8:	60g Tris base (121g/mol)
	ad 900ml dH_2O
	adjust pH6.8 with 37% HCl (approx. 47ml)
	ad 1000ml dH_2O

3x Loading Buffer (Sample Buffer)

3x SDS-PAGE SB:	9.375ml Stacking Buffer
	17.2ml 87% glycerol
	15ml 10% SDS
	some grains bromophenol blue
	ad 47.5ml dH_2O
	store at RT
working solution:	950µl (47.5ml) 3x Loading Buffer
	50µl (2.5ml) beta-Mercaptoethanol
	store at –20°C

10x Running Buffer

10x SDS-PAGE RB:	250mM Tris base (121g/mol)	→ 30.3g
	1.92M Glycine (75g/mol)	→ 144.1g
	100ml 10% SDS	
	ad 1000ml dH_2O	

II Buffers for western blotting

10x Transferbuffer:	250mM Tris base (121g/mol)	→ 30.3g
	1.92M Glycine (75g/mol)	→ 144.1g
	ad 1000ml dH_2O	
1x Transferbuffer:	100ml 10x Transferbuffer	
	200ml Methanol	
	ad 1000ml dH_2O	
1M Tris-HCl pH7.6:	120g Tris base (121g/mol)	
	ad 900ml dH_2O	
	adjust pH7.6 with 37% HCl	
	ad 1000ml dH_2O	
1x TBS:	8g Sodium Chloride	
	20ml 1M Tris-Hcl pH7.6	
	ad 1000ml dH_2O	
1x TBST:	1000 ml 1x TBS	
	1 ml Tween 20	
Blocking solution:	3% milk powder → 1.5g	
	ad 50ml 1x TBST	

III Target gene lists

Table X.1 Target gene list for human skin fibroblasts.

Symbol	Definition	ImageID	Ratio	PValue
	Increased with age (Top 50)			
ZDHHC18	Zinc finger, DHHC-type containing 18	4997435	3.93	1.9E-03
WNK3	WNK lysine deficient protein kinase 3	1733978	2.45	4.9E-04
MAPBPIP	Mitogen-activated protein-binding protein-interacting protein	4795043	1.84	2.8E-03
ZC3HC1	Zinc finger, C3HC-type containing 1	5454143	1.82	5.6E-03
GCL	Germ cell-less homolog 1 (Drosophila)	1356475	1.81	1.9E-03
EDD	E3 identified by differential display	358125	1.76	4.0E-02
GCA	Grancalcin, EF-hand calcium binding protein	141321	1.61	2.8E-03
CRIM1	Cysteine-rich motor neuron 1	267780	1.60	1.4E-02
LOC389677	Similar to RIKEN cDNA 3000004N20	134163	1.56	1.2E-03
SLC35C1	Solute carrier family 35, member C1	4300145	1.54	7.8E-04
PLXND1	Plexin D1	47314	1.53	1.1E-02
FLJ12666	Chromosome 1 open reading frame 108	5563088	1.50	1.4E-02
ZDHHC2	Zinc finger, DHHC-type containing 2	127682	1.47	3.1E-02
QPRT	Quinolinate phosphoribosyltransferase (nicotinate-nucleotide pyrophosphorylase (carboxylating))	4872092	1.43	2.4E-02
MYO1C	Myosin IC	5562766	1.38	1.4E-02
DDIT4	DNA-damage-inducible transcript 4	360717	1.38	1.2E-03
PGEA1	PKD2 interactor, golgi and endoplasmic reticulum associated 1	5269011	1.37	7.8E-03
CTGF	Connective tissue growth factor	267256	1.35	1.9E-02
---	Hypothetical LOC554202	5139119	1.32	2.8E-03
SPAG9	Sperm associated antigen 9	4446514	1.31	2.4E-02
182-FIP	82-kD FMRP Interacting Protein	3208514	1.29	1.9E-02
METTL2	Methyltransferase like 2	137934	1.26	5.6E-03
PMS2L5	Postmeiotic segregation increased 2-like 5	4397924	1.23	3.1E-02
C7orf23	Chromosome 7 open reading frame 23	129466	1.20	2.8E-03
C17orf31	Chromosome 17 open reading frame 31	6176178	1.20	7.8E-03
LOC284323	Hypothetical protein LOC284323	2722002	1.19	1.4E-02
PDF	Peptide deformylase-like protein	4360858	1.19	2.8E-03
---	Transcribed locus	265	1.19	3.1E-02
ANP32A	Acidic (leucine-rich) nuclear phosphoprotein 32 family, member A	4500255	1.19	5.6E-03
LOC112885	PHD finger protein 21B	384358	1.18	7.8E-03
IDH1	Isocitrate dehydrogenase 1 (NADP+), soluble	263446	1.18	4.0E-03
FLJ20580	Chromosome 1 open reading frame 123	134213	1.18	1.9E-02
PPIA	Peptidylprolyl isomerase A (cyclophilin A)	5264185	1.14	9.4E-02
TARDBP	TAR DNA binding protein	27469	1.13	7.8E-03
NT5C3	5'-nucleotidase, cytosolic III	2063633	1.13	4.0E-03
SP100	Nuclear antigen Sp100	324848	1.12	7.8E-04
SKIP	Skeletal muscle and kidney enriched inositol phosphatase	127715	1.11	2.8E-03
---	---	745698	1.07	1.4E-02
KIAA0672	KIAA0672 gene product	46488	1.06	9.4E-02
GBP1	Guanylate binding protein 1, interferon-inducible, 67kDa	1678893	1.06	4.0E-02
CLECSF2	C-type lectin domain family 2, member B	5587577	1.06	1.9E-03
UQCRFS1	Ubiquinol-cytochrome c reductase, Rieske iron-sulfur polypeptide 1	234347	1.05	1.1E-02
PCDH17	Protocadherin 17	1960190	1.05	7.7E-02
WAS	Wiskott-Aldrich syndrome (eczema-thrombocytopenia)	4849179	1.05	4.0E-03
NDUFB7	NADH dehydrogenase (ubiquinone) 1 beta subcomplex, 7, 18kDa	132618	1.04	1.9E-02
EXOSC1	Exosome component 1	145635	1.03	4.0E-02
---	Full-length cDNA clone CS0DB001YJ03 of Neuroblastoma Cot 10-normalized of Homo sapiens (human)	3610555	1.03	4.0E-02
Pfs2	DNA replication complex GINS protein PSF2	205460	1.02	2.4E-02
CCDC5	Coiled-coil domain containing 5 (spindle associated)	5492935	1.02	5.6E-03
GADD45GIP1	Growth arrest and DNA-damage-inducible, gamma interacting protein 1	141372	1.01	7.7E-02
	Decreased with age (Top 50)			
---	---	172289	-2.87	2.4E-02
C1orf22	Chromosome 1 open reading frame 22	151486	-2.54	1.7E-04
NR5A1	Nuclear receptor subfamily 5, group A, member 1	1737234	-2.51	6.3E-02
SMO	Smoothened homolog (Drosophila)	158237	-2.50	1.1E-02
HIPK2	Homeodomain interacting protein kinase 2	120533	-2.49	3.2E-02
MYH11	Myosin, heavy polypeptide 11, smooth muscle	123678	-2.44	5.6E-03
PBX2	Pre-B-cell leukemia transcription factor 2	757058	-2.40	1.1E-02
C10orf137	Chromosome 10 open reading frame 137	488861	-2.38	1.9E-02
---	---	743205	-2.38	4.0E-02
PIP	Prolactin-induced protein	985457	-2.36	2.4E-02
TYROBP	TYRO protein tyrosine kinase binding protein	152679	-2.31	1.1E-02
GALNT14	UDP-N-acetyl-alpha-D-galactosamine:polypeptide N-acetylgalactosaminyltransferase 14 (GalNAc-T14)	124006	-2.30	4.9E-04
RABL2A	RAB, member of RAS oncogene family-like 2A	504484	-2.23	1.4E-02
CIZ1	CDKN1A interacting zinc finger protein 1	758643	-2.22	7.8E-03
LACTB2	Lactamase, beta 2	195159	-2.20	3.2E-02
RBBP5	Retinoblastoma binding protein 5	824863	-2.17	3.2E-02
SIAT4B	ST3 beta-galactoside alpha-2,3-sialyltransferase 2	1408710	-2.17	4.0E-02
IFRD1	Interferon-related developmental regulator 1	121948	-2.17	2.8E-03
DKFZP586L0724	DKFZP586L0724 protein	825282	-2.13	1.7E-04
LRP4	Low density lipoprotein receptor-related protein 4	38228	-2.11	5.6E-03
SLC22A4	Solute carrier family 22 (organic cation transporter), member 4	937635	-2.10	2.9E-04
MAP3K12	Mitogen-activated protein kinase kinase kinase 12	1682059	-2.03	1.9E-03
SCN1B	Sodium channel, voltage-gated, type I, beta	156983	-2.02	3.2E-02
SMYD5	SMYD family member 5	774488	-2.02	3.2E-02
BXDC1	Brix domain containing 1	773331	-2.01	2.9E-04
CASK	Calcium/calmodulin-dependent serine protein kinase (MAGUK family)	247107	-1.98	7.8E-03
GNAO1	Guanine nucleotide binding protein (G protein), alpha activating activity polypeptide O	1734348	-1.91	6.3E-02
TARBP2	TAR (HIV) RNA binding protein 2	156223	-1.89	1.4E-02
GRB10	Growth factor receptor-bound protein 10	31593	-1.87	2.8E-03
EDNRA	Endothelin receptor type A	487341	-1.87	1.9E-02
VCP	Valosin-containing protein	123873	-1.86	5.6E-03
---	Transcribed locus	728470	-1.84	1.1E-02
SETDB1	SET domain, bifurcated 1	25755	-1.82	2.8E-03
0	0	115454	-1.81	5.0E-02
IFNAR2	Interferon (alpha, beta and omega) receptor 2	123950	-1.79	2.4E-02
---	Transcribed locus	1744348	-1.79	4.0E-03
NFKBIL2	Nuclear factor of kappa light polypeptide gene enhancer in B-cells inhibitor-like 2	726311	-1.76	2.2E-01
FLJ10826	Hypothetical protein FLJ10826	34187	-1.76	1.4E-02
FLJ32731	Hypothetical protein FLJ32731	142851	-1.75	4.0E-03
RXRB	Retinoid X receptor, beta	724955	-1.74	2.4E-02
CHD1L	Chromodomain helicase DNA binding protein 1-like	145151	-1.74	5.6E-03
UBQLN4	Ubiquilin 4	114186	-1.71	1.9E-03
C1orf16	Chromosome 1 open reading frame 16	23108	-1.71	2.8E-03
MRPL30	Mitochondrial ribosomal protein L30	428568	-1.69	4.0E-02
DSC1	Desmocollin 1	1704980	-1.66	3.2E-02
PYCRL	Pyrroline-5-carboxylate reductase-like	754617	-1.66	4.0E-02
RARG	Retinoic acid receptor, gamma	298678	-1.65	4.0E-02
MRPS17	Mitochondrial ribosomal protein S17	1691741	-1.64	4.0E-02
HSPBP1	Hsp70-interacting protein	743114	-1.64	1.9E-02
---	---	2255603	-1.62	4.0E-03

Table X.2 Target gene list for human sebocytes.

Symbol	Definition	ImageID	Ratio	PValue
	Increased with age (Top 50)			
---	---	2241284	1.72	4.1E-03
FLJ10884	CDNA FLJ11111 FIS, CLONE PLACE1005923.	2723837	1.61	1.8E-02
KIAA0431	HYPOTHETICAL PROTEIN KIAA0431.	37271	0.96	2.6E-02
FZD3	FRIZZLED 3 PRECURSOR (FRIZZLED-3) (FZ-3) (HFZ3)	5562987	0.95	3.8E-02
---	---	2454105	0.93	2.3E-03
---	---	269470	0.92	5.8E-04
SDCCAG16	SIMILAR TO KIAA0266 GENE PRODUCT	3842230	0.91	1.1E-02
FLJ20080	CDNA FLJ20080 FIS, CLONE COL03184.	5201158	0.90	1.1E-02
---	---	1185708	0.89	1.8E-02
LOC56906	HYPOTHETICAL UNKNOWN PROTEIN PRODUCT.	190305	0.86	1.1E-02
FLJ14547	---	5535826	0.85	2.3E-03
KIAA0308,MGC17528	CDNA FLJ12178 FIS, CLONE MAMMA1000731.	147630	0.84	5.8E-04
EIF3S10	EUKARYOTIC TRANSLATION INITIATION FACTOR 3 SUBUNIT 10	125261	0.83	7.0E-03
---	---	5482492	0.82	2.3E-03
FLJ10719	CDNA FLJ10719 FIS, CLONE NT2RP3001109 (FRAGMENT).	5585739	0.82	1.8E-02
IQGAP1	RAS GTPASE-ACTIVATING-LIKE PROTEIN IQGAP1 (P195)	41500	0.82	7.0E-03
FEZ1	FASCICULATION AND ELONGATION PROTEIN ZETA 1 (ZYGIN I)	46305	0.82	7.0E-03
FLJ10824,KIAA0592	HYPOTHETICAL 30.5 KDA PROTEIN	140020	0.79	2.6E-02
MTERF	TRANSCRIPTION TERMINATION FACTOR, MITOCHONDRIAL PRECURSOR	810951	0.79	1.1E-02
RACGAP1	CDNA FLJ12664 FIS, CLONE NT2RM4002226	726783	0.77	1.8E-02
EPRS	BIFUNCTIONAL AMINOACYL-TRNA SYNTHETASE	5473525	0.76	7.0E-03
MBD2	METHYL-CPG BINDING DOMAIN PROTEIN 2, ISOFORM 1	713558	0.75	7.0E-03
KTN1	KINECTIN 1; CG-1 ANTIGEN	502136	0.75	1.8E-02
EGFL3	MEGF6 (FRAGMENT).	2155017	0.75	1.8E-02
FLJ20048	CDNA FLJ20048 FIS, CLONE COL00659.	278926	0.74	7.0E-03
SYBL1	SYNAPTOBREVIN-LIKE PROTEIN 1	743221	0.74	1.1E-02
PCM1	RET/PCM-1 PROTEIN (FRAGMENT).	5141807	0.74	4.1E-03
HT010	UNCHARACTERIZED HYPOTHALAMUS PROTEIN HT010	145676	0.73	1.8E-02
---	---	5459635	0.73	2.6E-02
MGC4268	HYPOTHETICAL 3.3 KDA PROTEIN.	3532352	0.72	4.1E-03
---	---	2010707	0.72	7.3E-02
FLJ21816	CDNA: FLJ21816 FIS, CLONE HEP01116.	773527	0.72	1.1E-02
CXCL1	GROWTH REGULATED PROTEIN PRECURSOR	323238	0.72	4.1E-03
---	---	3633831	0.72	2.3E-03
---	---	1876862	0.71	1.1E-02
---	---	114997	0.70	7.0E-03
---	---	347118	0.70	1.1E-02
KIF5B	KINESIN HEAVY CHAIN (UBIQUITOUS KINESIN HEAVY CHAIN) (UKHC).	5557202	0.69	5.3E-02
USP15	UBIQUITIN CARBOXYL-TERMINAL HYDROLASE 15	136304	0.69	1.1E-02
KIAA0450	HYPOTHETICAL PROTEIN KIAA0450.	153543	0.69	1.1E-02
SMURF2	NEDD 4 PROTEIN EC 6.3.2.-	754026	0.69	1.8E-02
CMKLR1	CHEMOKINE RECEPTOR-LIKE 1 (G-PROTEIN COUPLED RECEPTOR DEZ)	3032869	0.69	1.8E-02
GBP1	INTERFERON-INDUCED GUANYLATE-BINDING PROTEIN 1	1678893	0.69	3.8E-02
---	---	4372994	0.68	4.1E-03
EIF3S1	CDNA: FLJ21439 FIS, CLONE COL04352.	51827	0.68	1.2E-03
PAG	PHOSPHOPROTEIN ASSOCIATED WITH GLYCOSPHINGOLIPID-ENRICHED MICRODOMAINS	282779	0.68	1.2E-03
ENAH	CDNA FLJ10773 FIS, CLONE NT2RP4000246	124369	0.68	2.6E-02
---	---	1326140	0.68	7.0E-03
TYROBP	TYRO PROTEIN TYROSINE KINASE-BINDING PROTEIN PRECURSOR	152679	0.68	2.6E-02
GALNT7	POLYPEPTIDE N-ACETYLGALACTOSAMINYLTRANSFERASE 7	2187813	0.67	3.8E-02
	Decreased with age (Top 50)			
MGC8902	AMBIGUOUS	3850514	1.73	5.8E-04
VCP	26S PROTEASE REGULATORY SUBUNIT	5737119	1.68	5.8E-04
TCP11	T-COMPLEX 11 (MOUSE); T-COMPLEX HOMOLOG TCP-11; T-COMPLEX 11	1644999	1.48	2.6E-02
---	KERATIN, HAIR, BASIC, 4; HARD KERATIN, TYPE II, 4	1618942	1.48	5.8E-04
MGC4170	HYPOTHETICAL 8.4 KDA PROTEIN.	3278043	1.31	1.1E-02
HLA-C	HLA CLASS I HISTOCOMPATIBILITY ANTIGEN, A-1 ALPHA CHAIN PRECURSOR	2125838	1.31	5.8E-04
EEF2	ELONGATION FACTOR 2 (EF-2).	704464	1.29	5.8E-04
SAFB	KIAA0138 PROTEIN.	363287	1.29	2.3E-03
---	---	2210175	1.23	1.2E-03
MVD	DIPHOSPHOMEVALONATE DECARBOXYLASE	155866	1.19	5.8E-04
FLJ12592	NT2RM4001316 PROTEIN.	6048624	1.18	4.1E-03
---	---	1737519	1.15	1.1E-02
---	---	2296343	1.10	2.6E-02
DJ328E19.C1.1	AMBIGUOUS	4536659	1.09	5.8E-04
---	---	358599	1.05	2.6E-02
DKFZP434A0131	NUCLEAR	5416073	1.05	4.1E-03
HOXB9	HOXB9.	784578	1.03	2.6E-02
---	---	2164556	1.02	3.8E-02
---	---	2143952	1.02	1.1E-02
---	---	1960523	1.02	3.8E-02
C20ORF28	HYPOTHETICAL 18.4 KDA PROTEIN (DJ1009E24.4) (DKFZ434I114).	2444239	1.01	1.1E-02
TMPRSS3	TRANSMEMBRANE PROTEASE, SERINE 3	2155792	1.01	7.0E-03
MGC2835	ATP-DEPENDENT RNA HELICASE; APOPTOSIS RELATED PROTEIN APR-5	743268	1.01	7.3E-02
FLJ12505	CDNA FLJ12505 FIS, CLONE NT2RM2001699.	1707965	1.01	5.8E-04
FLJ35119		1623114	1.00	2.3E-03
TNFRSF25	WSL 1 PROTEIN PRECURSOR	177245	0.99	2.6E-02
FBXW7	F-BOX PROTEIN FBW7, ISOFORM 2	2211511	0.98	1.8E-02
---	---	2027767	0.97	5.3E-02
---	---	712909	0.96	3.8E-02
---	---	2393739	0.96	1.2E-03
---	---	1621717	0.96	5.8E-04
RAB1A	RAS-RELATED PROTEIN RAB-1A (YPT1-RELATED PROTEIN)	202868	0.96	5.8E-04
KIAA1962	ZINC FINGER PROTEIN	1755636	0.96	2.3E-03
---	PRO2168.	362672	0.95	2.6E-02
MRS3/4	NPD016.	5114190	0.95	3.8E-02
LYAR	HYPOTHETICAL 43.6 KDA PROTEIN.	767163	0.95	2.3E-03
---	---	810482	0.94	1.8E-02
GRF2	GUANINE NUCLEOTIDE-RELEASING FACTOR 2	143729	0.93	4.1E-03
DKFZP434N1235	HYPOTHETICAL 35.0 KDA PROTEIN.	1751497	0.93	2.3E-03
TREX1	CDNA FLJ12343 FIS, CLONE MAMMA1002292.	2327763	0.93	3.8E-02
ACTN1	ALPHA-ACTININ 1	6156839	0.92	2.3E-03
---	---	2171954	0.92	4.1E-03
---	---	1989546	0.91	5.8E-04
---	---	3177823	0.90	1.8E-02
MYO1C	MYOSIN IC (MYOSIN I BETA) (MMI-BETA) (MMIB).	5562766	0.89	2.3E-03
MFGE8	LACTADHERIN PRECURSOR (MILK FAT GLOBULE-EGF FACTOR 8)	44854	0.89	5.8E-04
PGLS	6-PHOSPHOGLUCONOLACTONASE (EC 3.1.1.31) (6PGL)	725475	0.88	7.0E-03
---	---	814273	0.88	1.8E-02
---	---	745644	0.88	2.3E-03
MGC8902	SH2 DOMAIN PROTEIN 2A (T CELL-SPECIFIC ADAPTER PROTEIN)	2454476	0.88	5.8E-04

Table X.3 Target gene list for female human skin biopsies.

Symbol	Definition	Accession	Ratio	PValue
	Increased with age (Top 50)			
LOC440157	hypothetical gene supported by AK096951; BC066547	NM_001013701.1	2.30	2.0E-02
POLN	polymerase (DNA directed) nu	NM_181808.1	1.81	3.5E-02
LRAP	leukocyte-derived arginine aminopeptidase	NM_022350.1	1.76	5.8E-03
FOLR3	folate receptor 3 (gamma)	NM_000804.2	1.73	4.0E-02
SIRT6	sirtuin (silent mating type information regulation 2 homolog) 6 (S. cerevisiae)	NM_016539.1	1.72	4.3E-02
TRIM15	tripartite motif-containing 15, transcript variant 2	NM_052812.1	1.65	4.0E-02
HBQ1	hemoglobin, theta 1	NM_005331.3	1.42	3.5E-02
WBSCR27	Williams Beuren syndrome chromosome region 27	NM_152559.2	1.31	4.4E-02
LOC115648	similar to hypothetical protein FLJ13659	NM_145326.1	1.27	3.4E-02
SLC25A16	solute carrier family 25 (mitochondrial carrier; Graves disease autoantigen), member 16	NM_152707.2	1.15	3.1E-02
CPT1B	carnitine palmitoyltransferase 1B (muscle), transcript variant 3	NM_152246.1	1.12	7.2E-03
ARHGAP26	Rho GTPase activating protein 26	NM_015071.2	1.10	3.5E-02
ITGA2B	integrin, alpha 2b (platelet glycoprotein IIb of IIb/IIIa complex, antigen CD41B)	NM_000419.2	1.09	2.7E-02
C14orf50	chromosome 14 open reading frame 50	NM_172365.1	1.08	4.6E-02
SFRS14	splicing factor, arginine/serine-rich 14, transcript variant 1	NM_001017392.1	1.07	1.2E-02
DMD	dystrophin (muscular dystrophy, Duchenne and Becker types), transcript variant Dp40	NM_004019.1	1.02	4.5E-02
DYNC2LI1	dynein, cytoplasmic 2, light intermediate chain 1, transcript variant 3	NM_001012665.1	1.01	2.8E-02
SEC31L2	SEC31-like 2 (S. cerevisiae), transcript variant 2	NM_198138.1	1.01	2.0E-02
NDUFV3	NADH dehydrogenase (ubiquinone) flavoprotein 3, 10kDa, transcript variant 1	NM_021075.3	0.99	3.8E-03
ZBTB16	zinc finger and BTB domain containing 16, transcript variant 1	NM_006006.4	0.98	2.4E-02
CDC42BPA	CDC42 binding protein kinase alpha (DMPK-like), transcript variant A	NM_014826.3	0.97	3.4E-02
SPAG8	sperm associated antigen 8, transcript variant 2	NM_172312.1	0.96	1.1E-02
TMEM52	transmembrane protein 52	NM_178545.2	0.96	3.4E-02
C10orf125	chromosome 10 open reading frame 125	NM_198472.1	0.95	4.0E-02
ALDH4A1	aldehyde dehydrogenase 4 family, member A1, transcript variant P5CDhS	NM_170726.1	0.95	2.2E-02
C19orf18	chromosome 19 open reading frame 18	NM_152474.2	0.94	3.6E-02
ALDH4A1	aldehyde dehydrogenase 4 family, member A1, transcript variant P5CDhL	NM_003748.2	0.94	9.7E-03
DNHD1	dynein heavy chain domain 1	NM_144666.1	0.93	4.3E-02
SLC1A3	solute carrier family 1 (glial high affinity glutamate transporter), member 3	NM_004172.3	0.93	4.3E-02
EIF4EBP1	eukaryotic translation initiation factor 4E binding protein 1	NM_004095.2	0.93	2.8E-02
ABCB9	ATP-binding cassette, sub-family B (MDR/TAP), member 9, transcript variant 2	NM_019624.2	0.92	2.9E-02
NR1H4	nuclear receptor subfamily 1, group H, member 4	NM_005123.1	0.92	4.7E-02
GLI4	GLI-Kruppel family member GLI4	NM_138465.3	0.92	2.2E-03
HEMK1	HemK methyltransferase family member 1	NM_016173.3	0.88	2.3E-02
LOC51252	hypothetical protein LOC51252	NM_016490.3	0.88	3.5E-02
FLT1	fms-related tyrosine kinase 1 (vascular endothelial growth factor/vascular permeability factor receptor)	NM_002019.2	0.87	3.2E-02
C17orf53	chromosome 17 open reading frame 53	NM_024032.2	0.85	3.1E-02
FLJ23554	hypothetical protein FLJ23554, transcript variant 1	NM_024806.2	0.84	2.0E-02
C3orf62	chromosome 3 open reading frame 62	NM_198562.1	0.83	8.0E-03
ABHD14B	abhydrolase domain containing 14B	NM_032750.1	0.82	2.9E-02
FLJ12700	hypothetical protein FLJ12700	NM_024910.1	0.82	2.3E-02
KIAA0408	KIAA0408	NM_014702.3	0.81	2.1E-02
LOC81691	exonuclease NEF-sp	NM_030941.1	0.81	7.1E-03
MRPL27	mitochondrial ribosomal protein L27, transcript variant 2	NM_148571.1	0.81	1.9E-04
KLHDC8B	kelch domain containing 8B	NM_173546.1	0.79	1.6E-02
HYAL3	hyaluronoglucosaminidase 3	NM_003549.2	0.79	1.2E-02
HSDL2	hydroxysteroid dehydrogenase like 2	NM_032303.2	0.78	1.7E-02
SPIC	Spi-C transcription factor (Spi-1/PU.1 related)	NM_152323.1	0.78	4.8E-02
PRDM1	PR domain containing 1, with ZNF domain, transcript variant 2	NM_182907.1	0.77	2.3E-02
GPT	glutamic-pyruvate transaminase (alanine aminotransferase)	NM_005309.1	0.77	1.8E-02
	Decreased with age (Top 50)			
CORIN	corin, serine peptidase	NM_006587.2	-3.42	1.3E-03
MUC7	mucin 7, salivary	NM_152291.1	-2.64	2.3E-02
SELE	selectin E (endothelial adhesion molecule 1)	NM_000450.1	-2.59	4.2E-02
WIF1	WNT inhibitory factor 1	NM_007191.2	-2.48	1.7E-03
COL1A1	collagen, type I, alpha 1	NM_000088.2	-2.33	2.9E-03
GREM1	gremlin 1, cysteine knot superfamily, homolog (Xenopus laevis)	NM_013372.5	-2.14	3.0E-02
CPZ	carboxypeptidase Z, transcript variant 1	NM_001014447.1	-2.08	4.3E-03
BCMP11	breast cancer membrane protein 11	NM_176813.3	-2.06	1.4E-02
ACCN1	amiloride-sensitive cation channel 1, neuronal (degenerin), transcript variant 1	NM_183377.1	-2.04	2.0E-02
MATN4	matrilin 4, transcript variant 2	NM_030590.1	-1.99	9.4E-03
CLDN11	claudin 11 (oligodendrocyte transmembrane protein)	NM_005602.4	-1.95	2.0E-02
MATN4	matrilin 4, transcript variant 1	NM_003833.2	-1.95	1.8E-03
COL3A1	collagen, type III, alpha 1 (Ehlers-Danlos syndrome type IV, autosomal dominant)	NM_000090.2	-1.93	1.5E-03
FLJ13391	hypothetical protein FLJ13391	NM_032181.1	-1.91	3.8E-03
NPTX2	neuronal pentraxin II	NM_002523.1	-1.82	2.8E-02
HLA-DRB4	major histocompatibility complex, class II, DR beta 4	NM_021983.4	-1.79	1.8E-02
TMEM46	transmembrane protein 46	NM_001007538.1	-1.74	2.3E-02
C1QTNF3	C1q and tumor necrosis factor related protein 3, transcript variant 2	NM_181435.4	-1.73	2.3E-02
ELA2	elastase 2, neutrophil	NM_001972.2	-1.73	3.5E-02
EDAR	ectodysplasin A receptor	NM_022336.1	-1.70	2.8E-02
KIAA1913	KIAA1913	NM_052913.2	-1.69	5.2E-03
SFRP2	secreted frizzled-related protein 2	NM_003013.2	-1.69	2.5E-03
CLDN10	claudin 10, transcript variant 2	NM_006984.3	-1.68	1.8E-02
GREM2	gremlin 2, cysteine knot superfamily, homolog (Xenopus laevis)	NM_022469.3	-1.64	1.2E-02
COL1A2	collagen, type I, alpha 2	NM_000089.3	-1.63	6.2E-04
HOXD10	homeo box D10	NM_002148.2	-1.62	1.5E-02
MMP27	matrix metallopeptidase 27	NM_022122.2	-1.57	3.4E-03
ADCY8	adenylate cyclase 8 (brain)	NM_001115.1	-1.50	4.1E-02
FNDC1	fibronectin type III domain containing 1	NM_032532.1	-1.50	4.9E-02
MASP1	mannan-binding lectin serine peptidase 1 (C4/C2 activating component of Ra-reactive factor), transcript variant 2	NM_139125.2	-1.48	2.8E-04
DUSP7	dual specificity phosphatase 7	NM_001947.1	-1.47	1.0E-02
CSPG2	chondroitin sulfate proteoglycan 2 (versican)	NM_004385.2	-1.47	1.6E-02
BARX2	BarH-like homeobox 2	NM_003658.3	-1.46	6.9E-04
HRNR	hornerin	NM_001009931.1	-1.46	7.2E-03
CA6	carbonic anhydrase VI	NM_001215.2	-1.44	4.9E-02
MB	myoglobin, transcript variant 1	NM_005368.2	-1.44	4.6E-02
HLA-C	major histocompatibility complex, class I, C	NM_002117.4	-1.43	2.2E-02
PRB2	proline-rich protein BstNI subfamily 2	NM_006248.1	-1.41	2.8E-02
WNT7B	wingless-type MMTV integration site family, member 7B	NM_058238.1	-1.41	1.0E-02
F5	coagulation factor V (proaccelerin, labile factor)	NM_000130.2	-1.40	1.3E-03
NFATC4	nuclear factor of activated T-cells, cytoplasmic, calcineurin-dependent 4	NM_004554.3	-1.40	2.4E-02
DIRAS3	DIRAS family, GTP-binding RAS-like 3	NM_004675.2	-1.39	2.1E-02
ST8SIA1	ST8 alpha-N-acetyl-neuraminide alpha-2,8-sialyltransferase 1	NM_003034.2	-1.38	2.7E-02
E2F8	E2F transcription factor 8	NM_024680.2	-1.37	2.5E-03
TRPC6	transient receptor potential cation channel, subfamily C, member 6	NM_004621.3	-1.37	3.6E-02
NOV	nephroblastoma overexpressed gene	NM_002514.2	-1.37	1.0E-02
SLC12A2	solute carrier family 12 (sodium/potassium/chloride transporters), member 2	NM_001046.2	-1.37	1.8E-02
WNT5A	wingless-type MMTV integration site family, member 5A	NM_003392.3	-1.36	3.5E-03
FAP	fibroblast activation protein, alpha	NM_004460.2	-1.35	3.3E-02
CHURC1	churchill domain containing 1	NM_145165.2	-1.34	3.6E-02

Table X.4 Target gene list for male human skin biopsies.

Symbol	Definition	Accession	Ratio	PValue
	Increased with age (Top 50)			
WDR66	WD repeat domain 66	NM_144668.3	2.00	7.0E-04
GUCY2C	guanylate cyclase 2C (heat stable enterotoxin receptor)	NM_004963.1	1.60	2.9E-02
SIRT6	sirtuin (silent mating type information regulation 2 homolog) 6 (S. cerevisiae)	NM_016539.1	1.29	4.1E-02
FETUB	fetuin B	NM_014375.2	1.28	7.9E-06
LRMP	lymphoid-restricted membrane protein	NM_006152.2	1.23	5.7E-03
FMO3	flavin containing monooxygenase 3, transcript variant 1	NM_006894.4	1.23	1.2E-02
ALDH1L1	aldehyde dehydrogenase 1 family, member L1	NM_012190.2	1.17	3.9E-02
ZSCAN4	zinc finger and SCAN domain containing 4	NM_152677.1	1.14	1.1E-02
PEX6	peroxisomal biogenesis factor 6	NM_000287.2	1.13	1.9E-02
RDH16	retinol dehydrogenase 16 (all-trans and 13-cis)	NM_003708.2	1.13	4.3E-03
MGC33839	hypothetical protein MGC33839	NM_152353.1	1.08	2.4E-02
FMO2	flavin containing monooxygenase 2	NM_001460.2	1.07	4.3E-02
ALDH4A1	aldehyde dehydrogenase 4 family, member A1, transcript variant P5CDhL	NM_003748.2	1.05	1.0E-02
METRN	meteorin, glial cell differentiation regulator	NM_024042.2	1.04	4.4E-03
CLDN15	claudin 15, transcript variant 2	NM_138429.1	1.03	9.2E-03
KRT1B	keratin 1B	NM_175078.1	1.02	8.0E-03
ICEBERG	ICEBERG caspase-1 inhibitor	NM_021571.2	1.01	3.4E-02
WNK2	WNK lysine deficient protein kinase 2	NM_006648.3	1.00	1.6E-02
CAMK1G	calcium/calmodulin-dependent protein kinase IG	NM_020439.2	1.00	7.8E-03
CENTA1	centaurin, alpha 1	NM_006869.1	0.97	7.3E-03
SPRR1B	small proline-rich protein 1B (cornifin)	NM_003125.1	0.97	3.3E-02
CPT1B	carnitine palmitoyltransferase 1B (muscle), transcript variant 3	NM_152246.1	0.96	2.6E-02
MAMDC4	MAM domain containing 4	NM_206920.1	0.95	6.0E-04
VMD2L2	vitelliform macular dystrophy 2-like 2	NM_153274.1	0.95	4.5E-02
FOXJ1	forkhead box J1	NM_001454.2	0.92	1.6E-02
CRTC1	CREB regulated transcription coactivator 1, transcript variant 1	NM_015321.1	0.90	4.6E-02
SAMD10	sterile alpha motif domain containing 10	NM_080621.3	0.88	4.4E-04
WNT3	wingless-type MMTV integration site family, member 3	NM_030753.3	0.87	1.6E-02
CIB2	calcium and integrin binding family member 2	NM_006383.2	0.86	6.2E-03
MGC3101	hypothetical protein MGC3101	NM_024043.2	0.85	3.2E-04
FLJ43374	FLJ43374 protein	NM_198582.1	0.84	3.7E-02
PTP4A3	protein tyrosine phosphatase type IVA, member 3, transcript variant 2	NM_007079.2	0.83	9.6E-03
MFSD7	major facilitator superfamily domain containing 7	NM_032219.2	0.82	2.6E-03
VWCE	von Willebrand factor C and EGF domains	NM_152718.1	0.82	1.2E-02
MGC17624	MGC17624 protein	NM_206967.1	0.81	2.5E-02
C12orf28	chromosome 12 open reading frame 28	NM_182530.1	0.81	1.9E-02
SCRIB	scribbled homolog (Drosophila), transcript variant 1	NM_182706.2	0.80	1.2E-02
LRRC61	leucine rich repeat containing 61	NM_023942.1	0.80	5.2E-03
H1FX	H1 histone family, member X	NM_006026.2	0.79	1.4E-02
KCNJ12	potassium inwardly-rectifying channel, subfamily J, member 12	NM_021012.3	0.76	4.4E-02
ACBD4	acyl-Coenzyme A binding domain containing 4	NM_024722.1	0.75	1.6E-02
MGC34647	hypothetical protein MGC34647 (MGC34647)	NM_152456.1	0.75	3.4E-02
PLA2G6	phospholipase A2, group VI (cytosolic, calcium-independent), transcript variant 1	NM_003560.2	0.74	1.9E-02
EGLN3	egl nine homolog 3 (C. elegans)	NM_022073.2	0.72	1.7E-02
LRRC54	leucine rich repeat containing 54	NM_015516.3	0.72	5.7E-03
MMP28	matrix metallopeptidase 28, transcript variant 1	NM_024302.3	0.71	1.9E-02
PLA2G4F	phospholipase A2, group IVF	NM_213600.2	0.71	2.2E-02
CYP2E1	cytochrome P450, family 2, subfamily E, polypeptide 1	NM_000773.3	0.71	2.6E-02
SCCPDH	saccharopine dehydrogenase (putative)	NM_016002.2	0.70	1.7E-02
DPH1	DPH1 homolog (S. cerevisiae)	NM_001383.2	0.70	1.7E-02
	Decreased with age (Top 50)			
LHX2	LIM homeobox 2	NM_004789.3	-2.44	3.5E-02
MATN4	matrilin 4, transcript variant 2	NM_030590.1	-1.88	2.4E-02
MPZ	myelin protein zero (Charcot-Marie-Tooth neuropathy 1B)	NM_000530.3	-1.76	6.7E-03
WIF1	WNT inhibitory factor 1	NM_007191.2	-1.76	4.7E-02
PMP2	peripheral myelin protein 2	NM_002677.3	-1.74	6.5E-03
CPZ	carboxypeptidase Z, transcript variant 1	NM_001014447.1	-1.69	1.3E-02
PDZRN4	PDZ domain containing RING finger 4	NM_013377.2	-1.56	1.8E-02
NOPE	likely ortholog of mouse neighbor of Punc E11	NM_020962.1	-1.51	2.2E-02
CEACAM7	carcinoembryonic antigen-related cell adhesion molecule 7	NM_006890.1	-1.47	4.0E-02
TUBB4	tubulin, beta 4	NM_006087.2	-1.45	4.4E-02
CRABP1	cellular retinoic acid binding protein 1	NM_004378.1	-1.43	9.0E-03
BCAN	brevican, transcript variant 1	NM_021948.3	-1.42	4.3E-03
MATN4	matrilin 4, transcript variant 1	NM_003833.2	-1.41	2.8E-02
TMEM46	transmembrane protein 46	NM_001007538.1	-1.39	4.3E-02
COL1A1	collagen, type I, alpha 1	NM_000088.2	-1.38	2.8E-02
PCSK2	proprotein convertase subtilisin/kexin type 2	NM_002594.2	-1.28	3.1E-02
ATXN3	ataxin 3, transcript variant 2	NM_030660.2	-1.26	9.7E-04
ZNF365	zinc finger protein 365, transcript variant A	NM_014951.1	-1.22	4.9E-03
OCA2	oculocutaneous albinism II (pink-eye dilution homolog, mouse)	NM_000275.1	-1.22	1.8E-02
FAM38B	family with sequence similarity 38, member B	NM_022068.1	-1.21	2.9E-02
RKHD3	ring finger and KH domain containing 3	NM_032246.3	-1.16	3.6E-02
PDE4B	phosphodiesterase 4B, cAMP-specific (phosphodiesterase E4 dunce homolog, Drosophila)	NM_002600.2	-1.15	3.7E-02
COL1A2	collagen, type I, alpha 2	NM_000089.3	-1.13	4.2E-02
ZNF608	zinc finger protein 608	NM_020747.1	-1.13	4.3E-02
ANGPTL1	angiopoietin-like 1	NM_004673.3	-1.11	4.7E-02
ZNF623	zinc finger protein 623	NM_014789.1	-1.11	3.3E-02
PMP22	peripheral myelin protein 22, transcript variant 2	NM_153321.1	-1.10	4.1E-02
MORC3	MORC family CW-type zinc finger 3	NM_015358.1	-1.09	1.7E-02
OTOP3	otopetrin 3	NM_178233.1	-1.08	2.2E-03
SLC45A3	solute carrier family 45, member 3	NM_033102.1	-1.06	1.3E-02
COL3A1	collagen, type III, alpha 1 (Ehlers-Danlos syndrome type IV, autosomal dominant)	NM_000090.2	-1.05	4.0E-02
ACADSB	acyl-Coenzyme A dehydrogenase, short/branched chain, nuclear gene encoding mitochondrial protein	NM_001609.2	-1.04	7.7E-05
FRAS1	Fraser syndrome 1, transcript variant 1	NM_025074.3	-0.99	1.6E-02
MRC2	mannose receptor, C type 2	NM_006039.2	-0.96	4.8E-02
C1QL4	complement component 1, q subcomponent-like 4	NM_001008223.1	-0.95	1.6E-02
NKD1	naked cuticle homolog 1 (Drosophila)	NM_033119.3	-0.92	3.8E-02
TUBAL3	tubulin, alpha-like 3	NM_024803.1	-0.92	4.3E-02
DCN	decorin, transcript variant A1	NM_001920.3	-0.90	3.3E-02
SEC23A	Sec23 homolog A (S. cerevisiae)	NM_006364.2	-0.88	3.2E-02
GNAQ	guanine nucleotide binding protein (G protein), q polypeptide	NM_002072.2	-0.86	3.2E-02
NUP43	nucleoporin 43kDa, transcript variant 1	NM_198887.1	-0.85	6.1E-03
ADH5	alcohol dehydrogenase 5 (class III), chi polypeptide	NM_000671.3	-0.85	9.9E-03
ARNT2	aryl-hydrocarbon receptor nuclear translocator 2	NM_014862.3	-0.84	1.2E-02
DBR1	debranching enzyme homolog 1 (S. cerevisiae)	NM_016216.2	-0.83	2.8E-02
BAPX1	bagpipe homeobox homolog 1 (Drosophila)	NM_001189.2	-0.82	3.4E-02
FLJ14503	hypothetical protein FLJ14503	NM_152780.2	-0.82	4.9E-02
ZNF545	zinc finger protein 545	NM_133466.1	-0.82	1.7E-02
ILF3	interleukin enhancer binding factor 3, 90kDa, transcript variant 3	NM_153464.1	-0.79	1.1E-02
SCRG1	scrapie responsive protein 1	NM_007281.1	-0.78	7.6E-03
CLK1	CDC-like kinase 1, transcript variant 1	NM_004071.2	-0.78	1.2E-02

Table X.5 Target gene list for mouse brain.

Symbol	Definition	Accession	Ratio	PValue
	Increased with age (Top 50)			
Ccl4	chemokine (C-C motif) ligand 4	NM_013652	2.87	1.8E-03
Igk-C	---	XM_132633	2.66	1.4E-02
Igk-C	---	XM_132633	2.45	1.7E-02
C4	complement component 4 (within H-2S)	NM_009780	2.14	2.2E-04
Slp	sex-limited protein	NM_011413	2.12	7.2E-04
Clecsf12	C-type (calcium dependent, carbohydrate recognition domain) lectin, superfamily member 12	NM_020008	2.07	2.3E-03
Slp	sex-limited protein	NM_011413	2.05	3.8E-04
Lgals3	lectin, galactose binding, soluble 3	NM_010705	1.91	2.4E-03
Mela	melanoma antigen	NM_008581	1.81	4.0E-03
C4	complement component 4 (within H-2S)	NM_009780	1.77	1.6E-04
S3-12	plasma membrane associated protein, S3-12	NM_020568	1.76	3.8E-03
Cd52	CD52 antigen	NM_013706	1.72	6.9E-03
Ppl	periplakin	NM_008909	1.68	1.2E-04
Fcrl3	Fc receptor-like 3	NM_144559	1.68	5.9E-03
C3	complement component 3	NM_009778	1.63	1.3E-04
A2m	alpha-2-macroglobulin (A2m)	NM_175628	1.61	7.8E-03
C4	complement component 4 (within H-2S)	NM_009780	1.49	1.7E-03
Abca8a	ATP-binding cassette, sub-family A (ABC1), member 8a	NM_153145	1.48	4.8E-03
Gpnmb	glycoprotein (transmembrane) nmb	NM_053110	1.47	2.8E-03
Lyzs	lysozyme	NM_017372	1.45	1.5E-03
Bcl2a1a	B-cell leukemia/lymphoma 2 related protein A1a	NM_009742	1.39	1.1E-03
2310061N23Rik	RIKEN cDNA 2310061N23 gene	NM_029803	1.37	5.0E-03
Igh-VJ558	---	XM_354700	1.30	3.6E-02
Xist	inactive X specific transcripts on chromosome X, transcript variant 1.	NR_001463	1.30	1.2E-02
Cyp2e1	cytochrome P450, family 2, subfamily e, polypeptide 1	NM_021282	1.29	1.7E-02
Gpnmb	glycoprotein (transmembrane) nmb	NM_053110	1.29	4.5E-03
Slamf9	SLAM family member 9	NM_029612	1.24	2.4E-02
Irak3	interleukin-1 receptor-associated kinase 3	NM_028679	1.23	2.3E-02
H2-K1	---	NM_001001892	1.21	1.9E-03
1810029C22Rik	RIKEN cDNA 1810029C22 gene	XM_284386	1.21	2.2E-02
Cox8b	cytochrome c oxidase, subunit VIIIb	NM_007751	1.16	3.2E-04
4833410I11Rik	---	---	1.15	2.2E-02
Cyp2e1	cytochrome P450, family 2, subfamily e, polypeptide 1	NM_021282	1.15	4.7E-02
Cd84	CD84 antigen	NM_013489	1.15	1.3E-03
Tlr2	toll-like receptor 2	NM_011905	1.15	1.8E-03
Bcl2a1d	B-cell leukemia/lymphoma 2 related protein A1d	NM_007536	1.15	6.5E-03
Cxcl5	chemokine (C-X-C motif) ligand 5	NM_009141	1.13	3.2E-02
Igh-1a	---	XM_354704	1.13	5.4E-03
4732467B22	hypothetical protein 4732467B22	NM_177822	1.07	3.1E-02
Tnfsf13b	tumor necrosis factor (ligand) superfamily, member 13b	NM_033622	1.06	3.2E-02
Capg	capping protein (actin filament), gelsolin-like	NM_007599	1.06	4.0E-03
Clecsf12	C-type (calcium dependent, carbohydrate recognition domain) lectin, superfamily member 12	NM_020008	1.05	2.0E-02
Psmb8	proteosome (prosome, macropain) subunit, beta type 8 (large multifunctional protease 7)	NM_010724	1.04	1.5E-02
Xdh	xanthine dehydrogenase	NM_011723	1.02	2.0E-02
Was	Wiskott-Aldrich syndrome homolog (human)	NM_009515	1.02	2.1E-02
B230204H03Rik	---	---	1.00	3.4E-03
Colec12	collectin sub-family member 12	NM_130449	0.99	7.5E-03
Arl11	---	NM_177337	0.99	1.3E-02
Pcdhb6	protocadherin beta 6	NM_053131	0.99	4.7E-04
Ii	Ia-associated invariant chain	NM_010545	0.99	4.0E-03
	Decreased with age (Top 50)			
F830002E14Rik	---	AK089567	-1.63	3.8E-02
Defb11	defensin beta 11	NM_139221	-1.57	5.7E-03
Mlp	MARCKS-like protein	NM_010807	-1.54	2.1E-02
Bid3	BH3 interacting (with BCL2 family) domain, apoptosis agonist	NM_007545	-1.16	4.5E-02
5031425E22Rik	RIKEN cDNA 5031425E22 gene	XM_149592	-1.05	3.2E-02
Emid2	EMI domain containing 2	NM_024474	-1.04	9.2E-03
Prc1	protein regulator of cytokinesis 1	NM_145150	-1.04	8.5E-03
Ube2j2	ubiquitin-conjugating enzyme E2, J2 homolog (yeast)	NM_021402	-1.00	1.4E-02
Sytl2	synaptotagmin-like 2	NM_031394	-0.98	9.1E-03
Cspg3	chondroitin sulfate proteoglycan 3	NM_007789	-0.96	6.2E-03
Uhrf1	ubiquitin-like, containing PHD and RING finger domains, 1	NM_010931	-0.94	3.7E-04
Dcamkl1	double cortin and calcium/calmodulin-dependent protein kinase-like 1	NM_019978	-0.88	2.5E-02
Mcart1	---	XM_131400	-0.85	2.0E-02
Mkrn3	makorin, ring finger protein, 3	NM_011746	-0.83	3.2E-02
Tnnc1	---	NM_009393	-0.83	3.2E-02
Avp	arginine vasopressin	NM_009732	-0.82	6.8E-03
Igsf1	immunoglobulin superfamily, member 1, transcript variant 2	NM_183336	-0.81	2.8E-02
BC016235	cDNA sequence BC016235	NM_145419	-0.80	1.1E-03
C030013G03Rik	---	---	-0.78	1.2E-03
Igsf1	immunoglobulin superfamily, member 1, transcript variant 2	NM_183336	-0.76	8.0E-03
Cenpa	centromere autoantigen A	NM_007681	-0.76	1.1E-02
Basp1	brain abundant, membrane attached signal protein 1	NM_027395	-0.74	2.4E-02
Rras2	related RAS viral (r-ras) oncogene homolog 2	NM_025846	-0.74	1.6E-02
4930417P05Rik	RIKEN cDNA 4930417P05 gene	XM_131829	-0.74	4.8E-04
---	---	---	-0.73	4.8E-02
2700067D09Rik	RIKEN cDNA 2700067D09 gene	NM_028301	-0.71	2.4E-02
Aoc3	amine oxidase, copper containing 3	NM_009675	-0.71	5.8E-03
1700051I12Rik	RIKEN cDNA 1700051I12 gene	XM_181390	-0.71	1.6E-02
Dpysl4	dihydropyrimidinase-like 4	NM_011993	-0.71	3.5E-02
Tmprss7	---	NM_172455	-0.71	1.4E-02
Slc17a5	solute carrier family 17 (anion/sugar transporter), member 5	NM_172773	-0.70	2.4E-02
Dact2	dapper homolog 2, antagonist of beta-catenin (xenopus)	NM_172826	-0.69	2.4E-02
Ppil6	---	---	-0.69	3.1E-02
Zfp580	---	XM_133134	-0.68	1.1E-02
Pim2	proviral integration site 2	NM_138606	-0.68	4.3E-02
Myh3	myosin, heavy polypeptide 3, skeletal muscle, embryonic	XM_354614	-0.68	1.3E-02
Bai1	brain-specific angiogenesis inhibitor 1	NM_174991	-0.68	1.4E-02
B230382K22Rik	RIKEN cDNA B230382K22 gene	NM_175502	-0.67	1.4E-02
C330012H03Rik	RIKEN cDNA C330012H03 gene	NM_183029	-0.67	3.2E-02
1810037B05Rik	RIKEN cDNA 1810037B05 gene	XM_129390	-0.67	9.2E-03
9130024F11Rik	---	---	-0.66	3.8E-03
2010317E24Rik	RIKEN cDNA 2010317E24 gene	XM_130053	-0.66	6.7E-03
---	hypothetical protein 9630059J11	XM_195221	-0.66	4.7E-02
Itm2a	integral membrane protein 2A	NM_008409	-0.66	4.4E-03
Tcrb-V8.2	---	---	-0.66	1.8E-02
Gpr21	G protein-coupled receptor 21	NM_177383	-0.65	2.9E-03
0610010F05Rik	RIKEN cDNA 0610010F05 gene	XM_203572	-0.65	1.7E-02
Adam19	a disintegrin and metalloproteinase domain 19 (meltrin beta)	NM_009616	-0.65	4.5E-04
Parp6	---	XM_134863	-0.65	2.7E-03
Myl9	myosin, light polypeptide 9, regulatory	XM_283793	-0.65	2.0E-02

Table X.6 Target gene list for mouse heart.

Symbol	Definition	Accession	Ratio	PValue
	Increased with age (Top 50)			
Igh-1a	---	XM_354704	3.89	3.6E-05
Igh-1a	---	XM_354704	3.62	8.2E-05
1810029C22Rik	RIKEN cDNA 1810029C22 gene	XM_284386	3.36	2.2E-02
Klk26	kallikrein 26	NM_010644	3.29	4.1E-03
Csprs	component of Sp100-rs	NM_033616	3.15	5.3E-04
AW120700	---	---	2.94	4.1E-05
Cyp2b20	---	NM_009999	2.90	2.1E-02
S100a9	S100 calcium binding protein A9 (calgranulin B)	NM_009114	2.80	1.1E-02
Serpina3n	serine (or cysteine) proteinase inhibitor, clade A, member 3N	NM_009252	2.80	3.9E-02
Aldob	---	NM_144903	2.66	9.9E-04
Myh7	myosin, heavy polypeptide 7, cardiac muscle, beta	NM_080728	2.62	1.9E-04
Mmp3	matrix metalloproteinase 3	NM_010809	2.57	2.2E-03
Slp	sex-limited protein	NM_011413	2.48	5.2E-03
H2-Bf	histocompatibility 2, complement component factor B	NM_008198	2.42	7.1E-03
Klk26	kallikrein 26	NM_010644	2.41	1.7E-03
Lzp-s	P lysozyme structural	NM_013590	2.36	1.1E-02
Cds1	CDP-diacylglycerol synthase 1	NM_173370	2.35	1.2E-02
Ccl11	small chemokine (C-C motif) ligand 11	NM_011330	2.24	3.4E-03
D5Bwg0834e	DNA segment, Chr 5, Brigham & Womens Genetics 0834 expressed	NM_144819	2.17	3.5E-02
Temt	thioether S-methyltransferase	NM_009349	2.13	8.8E-05
Tac1	tachykinin 1	NM_009311	2.11	9.8E-03
Ttid	titin immunoglobulin domain protein (myotilin)	NM_021484	2.08	9.5E-03
Gpnmb	glycoprotein (transmembrane) nmb	NM_053110	2.04	2.8E-04
Serpina3g	serine (or cysteine) proteinase inhibitor, clade A, member 3G	XM_354694	2.02	3.4E-02
Ifi205	interferon activated gene 205	NM_172648	2.00	1.1E-02
Gsta2	glutathione S-transferase, alpha 2 (Yc2)	NM_008182	1.98	5.6E-04
C4	complement component 4 (within H-2S)	NM_009780	1.98	2.0E-03
Cxcl14	chemokine (C-X-C motif) ligand 14	NM_019568	1.97	8.9E-05
Slp	sex-limited protein	NM_011413	1.96	2.8E-03
Gsta1	glutathione S-transferase, alpha 1 (Ya)	NM_008181	1.94	7.5E-04
Mmp3	matrix metalloproteinase 3	NM_010809	1.89	5.1E-03
Ear2	eosinophil-associated, ribonuclease A family, member 2	NM_007895	1.89	1.9E-02
Cxcl14	chemokine (C-X-C motif) ligand 14	NM_019568	1.83	1.1E-02
Ccl5	chemokine (C-C motif) ligand 5	NM_013653	1.81	8.6E-03
Prkcz	protein kinase C, zeta	NM_008860	1.77	1.3E-02
Ear2	eosinophil-associated, ribonuclease A family, member 2	NM_007895	1.76	2.1E-03
Ear1	eosinophil-associated, ribonuclease A family, member 1	NM_007894	1.76	3.8E-02
Fcrl3	Fc receptor-like 3	NM_144559	1.75	1.1E-02
---	10, 11 days embryo whole body cDNA, RIKEN full-length enriched library, clone:2810403D21 product:unclassifiable, full insert sequence.	AK012972	1.74	1.1E-02
Cib3	---	XM_356089	1.71	3.5E-02
Prkcq	protein kinase C, theta	NM_008859	1.70	1.7E-02
Bcl2a1a	B-cell leukemia/lymphoma 2 related protein A1a	NM_009742	1.70	1.4E-02
Ear10	eosinophil-associated, ribonuclease A family, member 10	NM_053112	1.67	2.9E-02
Mal	myelin and lymphocyte protein, T-cell differentiation protein	NM_010762	1.65	2.5E-04
Ifi205	interferon activated gene 205	NM_172648	1.62	5.0E-03
Gsta2	glutathione S-transferase, alpha 2 (Yc2)	NM_008182	1.61	5.9E-03
Retnla	resistin like alpha	NM_020509	1.60	2.1E-02
Amy2	amylase 2, pancreatic	NM_009669	1.59	6.7E-03
Abat	4-aminobutyrate aminotransferase	NM_172961	1.58	2.1E-02
Ifi205	interferon activated gene 205	NM_172648	1.57	2.7E-02
	Decreased with age (Top 50)			
Ddc	dopa decarboxylase	AK011834	-2.65	6.5E-04
Ddc	dopa decarboxylase	NM_016672	-2.60	9.1E-04
F830002E14Rik	---	AK089567	-2.28	1.3E-02
Kif1b	kinesin family member 1B, transcript variant 1	NM_008441	-1.95	1.2E-03
Tce4	---	XM_489778	-1.87	3.6E-03
Slc38a4	solute carrier family 38, member 4	NM_027052	-1.79	1.0E-02
Ddc	dopa decarboxylase	NM_016672	-1.79	2.2E-03
Col4a6	procollagen, type IV, alpha 6	NM_053185	-1.73	2.4E-02
6720403M19Rik	---	---	-1.67	2.9E-03
Psmb1	proteasome (prosome, macropain) subunit, beta type 1	NM_011185	-1.65	8.5E-03
Gats	opposite strand transcription unit to Stag3	XM_289726	-1.62	2.4E-04
2510002D24Rik	RIKEN cDNA 2510002D24 gene	XM_110173	-1.57	1.4E-03
2900072G11Rik	---	---	-1.48	9.6E-04
Prnd	prion protein dublet	NM_023043	-1.44	6.5E-03
D930038O18Rik	weakly similar to KIAA1036 PROTEIN [Homo sapiens]	AK086583	-1.41	1.9E-02
2900006F19Rik	RIKEN cDNA 2900006F19 gene	XM_355346	-1.40	1.2E-02
1110017D07Rik	---	---	-1.38	7.3E-03
Plekhh1	---	XM_126961	-1.36	1.3E-03
D0H4S114	DNA segment, human D4S114	NM_053078	-1.30	3.7E-03
BC026657	---	NM_029895	-1.29	6.8E-03
Mfap4	microfibrillar-associated protein 4	NM_029568	-1.28	1.9E-02
3526401B18Rik	---	---	-1.26	4.2E-02
Kcne1	potassium voltage-gated channel, Isk-related subfamily, member 1	NM_008424	-1.25	5.0E-03
Adamts12	a disintegrin-like and metalloprotease (reprolysin type) with thrombospondin type 1 motif, 12	NM_175501	-1.25	4.1E-03
2210407C18Rik	RIKEN cDNA 2210407C18 gene	NM_144544	-1.25	1.9E-03
C1qtnf2	---	XM_126141	-1.25	2.2E-02
Arfl4	---	NM_025404	-1.23	1.8E-02
Phkg1	---	NM_011079	-1.22	2.4E-05
4833431P16Rik	---	AK029415	-1.22	8.4E-03
Col3a1	procollagen, type III, alpha 1	NM_009930	-1.21	4.6E-03
4632418H02Rik	RIKEN cDNA 4632418H02 gene	XM_150247	-1.21	1.6E-02
Copg2as2	coatomer protein complex, subunit gamma 2, antisense 2	AK018238	-1.19	2.4E-02
BC029214	cDNA sequence BC029214	NM_153557	-1.19	7.5E-03
6430519N07Rik	---	---	-1.19	5.3E-03
D430036M17Rik	---	AK085102	-1.16	4.0E-02
Acta2	RIKEN cDNA 0610041G09 gene	NM_007392	-1.15	1.5E-02
Prc1	protein regulator of cytokinesis 1	NM_145150	-1.15	1.2E-02
Sec24b	---	XM_131192	-1.15	3.2E-02
6720460K10Rik	---	---	-1.13	1.1E-02
4831403C07Rik	---	---	-1.13	1.2E-02
B930083E23Rik	---	AK047526	-1.12	2.3E-02
9430064K01Rik	---	---	-1.11	6.7E-03
Gpc6	glypican 6	AK032866	-1.10	2.5E-02
3100003M19Rik	---	AK013928	-1.10	1.1E-02
2310007J06Rik	---	---	-1.10	1.2E-02
Col1a1	procollagen, type I, alpha 1	NM_007742	-1.09	1.2E-03
E330020G21Rik	---	AK054368	-1.09	2.3E-02
E530016P10Rik	weakly similar to ONCOGENE TLM [Mus musculus]	AK089149	-1.08	3.8E-03
6030440P17Rik	RIKEN cDNA 6030440P17 gene	NM_172862	-1.06	1.4E-03
9130009M17Rik	dopa decarboxylase	AK011834	-1.06	5.5E-03

Table X.7 Target gene list for mouse kidney.

Symbol	Definition	Accession	Ratio	PValue
	Increased with age (Top 50)			
Igh-1a	---	XM_354704	7.33	1.2E-02
Igh-6	---	XM_354710	6.03	2.8E-02
---	---	---	5.40	1.1E-03
Igh-6	---	XM_354710	5.39	3.2E-02
Igh-1a	---	XM_354704	5.33	6.5E-03
---	---	---	5.19	1.2E-04
AU044919	---	XM_354705	5.15	4.7E-02
Igl-V1	---	XM_148393	4.45	1.9E-02
LOC381783	---	XM_355782	4.32	9.9E-03
---	---	---	4.24	2.8E-02
Igl-V1	---	XM_148393	4.21	2.2E-02
IgK	---	M83099	3.86	1.8E-03
LOC333501	similar to immunoglobulin kappa light chain variable region precursor	XM_285436	3.84	8.4E-03
LOC213684	similar to immunoglobulin light chain variable region	XM_135590	3.76	4.1E-02
LOC384413	similar to immunoglobulin light chain variable region	XM_357631	3.68	1.8E-02
LOC381783	---	XM_355782	3.67	1.1E-02
LOC385109	similar to immunoglobulin light chain variable region	XM_358058	3.65	4.0E-02
Igk-C	---	XM_132633	3.61	1.6E-02
Igk-C	---	XM_132633	3.58	1.0E-02
LOC243430	similar to Ig kappa light chain precursor	XM_144780	3.53	4.8E-02
LOC382696	similar to Ig heavy chain precursor V region (3) - mouse	XM_138364	3.49	2.5E-03
Igl-V1	---	---	3.46	3.5E-02
Ear1	eosinophil-associated, ribonuclease A family, member 1	NM_007894	3.30	1.1E-02
Hdc	histidine decarboxylase	NM_008230	3.26	6.8E-03
---	---	---	3.19	1.0E-02
LOC243467	PREDICTED: similar to immunoglobulin light chain	XM_144849	3.18	2.1E-02
Ms4a6d	membrane-spanning 4-domains, subfamily A, member 11	NM_026835	3.15	4.5E-03
D6Mit97	---	---	3.14	1.1E-02
---	---	---	3.10	2.4E-02
Ear2	eosinophil-associated, ribonuclease A family, member 2	NM_007895	3.08	1.2E-02
2610305J24Rik	weakly similar to GAG PROTEIN [Mus dunni endogenous virus]	AK011989	3.06	1.4E-02
---	---	---	3.06	1.1E-02
Igh-VJ558	---	XM_354700	3.03	4.2E-02
LOC232065	similar to variable region of immunoglobulin kappa light chain	XM_132611	2.92	2.8E-02
---	---	---	2.90	3.9E-02
---	---	---	2.89	1.3E-02
---	---	---	2.88	9.2E-03
Ear10	eosinophil-associated, ribonuclease A family, member 10	NM_053112	2.85	3.1E-03
---	---	---	2.81	9.0E-03
---	---	---	2.81	8.8E-03
Igh-VJ558	---	XM_354700	2.80	2.6E-02
Igk-V1	---	XM_355776	2.80	3.6E-02
LOC232060	similar to monoclonal antibody kappa light chain	XM_132608	2.78	1.1E-02
---	---	---	2.77	3.7E-02
Slpi	secretory leukocyte protease inhibitor	NM_011414	2.75	1.5E-02
Speer7-ps1	spermatogenesis associated glutamate (E)-rich protein 7, pseudogene 1 on chromosome 5.	NR_001585	2.75	1.4E-02
LOC381774	similar to IgE antibody light chain (VJ)	XM_355772	2.74	2.4E-02
---	---	---	2.71	3.3E-02
LOC243433	---	XM_144783	2.67	1.8E-02
Igh-1a	---	XM_354704	2.61	9.2E-04
	Decreased with age (Top 50)			
Temt	thioether S-methyltransferase	NM_009349	-2.22	5.7E-04
Slitrk1	---	NM_199065	-2.18	2.1E-04
Mogat2	---	NM_177448	-1.94	8.3E-04
Akr1c18	aldo-keto reductase family 1, member C18	NM_134066	-1.83	1.4E-03
Emid2	EMI domain containing 2	NM_024474	-1.76	1.7E-03
Stab2	stabilin 2	NM_138673	-1.57	1.2E-03
Sah	SA rat hypertension-associated homolog	NM_016870	-1.53	2.6E-02
Chst3	carbohydrate (chondroitin 6/keratan) sulfotransferase 3	NM_016803	-1.52	2.2E-02
9030611N15Rik	RIKEN cDNA 9030611N15 gene	NM_134072	-1.50	1.7E-03
C730048C13Rik	RIKEN cDNA C730048C13 gene	NM_177002	-1.48	4.6E-03
C730048C13Rik	RIKEN cDNA C730048C13 gene	NM_177002	-1.44	5.7E-03
Serpina1d	serine (or cysteine) proteinase inhibitor, clade A, member 1d	NM_009246	-1.43	1.7E-02
Ly6f	lymphocyte antigen 6 complex, locus F	NM_008530	-1.36	9.8E-03
Es22	esterase 22	NM_133660	-1.34	1.3E-03
BC014805	cDNA sequence BC014805	NM_146232	-1.27	3.3E-02
Edg4	endothelial differentiation, lysophosphatidic acid G-protein-coupled receptor 4	NM_020028	-1.27	1.3E-02
Npy6r	neuropeptide Y receptor Y6	NM_010935	-1.25	7.1E-03
A230055I01Rik	---	AK038691	-1.24	7.7E-03
Hpd	4-hydroxyphenylpyruvic acid dioxygenase	NM_008277	-1.24	1.3E-02
4933417C16Rik	RIKEN cDNA 4933417C16 gene	NM_172568	-1.23	1.0E-02
Mogat1	---	NM_026713	-1.20	2.7E-03
Col1a1	procollagen, type I, alpha 1	NM_007742	-1.20	7.9E-03
Gadd45g	growth arrest and DNA-damage-inducible 45 gamma	NM_011817	-1.19	5.4E-03
Dnase1	deoxyribonuclease I	NM_010061	-1.16	1.1E-02
Thhl1	---	NM_027762	-1.13	2.7E-02
Serpinf2	serine (or cysteine) proteinase inhibitor, clade F, member 2	NM_008878	-1.13	2.1E-02
LOC381001	similar to beta-alanine-pyruvate aminotransferase	XM_354912	-1.13	1.2E-02
LOC268782	similar to beta-alanine-pyruvate aminotransferase	XM_193784	-1.13	7.7E-03
6430537F04	---	---	-1.08	5.8E-03
---	0 day neonate kidney cDNA, RIKEN full-length enriched library, clone:D630011L08 product:unknown EST, full insert sequence.	AK085322	-1.08	1.9E-02
Cyp2e1	cytochrome P450, family 2, subfamily e, polypeptide 1	NM_021282	-1.07	1.0E-02
Cyp2e1	cytochrome P450, family 2, subfamily e, polypeptide 1	NM_021282	-1.06	3.4E-02
5730521E12Rik	RIKEN cDNA 5730521E12 gene	NM_025684	-1.05	2.1E-02
Adra1a	adrenergic receptor, alpha 1a	NM_013461	-1.04	3.9E-03
Slc2a2	solute carrier family 2 (facilitated glucose transporter), member 2	NM_031197	-1.01	2.6E-02
2200001I15Rik	RIKEN cDNA 2200001I15 gene	NM_183278	-1.00	8.4E-03
Slc34a3	solute carrier family 34 (sodium phosphate), member 3	NM_080854	-1.00	3.9E-03
Mep1b	meprin 1 beta	NM_008586	-0.98	9.9E-04
Slc5a2	solute carrier family 5 (sodium/glucose cotransporter), member 2	NM_133254	-0.98	3.7E-02
Slc5a8	solute carrier family 5 (iodide transporter), member 8	NM_145423	-0.96	1.0E-03
C1qtnf3	C1q and tumor necrosis factor related protein 3	NM_030888	-0.96	2.0E-02
Mcph1	---	NM_173189	-0.96	3.4E-04
Serpina1b	serine (or cysteine) proteinase inhibitor, clade A, member 1b	NM_009244	-0.95	2.7E-02
Adamts12	a disintegrin-like and metalloprotease (reprolysin type) with thrombospondin type 1 motif, 12	NM_175501	-0.95	1.2E-02
Cpb2	carboxypeptidase B2 (plasma)	NM_019775	-0.95	3.0E-02
Cox6a2	cytochrome c oxidase, subunit VI a, polypeptide 2	NM_009943	-0.95	1.5E-03
Spnb2	spectrin beta 2, transcript variant 1	NM_175836	-0.94	3.3E-02
Car14	carbonic anhydrase 14	NM_011797	-0.94	3.6E-03
Acy1	aminoacylase 1	NM_025371	-0.93	5.1E-03
Slc2a2	solute carrier family 2 (facilitated glucose transporter), member 2	NM_031197	-0.92	5.3E-03

IV David output tables

Table X.8 Kegg pathways and biological processes for human skin fibroblasts.

Category	Term	Count	%	PValue
	Kegg pathway up			
KEGG_PATHWAY	RIBOSOME	11	5.1	2,9E-07
KEGG_PATHWAY	GLUTATHIONE METABOLISM	4	1.9	1,5E-02
	Kegg pathway down			
	GO – BP up			
GO - BP	PROTEIN BIOSYNTHESIS	19	8.8	1.4E-05
GO – BP	BIOSYNTHESIS	27	12.6	4.8E-05
GO – BP	MACROMOLECULE BIOSYNTHESIS	20	9.3	3.6E-04
GO – BP	RNA PROCESSING	11	5.1	8.5E-04
GO – BP	RNA METABOLISM	11	5.1	5.5E-03
GO – BP	MRNA METABOLISM	7	3.3	6.3E-03
GO – BP	MRNA PROCESSING	6	2.8	1.6E-02
GO – BP	GLYOXYLATE CYCLE	2	0.9	1.9E-02
GO – BP	GLYOXYLATE METABOLISM	2	0.9	1.9E-02
GO – BP	CELLULAR PHYSIOLOGICAL PROCESS	57	26.5	2.1E-02
GO – BP	CELLULAR MORPHOGENESIS	6	2.8	2.4E-02
GO – BP	RNA SPLICING	5	2.3	3.4E-02
GO – BP	CELL ORGANIZATION AND BIOGENESIS	14	6.5	3.8E-02
GO – BP	COENZYME BIOSYNTHESIS	5	2.3	4.2E-02
GO – BP	CYTOPLASM ORGANIZATION AND BIOGENESIS	9	4.2	4.6E-02
	GO – BP down			
GO – BP	CELLULAR PHYSIOLOGICAL PROCESS	59	31,7	7,3E-05
GO – BP	CELL GROWTH AND/OR MAINTENANCE	52	28.0	2,2E-04
GO – BP	CELLULAR PROCESS	77	41,4	1,4E-03
GO – BP	MRNA PROCESSING	7	3,8	1,6E-03
GO – BP	MRNA METABOLISM	7	3,8	2,8E-03
GO – BP	PROTEIN METABOLISM	37	19,9	4,5E-03
GO – BP	INTRACELLULAR PROTEIN TRANSPORT	8	4,3	7,9E-03
GO – BP	INTRACELLULAR TRANSPORT	10	5,4	8,9E-03
GO – BP	MACROMOLECULE METABOLISM	41	22.0	1,3E-02
GO – BP	RNA PROCESSING	8	4,3	1,4E-02
GO – BP	PROTEIN MODIFICATION	21	11,3	1,5E-02
GO – BP	PROTEIN TARGETING	5	2,7	2,3E-02
GO – BP	PROTEIN TRANSPORT	9	4,8	2,5E-02
GO – BP	INTRACELLULAR SIGNALING CASCADE	16	8,6	2,7E-02
GO – BP	CELL PROLIFERATION	17	9,1	2,9E-02
GO – BP	TRANSCRIPTION FROM POL II PROMOTER	9	4,8	3,6E-02
GO – BP	NUCLEAR MRNA SPLICING, VIA SPLICEOSOME	4	2,2	3,9E-02
GO – BP	RNA SPLICING, VIA TRANSESTERIFICATION REACTIONS	4	2,2	3,9E-02
GO – BP	RNA SPLICING, VIA TRANSESTERIFICATION REACTIONS WITH BULGED ADENOSINE AS NUCLEOPHILE	4	2,2	3,9E-02
GO – BP	NUCLEOCYTOPLASMIC TRANSPORT	4	2,2	4,4E-02
GO – BP	ENZYME LINKED RECEPTOR PROTEIN SIGNALING PATHWAY	5	2,7	4,7E-02
GO – BP	RNA METABOLISM	8	4,3	4,7E-02

Table X.9 Kegg pathways and biological processes for human sebocytes.

Category	Term	Count	%	PValue
	Kegg pathway up			
KEGG_PATHWAY	AMINOACYL-TRNA BIOSYNTHESIS	5	1.1	1.7E-03
	Kegg pathway down			
KEGG_PATHWAY	PENTOSE PHOSPHATE PATHWAY	4	0.9	2.5E-02
	GO – BP up (Top 40)			
GO - BP	PROTEIN METABOLISM	92	19.5	8.2E-06
GO – BP	CELLULAR PHYSIOLOGICAL PROCESS	131	27.8	9.7E-06
GO – BP	RNA METABOLISM	24	5.1	1.0E-05
GO – BP	METABOLISM	196	41.6	9.6E-05
GO – BP	MACROMOLECULE METABOLISM	102	21.7	1.1E-04
GO – BP	CELLULAR PROCESS	180	38.2	2.8E-04
GO – BP	PROTEIN COMPLEX ASSEMBLY	10	2.1	6.0E-04
GO – BP	CELL GROWTH AND/OR MAINTENANCE	109	23.1	6.2E-04
GO – BP	PROTEIN TRANSPORT	21	4.5	6.3E-04
GO – BP	NUCLEOBASE, NUCLEOSIDE, NUCLEOTIDE AND NUCLEIC ACID METABOLISM	90	19.1	1.0E-03
GO – BP	MITOTIC CELL CYCLE	13	2.8	1.1E-03
GO – BP	TRANSLATION	12	2.5	1.4E-03
GO – BP	MITOSIS	10	2.1	1.7E-03
GO – BP	CELL PROLIFERATION	40	8.5	1.8E-03
GO – BP	M PHASE OF MITOTIC CELL CYCLE	10	2.1	2.1E-03
GO – BP	TRANSCRIPTION FROM POL II PROMOTER	20	4.2	3.4E-03
GO – BP	INTRACELLULAR TRANSPORT	19	4.0	3.7E-03
GO – BP	PROTEIN MODIFICATION	46	9.8	4.1E-03
GO – BP	RNA PROCESSING	15	3.2	5.1E-03
GO – BP	CELL CYCLE	29	6.2	5.3E-03
GO – BP	AMINO ACID ACTIVATION	6	1.3	6.1E-03
GO – BP	TRNA AMINOACYLATION	6	1.3	6.1E-03
GO – BP	TRNA AMINOACYLATION FOR PROTEIN TRANSLATION	6	1.3	6.1E-03
GO – BP	AMINO ACID METABOLISM	12	2.5	6.8E-03
GO – BP	NUCLEAR DIVISION	10	2.1	8.5E-03
GO – BP	MRNA METABOLISM	10	2.1	9.1E-03
GO – BP	TRNA MODIFICATION	6	1.3	9.4E-03
GO – BP	RESPONSE TO DNA DAMAGE STIMULUS	12	2.5	1.0E-02
GO – BP	M PHASE	10	2.1	1.2E-02
GO – BP	RNA CATABOLISM	4	0.8	1.3E-02
GO – BP	REGULATION OF TRANSCRIPTION FROM POL II PROMOTER	12	2.5	1.4E-02
GO – BP	RESPONSE TO ENDOGENOUS STIMULUS	12	2.5	1.5E-02
GO – BP	TRNA METABOLISM	7	1.5	1.6E-02
GO – BP	RNA MODIFICATION	6	1.3	1.8E-02
GO – BP	ANTI-APOPTOSIS	7	1.5	1.8E-02
GO – BP	VESICLE-MEDIATED TRANSPORT	13	2.8	2.0E-02
GO – BP	NEGATIVE REGULATION OF APOPTOSIS	7	1.5	2.2E-02
GO – BP	AMINO ACID AND DERIVATIVE METABOLISM	12	2.5	2.2E-02
GO – BP	NEGATIVE REGULATION OF PROGRAMMED CELL DEATH	7	1.5	2.3E-02
GO – BP	APOPTOSIS	17	3.6	2.4E-02
	GO – BP down			
GO – BP	CELLULAR PHYSIOLOGICAL PROCESS	125	26.8	1.6E-04
GO – BP	CELL PROLIFERATION	42	9.0	5.0E-04
GO – BP	CELL CYCLE	32	6.9	6.6E-04
GO – BP	CELL GROWTH AND/OR MAINTENANCE	105	22.5	2.8E-03
GO – BP	MACROMOLECULE BIOSYNTHESIS	29	6.2	6.3E-03
GO – BP	REGULATION OF CELL CYCLE	17	3.6	1.2E-02
GO – BP	ORGANOGENESIS	31	6.6	1.2E-02
GO – BP	EPIDERMIS DEVELOPMENT	6	1.3	1.2E-02
GO – BP	LIPID BIOSYNTHESIS	10	2.1	1.3E-02
GO – BP	INDUCTION OF APOPTOSIS	8	1.7	1.7E-02
GO – BP	INDUCTION OF PROGRAMMED CELL DEATH	8	1.7	1.7E-02
GO – BP	MORPHOGENESIS	36	7.7	1.9E-02
GO – BP	MUSCLE DEVELOPMENT	8	1.7	1.9E-02
GO – BP	ECTODERM DEVELOPMENT	6	1.3	2.1E-02
GO – BP	POSITIVE REGULATION OF APOPTOSIS	8	1.7	2.1E-02
GO – BP	POSITIVE REGULATION OF PROGRAMMED CELL DEATH	8	1.7	2.2E-02
GO – BP	DEVELOPMENT	51	10.9	2.3E-02
GO – BP	MACROMOLECULE METABOLISM	88	18.8	2.6E-02
GO – BP	MEMBRANE LIPID BIOSYNTHESIS	5	1.1	2.7E-02
GO – BP	MEMBRANE LIPID METABOLISM	7	1.5	3.7E-02
GO – BP	CELLULAR PROCESS	165	35.3	3.7E-02
GO – BP	LIPID METABOLISM	19	4.1	4.3E-02
GO – BP	UBIQUITIN CYCLE	14	3.0	4.7E-02

Table X.10 Kegg pathways and biological processes for female human skin biopsies.

Category	Term	Count	%	PValue
	Kegg pathway up			
KEGG_PATHWAY	GLYCEROPHOSPHOLIPID METABOLISM	5	1.77	2.1E-02
KEGG_PATHWAY	AMINOPHOSPHONATE METABOLISM	3	1.06	3.2E-02
KEGG_PATHWAY	HISTIDINE METABOLISM	4	1.41	3.3E-02
KEGG_PATHWAY	BUTANOATE METABOLISM	4	1.41	3.8E-02
KEGG_PATHWAY	TYROSINE METABOLISM	4	1.41	4.7E-02
KEGG_PATHWAY	1- AND 2-METHYLNAPHTHALENE DEGRADATION	3	1.06	4.8E-02
	Kegg pathway down			
KEGG_PATHWAY	RIBOSOME	36	6.19	6.1E-11
KEGG_PATHWAY	CELL COMMUNICATION	19	3.26	1.1E-05
KEGG_PATHWAY	WNT SIGNALING PATHWAY	18	3.09	4.4E-04
	GO – BP up			
GO - BP	macromolecule metabolism	82	28.98	5.9E-04
GO – BP	biopolymer metabolism	54	19.08	1.8E-03
GO – BP	cellular protein metabolism	59	20.85	2.3E-03
GO – BP	cellular macromolecule metabolism	59	20.85	3.3E-03
GO – BP	metabolism	126	44.52	4.2E-03
GO – BP	protein metabolism	61	21.55	5.3E-03
GO – BP	biosynthesis	31	10.95	6.1E-03
GO – BP	cell organization and biogenesis	31	10.95	8.9E-03
GO – BP	cellular biosynthesis	28	9.89	9.2E-03
GO – BP	cellular metabolism	117	41.34	9.6E-03
GO – BP	protein transport	15	5.30	1.1E-02
GO – BP	primary metabolism	113	39.93	1.2E-02
GO – BP	establishment of protein localization	15	5.30	1.5E-02
GO – BP	cellular physiological process	151	53.36	1.8E-02
GO – BP	protein localization	15	5.30	1.9E-02
GO – BP	protein modification	32	11.31	1.9E-02
GO – BP	organelle organization and biogenesis	19	6.71	2.0E-02
GO – BP	biopolymer modification	32	11.31	2.7E-02
GO – BP	physiological process	170	60.07	3.2E-02
GO – BP	DNA packaging	8	2.83	3.9E-02
GO – BP	DNA metabolism	15	5.30	4.5E-02
GO – BP	carboxylic acid metabolism	12	4.24	4.9E-02
GO – BP	actin cytoskeleton organization and biogenesis	6	2.12	4.9E-02
	GO – BP down			
GO – BP	ectoderm development	19	3.26	2.3E-10
GO – BP	epidermis development	16	2.75	2.0E-08
GO – BP	development	97	16.67	2.1E-08
GO – BP	protein biosynthesis	53	9.11	1.4E-07
GO – BP	tissue development	22	3.78	2.2E-07
GO – BP	macromolecule biosynthesis	55	9.45	6.0E-07
GO – BP	Wnt receptor signaling pathway	15	2.58	1.7E-06
GO – BP	phosphate transport	13	2.23	6.1E-05
GO – BP	cellular biosynthesis	65	11.17	9.2E-05
GO – BP	biosynthesis	68	11.68	3.6E-04
GO – BP	inorganic anion transport	15	2.58	4.6E-04
GO – BP	cellular macromolecule metabolism	128	21.99	8.5E-04
GO – BP	cell adhesion	36	6.19	1.1E-03
GO – BP	cellular protein metabolism	125	21.48	1.4E-03
GO – BP	frizzled signaling pathway	5	0.86	1.6E-03
GO – BP	protein metabolism	133	22.85	1.7E-03
GO – BP	anion transport	15	2.58	2.7E-03
GO – BP	organ development	26	4.47	1.7E-02
GO – BP	Notch signaling pathway	5	0.86	1.9E-02
GO – BP	antigen presentation, endogenous antigen	5	0.86	1.9E-02
GO – BP	enzyme linked receptor protein signaling pathway	12	2.06	2.4E-02
GO – BP	positive regulation of transcription	9	1.55	2.7E-02
GO – BP	positive regulation of nucleobase, nucleoside, nucleotide and nucleic acid metabolism	9	1.55	3.2E-02
GO – BP	morphogenesis	27	4.64	3.5E-02
GO – BP	positive regulation of cellular metabolism	10	1.72	4.6E-02
GO – BP	transmembrane receptor protein tyrosine kinase signaling pathway	9	1.55	4.6E-02

Table X.11 Kegg pathways and biological processes for male human skin biopsies.

Category	Term	Count	%	PValue
	Kegg pathway up			
KEGG_PATHWAY	ARGININE AND PROLINE METABOLISM	4	1.85%	3.4E-02
	Kegg pathway down			
	GO – BP up			
GO - BP	protein amino acid phosphorylation	16	7.41	1.3E-03
GO – BP	phosphorylation	16	7.41	9.6E-03
GO – BP	phosphorus metabolism	18	8.33	1.1E-02
GO – BP	phosphate metabolism	18	8.33	1.1E-02
GO – BP	protein modification	27	12.50	1.2E-02
GO – BP	biopolymer modification	27	12.50	1.6E-02
GO – BP	protein metabolism	46	21.30	2.5E-02
GO – BP	cellular physiological process	117	54.17	3.7E-02
GO – BP	membrane lipid metabolism	5	2.31	4.0E-02
GO – BP	cellular protein metabolism	42	19.44	4.1E-02
GO – BP	programmed cell death	11	5.09	4.7E-02
	GO – BP down			
GO – BP	protein amino acid ADP-ribosylation	4	2.40	2.1E-03
GO – BP	development	26	15.57	4.1E-03
GO – BP	ionic insulation of neurons by glial cells	3	1.80	4.4E-03
GO – BP	cellular nerve ensheathment	3	1.80	4.4E-03
GO – BP	transcription, DNA-dependent	29	17.37	6.7E-03
GO – BP	nerve ensheathment	3	1.80	7.5E-03
GO – BP	neuron differentiation	5	2.99	7.6E-03
GO – BP	frizzled signaling pathway	3	1.80	8.4E-03
GO – BP	regulation of action potential	3	1.80	8.4E-03
GO – BP	regulation of transcription, DNA-dependent	28	16.77	8.5E-03
GO – BP	phosphate transport	5	2.99	9.0E-03
GO – BP	neurogenesis	5	2.99	9.0E-03
GO – BP	regulation of cellular process	40	23.95	1.0E-02
GO – BP	regulation of transcription	29	17.37	1.1E-02
GO – BP	transcription	30	17.96	1.1E-02
GO – BP	cellular process	111	66.47	1.2E-02
GO – BP	regulation of nucleobase, nucleoside, nucleotide and nucleic acid metabolism	29	17.37	1.3E-02
GO – BP	regulation of physiological process	39	23.35	1.3E-02
GO – BP	protein amino acid autophosphorylation	3	1.80	1.4E-02
GO – BP	regulation of cellular physiological process	38	22.75	1.4E-02
GO – BP	protein autoprocessing	3	1.80	1.5E-02
GO – BP	regulation of cellular metabolism	30	17.96	1.5E-02
GO – BP	neuron maturation	3	1.80	1.6E-02
GO – BP	regulation of biological process	41	24.55	1.8E-02
GO – BP	regulation of metabolism	30	17.96	2.1E-02
GO – BP	neuron development	4	2.40	2.7E-02
GO – BP	cell maturation	3	1.80	3.0E-02
GO – BP	nervous system development	9	5.39	3.3E-02
GO – BP	system development	9	5.39	3.4E-02
GO – BP	chromatin remodeling	3	1.80	3.7E-02
GO – BP	mechanosensory behavior	2	1.20	3.8E-02
GO – BP	inorganic anion transport	5	2.99	4.2E-02
GO – BP	Wnt receptor signaling pathway	4	2.40	4.5E-02

Table X.12 Kegg pathways and biological processes for mouse brain.

Category	Term	Count	%	PValue
	Kegg pathway up			
KEGG_PATHWAY	ANTIGEN PROCESSING AND PRESENTATION	15	3.42	3.7E-06
KEGG_PATHWAY	TYPE I DIABETES MELLITUS	11	2.51	9.2E-05
KEGG_PATHWAY	CELL ADHESION MOLECULES (CAMS)	14	3.19	2.8E-03
KEGG_PATHWAY	COMPLEMENT AND COAGULATION CASCADES	9	2.05	4.0E-03
	Kegg pathway down			
	GO – BP up (Top 40)			
GO - BP	antigen processing	16	3.64	1.2E-11
GO – BP	antigen presentation	18	4.10	1.4E-11
GO – BP	immune response	48	10.93	1.2E-10
GO – BP	response to biotic stimulus	55	12.53	3.5E-10
GO – BP	defense response	51	11.62	8.8E-09
GO – BP	humoral defense mechanism (sensu Vertebrata)	12	2.73	2.3E-08
GO – BP	antigen processing, endogenous antigen via MHC class I	9	2.05	1.6E-06
GO – BP	antigen presentation, endogenous antigen	9	2.05	1.9E-06
GO – BP	antigen presentation, exogenous antigen via MHC class II	6	1.37	4.4E-06
GO – BP	inflammatory response	14	3.19	1.1E-05
GO - BP	complement activation	8	1.82	1.6E-05
GO – BP	response to other organism	30	6.83	2.9E-05
GO – BP	humoral immune response	14	3.19	2.9E-05
GO – BP	response to pest, pathogen or parasite	29	6.61	4.1E-05
GO – BP	regulation of immune response	12	2.73	4.4E-05
GO – BP	phagocytosis	7	1.59	4.8E-05
GO – BP	antigen presentation, exogenous antigen	7	1.59	5.7E-05
GO – BP	innate immune response	8	1.82	5.7E-05
GO – BP	complement activation, classical pathway	6	1.37	1.2E-04
GO – BP	positive regulation of immune response	9	2.05	1.9E-04
GO - BP	establishment of cellular localization	28	6.38	2.0E-04
GO – BP	establishment of localization	84	19.13	2.0E-04
GO – BP	cellular localization	28	6.38	2.2E-04
GO – BP	localization	84	19.13	2.7E-04
GO – BP	tumor necrosis factor-alpha biosynthesis	4	0.91	3.6E-04
GO – BP	regulation of tumor necrosis factor-alpha biosynthesis	4	0.91	3.6E-04
GO – BP	positive regulation of tumor necrosis factor-alpha biosynthesis	4	0.91	3.6E-04
GO – BP	transport	77	17.54	3.9E-04
GO – BP	intracellular transport	27	6.15	4.2E-04
GO – BP	regulation of phagocytosis	5	1.14	5.0E-04
GO - BP	positive regulation of phagocytosis	5	1.14	5.0E-04
GO – BP	regulation of organismal physiological process	13	2.96	5.8E-04
GO – BP	positive regulation of organismal physiological process	9	2.05	6.3E-04
GO – BP	positive regulation of endocytosis	5	1.14	1.0E-03
GO – BP	antigen processing, exogenous antigen via MHC class II	5	1.14	1.4E-03
GO – BP	response to wounding	19	4.33	1.8E-03
GO – BP	regulation of programmed cell death	16	3.64	1.9E-03
GO – BP	cell organization and biogenesis	52	11.85	2.1E-03
GO – BP	phagocytosis, engulfment	4	0.91	2.2E-03
GO – BP	response to external stimulus	22	5.01	2.2E-03
	GO – BP down			
GO – BP	cellular physiological process	119	55.35	2.0E-03
GO – BP	nervous system development	13	6.05	5.1E-03
GO – BP	cytoskeleton organization and biogenesis	12	5.58	6.1E-03
GO – BP	localization	45	20.93	8.4E-03
GO – BP	system development	13	6.05	9.7E-03
GO – BP	development	32	14.88	1.2E-02
GO – BP	establishment of localization	44	20.47	1.2E-02
GO – BP	ion transport	15	6.98	1.4E-02
GO – BP	regulation of apoptosis	9	4.19	2.0E-02
GO – BP	cell differentiation	17	7.91	2.0E-02
GO – BP	regulation of programmed cell death	9	4.19	2.2E-02
GO – BP	cell organization and biogenesis	28	13.02	2.4E-02
GO – BP	negative regulation of apoptosis	5	2.33	3.4E-02
GO – BP	negative regulation of programmed cell death	5	2.33	3.5E-02
GO – BP	muscle contraction	4	1.86	3.5E-02
GO – BP	phosphate transport	4	1.86	3.7E-02
GO – BP	microtubule-based process	6	2.79	3.7E-02
GO – BP	axonogenesis	5	2.33	4.2E-02
GO – BP	neuron development	6	2.79	4.5E-02
GO – BP	di-, tri-valent inorganic cation transport	5	2.33	4.7E-02
GO – BP	anti-apoptosis	4	1.86	4.9E-02

Table X.13 Kegg pathways and biological processes for mouse heart.

Category	Term	Count	%	PValue
	Kegg pathway up			
KEGG_PATHWAY	ANTIGEN PROCESSING AND PRESENTATION	18	3.64	1.4E-07
KEGG_PATHWAY	TYPE I DIABETES MELLITUS	13	2.63	1.1E-05
KEGG_PATHWAY	CELL ADHESION MOLECULES (CAMS)	20	4.04	1.1E-05
KEGG_PATHWAY	GLUTATHIONE METABOLISM	10	2.02	6.7E-05
KEGG_PATHWAY	METABOLISM OF XENOBIOTICS BY CYTOCHROME P450	12	2.42	1.2E-04
KEGG_PATHWAY	COMPLEMENT AND COAGULATION CASCADES	9	1.82	9.5E-03
KEGG_PATHWAY	STARCH AND SUCROSE METABOLISM	7	1.41	3.1E-02
	Kegg pathway down			
KEGG_PATHWAY	ECM-RECEPTOR INTERACTION	13	4.25	9.0E-09
KEGG_PATHWAY	FOCAL ADHESION	16	5.23	7.3E-07
KEGG_PATHWAY	CELL COMMUNICATION	12	3.92	4.0E-06
KEGG_PATHWAY	BENZOATE DEGRADATION VIA COA LIGATION	4	1.31	3.8E-02
	GO – BP up (Top 30)			
GO - BP	immune response	60	12.12	5.1E-13
GO – BP	antigen processing	17	3.43	2.7E-11
GO – BP	response to biotic stimulus	66	13.33	3.7E-11
GO – BP	antigen presentation	19	3.84	5.8E-11
GO – BP	defense response	63	12.73	2.5E-10
GO – BP	antigen processing, endogenous antigen via MHC class I	10	2.02	8.3E-07
GO – BP	antigen presentation, endogenous antigen	10	2.02	1.0E-06
GO – BP	inflammatory response	16	3.23	6.5E-06
GO – BP	antigen presentation, exogenous antigen via MHC class II	6	1.21	1.3E-05
GO – BP	humoral defense mechanism (sensu Vertebrata)	10	2.02	1.6E-05
GO - BP	complement activation	8	1.62	6.8E-05
GO – BP	antigen presentation, exogenous antigen	7	1.41	2.0E-04
GO – BP	innate immune response	8	1.62	2.3E-04
GO – BP	antigen processing, exogenous antigen via MHC class II	6	1.21	3.4E-04
GO – BP	complement activation, classical pathway	6	1.21	3.4E-04
GO – BP	response to pest, pathogen or parasite	30	6.06	8.3E-04
GO – BP	response to external stimulus	27	5.45	8.7E-04
GO – BP	humoral immune response	13	2.63	1.0E-03
GO – BP	response to stress	44	8.89	1.1E-03
GO – BP	response to other organism	30	6.06	1.4E-03
GO - BP	response to wounding	22	4.44	2.0E-03
GO – BP	mast cell activation	4	0.81	2.6E-03
GO – BP	taxis	9	1.82	3.2E-03
GO – BP	chemotaxis	9	1.82	3.2E-03
GO – BP	positive regulation of immune response	8	1.62	3.8E-03
GO – BP	positive regulation of enzyme activity	9	1.82	4.1E-03
GO – BP	regulation of immune response	10	2.02	4.4E-03
GO – BP	oxygen and reactive oxygen species metabolism	7	1.41	4.7E-03
GO – BP	transport	87	17.58	4.9E-03
GO – BP	locomotory behavior	11	2.22	5.7E-03
	GO – BP down (Top 30)			
GO – BP	cell adhesion	28	9.15	6.0E-08
GO – BP	cellular physiological process	174	56.86	1.3E-05
GO – BP	cellular protein metabolism	64	20.92	1.6E-04
GO – BP	cellular macromolecule metabolism	64	20.92	2.4E-04
GO – BP	protein metabolism	66	21.57	2.8E-04
GO – BP	regulation of transforming growth factor beta receptor signaling pathway	4	1.31	3.5E-04
GO – BP	negative regulation of cellular process	23	7.52	4.1E-04
GO – BP	regulation of cellular process	68	22.22	5.1E-04
GO – BP	phosphorus metabolism	25	8.17	1.0E-03
GO – BP	phosphate metabolism	25	8.17	1.0E-03
GO – BP	negative regulation of biological process	23	7.52	1.2E-03
GO – BP	regulation of biological process	70	22.88	1.5E-03
GO – BP	protein modification	37	12.09	1.8E-03
GO – BP	enzyme linked receptor protein signaling pathway	11	3.59	1.9E-03
GO – BP	regulation of cellular physiological process	63	20.59	2.0E-03
GO – BP	macromolecule metabolism	78	25.49	2.4E-03
GO – BP	regulation of physiological process	64	20.92	2.9E-03
GO – BP	biopolymer modification	37	12.09	3.4E-03
GO – BP	phosphate transport	6	1.96	3.9E-03
GO – BP	negative regulation of cellular physiological process	18	5.88	4.9E-03
GO – BP	protein amino acid alkylation	4	1.31	6.3E-03
GO – BP	biopolymer metabolism	52	16.99	6.7E-03
GO – BP	negative regulation of physiological process	18	5.88	7.6E-03
GO – BP	ion transport	20	6.54	8.1E-03
GO – BP	epidermal growth factor receptor signaling pathway	3	0.98	1.1E-02
GO – BP	regulation of transcription from RNA polymerase II promoter	11	3.59	1.2E-02
GO – BP	DNA replication	7	2.29	1.3E-02
GO – BP	vesicle-mediated transport	12	3.92	1.3E-02
GO – BP	establishment of localization	59	19.28	1.4E-02
GO – BP	transcription from RNA polymerase II promoter	12	3.92	1.4E-02

Table X.14 Kegg pathways and biological processes for mouse kidney.

Category	Term	Count	%	PValue
	Kegg pathway up			
KEGG_PATHWAY	T CELL RECEPTOR SIGNALING PATHWAY	20	2.41	9.4E-07
KEGG_PATHWAY	B CELL RECEPTOR SIGNALING PATHWAY	15	1.81	1.5E-05
KEGG_PATHWAY	HEMATOPOIETIC CELL LINEAGE	16	1.93	3.8E-05
KEGG_PATHWAY	NATURAL KILLER CELL MEDIATED CYTOTOXICITY	19	2.29	9.6E-05
KEGG_PATHWAY	CELL ADHESION MOLECULES (CAMS)	20	2.41	6.8E-04
KEGG_PATHWAY	LEUKOCYTE TRANSENDOTHELIAL MIGRATION	16	1.93	3.0E-03
KEGG_PATHWAY	FC EPSILON RI SIGNALING PATHWAY	12	1.45	4.3E-03
KEGG_PATHWAY	ANTIGEN PROCESSING AND PRESENTATION	13	1.57	4.9E-03
KEGG_PATHWAY	FOCAL ADHESION	22	2.65	5.6E-03
KEGG_PATHWAY	TOLL-LIKE RECEPTOR SIGNALING PATHWAY	12	1.45	1.4E-02
KEGG_PATHWAY	ADIPOCYTOKINE SIGNALING PATHWAY	10	1.20	1.6E-02
KEGG_PATHWAY	TIGHT JUNCTION	14	1.69	1.6E-02
KEGG_PATHWAY	O-GLYCAN BIOSYNTHESIS	6	0.72	2.0E-02
KEGG_PATHWAY	APOPTOSIS	11	1.33	2.6E-02
KEGG_PATHWAY	CYTOKINE-CYTOKINE RECEPTOR INTERACTION	22	2.65	2.7E-02
KEGG_PATHWAY	TYPE I DIABETES MELLITUS	9	1.08	2.8E-02
KEGG_PATHWAY	REGULATION OF ACTIN CYTOSKELETON	19	2.29	3.0E-02
KEGG_PATHWAY	JAK-STAT SIGNALING PATHWAY	15	1.81	3.9E-02
	Kegg pathway down			
KEGG_PATHWAY	UREA CYCLE AND METABOLISM OF AMINO GROUPS	6	1.63	7.8E-04
KEGG_PATHWAY	NITROGEN METABOLISM	5	1.36	2.9E-03
KEGG_PATHWAY	ARGININE AND PROLINE METABOLISM	7	1.91	4.0E-03
KEGG_PATHWAY	GLUTATHIONE METABOLISM	5	1.36	3.6E-02
KEGG_PATHWAY	ALANINE AND ASPARTATE METABOLISM	4	1.09	4.2E-02
	GO – BP up (Top 24)			
GO - BP	regulation of biological process	178	21.45	3.3E-09
GO – BP	immune response	66	7.95	8.6E-09
GO – BP	regulation of cellular process	166	20.00	1.0-08E
GO – BP	response to biotic stimulus	78	9.40	1.6E-08
GO – BP	regulation of physiological process	161	19.40	7.4E-08
GO – BP	regulation of cellular physiological process	156	18.80	1.0E-07
GO – BP	defense response	74	8.92	1.1E-07
GO – BP	antigen presentation, peptide antigen	7	0.84	1.4E-06
GO – BP	immune cell activation	21	2.53	2.1E-06
GO – BP	cell activation	21	2.53	2.3E-06
GO – BP	death	42	5.06	4.1E-06
GO – BP	positive regulation of immune response	14	1.69	6.2E-06
GO – BP	cell death	41	4.94	7.0E-06
GO – BP	positive regulation of organismal physiological process	15	1.81	9.3E-06
GO – BP	programmed cell death	39	4.70	1.2E-05
GO – BP	lymphocyte activation	18	2.17	2.2E-05
GO – BP	T cell activation	14	1.69	2.2E-05
GO – BP	mast cell activation	6	0.72	3.4E-05
GO – BP	regulation of organismal physiological process	21	2.53	3.6E-05
GO – BP	apoptosis	37	4.46	4.2E-05
GO – BP	inflammatory response	18	2.17	4.3E-05
GO – BP	positive regulation of cellular physiological process	38	4.58	4.6E-05
GO – BP	hemopoietic or lymphoid organ development	20	2.41	4.6E-05
GO – BP	regulation of programmed cell death	28	3.37	4.9E-05
	GO – BP down (Top 24)			
GO – BP	cellular physiological process	221	60.22	1.1E-08
GO – BP	carboxylic acid metabolism	28	7.63	3.7E-08
GO – BP	organic acid metabolism	28	7.63	3.7E-08
GO – BP	metabolism	174	47.41	3.8E-07
GO – BP	nitrogen compound metabolism	21	5.72	3.2E-06
GO – BP	amine metabolism	20	5.45	5.1E-06
GO – BP	cellular lipid metabolism	24	6.54	6.6E-06
GO – BP	physiological process	248	67.57	1.5E-05
GO – BP	lipid metabolism	26	7.08	1.5E-05
GO – BP	sodium ion transport	11	3.00	2.8E-05
GO – BP	amino acid and derivative metabolism	17	4.63	3.8E-05
GO – BP	transport	76	20.71	9.7E-05
GO – BP	cofactor metabolism	14	3.81	1.2E-04
GO – BP	amino acid biosynthesis	7	1.91	1.3E-04
GO – BP	coenzyme metabolism	13	3.54	1.4E-04
GO – BP	amino acid metabolism	14	3.81	2.0E-04
GO – BP	localization	80	21.80	2.9E-04
GO – BP	establishment of localization	79	21.53	3.7E-04
GO – BP	cellular metabolism	152	41.42	4.2E-04
GO – BP	amine biosynthesis	7	1.91	1.0E-03
GO – BP	nitrogen compound biosynthesis	7	1.91	1.0E-03
GO – BP	amino acid catabolism	6	1.63	1.1E-03
GO – BP	anion transport	11	3.00	1.3E-03
GO – BP	fatty acid metabolism	10	2.72	1.5E-03